Characterization of habenular neurocircuitry. A potential novel target for treating depression.

Jester-Broms, Jonas

2018

Document Version:
Publisher's PDF, also known as Version of record

Characterization of habenular neurocircuitry

a potential novel target for treating depression

JONAS JESTER-BROMS
FACULTY OF MEDICINE | LUND UNIVERSITY

Characterization of habenular neurocircuitry

Characterization of habenular neurocircuitry

a potential novel target for treating depression

by Jonas Jester-Broms

LUND
UNIVERSITY

Doctoral dissertation
Thesis advisors: Prof. Anders Tingström, Dr. Joakim Ekstrand, Dr. Martin Lundblad
Faculty opponent: Prof. emeritus Jon Storm-Mathisen

To be presented, with the permission of the Faculty of Medicine of Lund University, for public criticism in the Belfrage lecture hall (Belfragesalen) at the Biomedical Centre on Friday, the 30th of November 2018 at 13:00.

Organization	Document name
LUND UNIVERSITY Department of Psychiatry Psychiatric Neuromodulation Unit Klinikgatan 30, BMC D11 221 84 Lund, Sweden	**DOCTORAL DISSERTATION** Date of disputation 2018-11-30 Sponsoring organization
Author(s) Jonas Jester-Broms	

Title and subtitle

Characterization of habenular neurocircuitry

Abstract

In the last decade, there has been an explosion of interest within the psychiatric research community in a small diencephalic brain region called the habenula. It has been uncovered as a key regulator of monoaminergic transmission, playing a fundamental role in decision making, behavioral flexibility, inhibitory control, sleep, pain and analgesia. Perturbation of the habenular neurocircuitry in animals produce effects that mimic rewards and punishments, animals actively seek habenula inactivation while avoiding activation. From a psychiatric viewpoint, the habenula is a promising target for diseases like depression, drug dependence and ADHD. Given that the morphology and connectivity of the habenula is highly conserved throughout the vertebrate subphylum, animal research is both valid and necessary to map the circuitry and neuronal populations that constitute the habenular complex. Due to the small size and position of the habenula, techniques for modulating this brain area in humans are both invasive, difficult and risky. To overcome this issue, we have characterized an orphan G protein-coupled receptor (Gpr151) that may serve as a future non-invasive target for habenula modulation. We demonstrate that it is highly enriched in the habenular circuitry, with a pattern that is evolutionary conserved. Using monosynaptic pseudorabies and adenoassociated viral tracing techniques we have dissected the connectivity of the habenular neurons expressing the orphan G-protein coupled receptor Gpr151. We have also performed initial screening experiments with the aim of identifying ligands to the receptor. Our results indicate that Gpr151 can possibly modulate a brain network providing a link between the basal forebrain and neuromodulatory brain stem targets, a circuitry with a involved in a multitude of functions with importance for psychiatric disease. Moreover, we continued the characterization of the inhibitory interneurons in the habenula, a neuronal population which has received very little attention previously. The existence of various types of intrinsic neurons within the habenular nucleus adds to the already very complex picture of this intriguing structure. Psychiatry is in dire need of new effective treatments, and the habenula and Gpr151 might provide possible novel targets for psychopharmacological research and future drug development.

Key words

habenula, Gpr151, depression, psychiatry, GABA, interneuron

Classification system and/or index terms (if any)

Supplementary bibliographical information	Language English
ISSN and key title	ISBN 978-91-7619-707-3 (print)

Recipient's notes	Number of pages 176	Price
	Security classification	

Characterization of habenular neurocircuitry

a potential novel target for treating depression

by Jonas Jester-Broms

LUND
UNIVERSITY

A doctoral thesis at a university in Sweden takes either the form of a single, cohesive research study (monograph) or a summary of research papers (compilation thesis), which the doctoral student has written alone or together with one or several other author(s).

In the latter case the thesis consists of two parts. An introductory text puts the research work into context and summarizes the main points of the papers. Then, the research publications themselves are reproduced, together with a description of the individual contributions of the authors. The research papers may either have been already published or are manuscripts at various stages (in press, submitted, or in draft).

Cover illustration front: neurons.

Cover illustration back: picture of the author.

Funding information: This work was funded by grants from the Swedish Research Council, the Royal Physiographic Society of Lund, Stiftelsen Professor Bror Gadelius minnesfond, Gyllenstiernska Krapperupsstiftelsen, and Stiftelsen Ellen och Henrik Sjöbrings minnesfond.

Faculty of Medicine, Department of Psychiatry

ISBN: 978-91-7619-707-3 (print)
ISSN: 1652-8220

Printed in Sweden by Media-Tryck, Lund University, Lund 2018

The most merciful thing in the world, I think, is the inability of the human mind to correlate all its contents. We live on a placid island of ignorance in the midst of black seas of infinity, and it was not meant that we should voyage far. The sciences, each straining in its own direction, have hitherto harmed us little; but some day the piecing together of dissociated knowledge will open up such terrifying vistas of reality, and of our frightful position therein, that we shall either go mad from the revelation or flee from the deadly light into the peace and safety of a new dark age.

–H. P. Lovecraft, *The Call of Cthulhu*

Contents

List of publications

This thesis is based on the following publications, referred to by their Roman numerals:

I **Conserved expression of the Gpr151 receptor in habenular axonal projections of vertebrates.**

Broms, J., Antolin-Fontes, B., Tingström, A., & Ibañez-Tallon, I. (2014).
Journal of Comparative Neurology, 523(3), 359–380.

II **Monosynaptic retrograde tracing of neurons expressing the G-protein coupled receptor Gpr151 in the mouse brain.**

Broms, J., Grahm, M., Haugegaard, L., Blom, T., Meletis, K., & Tingström, A. (2017).
Journal of Comparative Neurology, 525(15), 3227–3250.

III **Investigating spexin and related neuropeptides as possible ligands of Gpr151.**

Jester-Broms, J., Haugegaard, L & Tingström, A. (unpublished).
Manuscript

IV *Gad2* **expressing interneurons in the mouse habenula.**

Jester-Broms, J., Haugegaard, L., Grahm, M., Ekstrand, J & Tingström, A. (unpublished).
Manuscript

Acknowledgements

I want to express my utmost gratitude and love to the following people. You have all been a part of my life during the 10 years that I have been doing research and I would like to thank you for the fun we've had and what is to come!

NAME	KEYWORDS
Jester-Broms, S & Jester-Broms, E	Loves of my life
Tingström, A	Main supervisor, guru, pal, cryptobillionaire (to be)
Ekstrand, J	Co-supervisor, sounding board, muckraker
Lundblad, M	Co-supervisor, laser operator, micro-tinkerer
Grahm, M	PhD-buddy, brain surgery team mate
Ekemohn, M	PhD-buddy, electrifying rat whisperer
Haugegaard, L.D	Lab magician
Broms & Jester *et al*.	Loving and supportive family
et al.	former MPU/PNU members
	helpful BMC people
	friends and collaborators

Popular summary in English

Major depressive disorder is a debilitating and potentially letal syndrome with symptoms including depressed mood, diminished interest in daily activities, feelings of worthlessness and cognitive impairment. In order to understand the underlying causes and to develop novel treatments, it is necessary to research the changes in the brain that occur in depressed individuals. One of the brain areas that has come into focus during the last decades is the habenula. The habenula receives information from the frontal parts of the brain and in turn, modulates parts of the brainstem. It is activated by stress, pain and disappointment and has been observed to be structurally and functionally dysregulated in depression.

Gpr151 is a G protein–coupled receptor with unknown ligand, and is almost exclusively found in the habenula. This fact makes this receptor a potential drug target for selectively modulating habenular function, which could have implications for treating depression. In this thesis, we map the expression pattern of Gpr151 as well as characterize the connectivity of the neurons that express this receptor. We find that the pattern of Gpr151 expression is remarkably conserved throughout the vertebrate lineage. Gpr151 is present in habenular axons contacting midbrain and brainstem structures with well established roles in goal-oriented behavior, stress, pain and depression. We also mapped the input to the Gpr151 expressing neurons, yielding a complete map of the circuits that are possibly modulated by Gpr151. We have also performed experiments with the aim of identifying the natural ligand to this receptor. Unfortunately, we did not find any promising candidates in these initial efforts. We have also further characterized a previously overlooked neuronal cell type in the habenula, the inhibitory interneurons, which was until recently assumed not to be present in this structure.

Our hope is that a characterization of habenular circuits and possible means of modulating its activity, may help to develop new treatment options for major depressive disorder in the future.

Populärvetenskaplig sammanfattning på svenska

Depression är en svårt handikappande och potentiellt livshotande sjukdom som karaktäriseras av sorg, känslor av tomhet och meningslöshet. För att bättre förstå hur depression uppkommer och för att kunna utveckla nya, mer specifika behandlingar, är det nödvändigt att förstå sjukdomens neurobiologi. Ett hjärnområde som det senaste decenniet har rönt mycket uppmärksamhet bland depressionsforskare är habenula. Området kopplar samman områden i de främre delarna av hjärnan med hjärnstammen och aktiveras bland annat vid stress, smärta och besvikelse. Avvikelser i habenulas storlek och funktion har påvisats hos patienter som drabbats av depression.

Gpr151 är en G–protein–kopplad receptor med okänd ligand, som finns nästan uteslutande i habenula. Detta faktum gör det möjligt att via denna receptor eventuellt kunna påverka habenulas funktion, vilket skulle kunna lindra depressiva symtom. Vi har i detta arbete gjort en extensiv kartläggning av de nervceller som producerar Gpr151. I den första studien, där vi undersökte Gpr151-proteinets lokalisation fann vi intressant nog att Gpr151-neuronens projektionsmönster är evolutionärt konserverat. Uttrycket hos mus och råtta var i det närmaste identiskt med det hos zebrafisk, och vi kan konstatera att denna receptors lokalisation (och möjligen även dess funktion) varit oförändrad i närmare en halv miljard år. Vi visade i denna studie att neuron vilka producerar Gpr151 i habenula kontaktar områden i hjärnstammen med väletablerad betydelse för motivationsstyrt beteende, stress, smärta och depression. I den andra studien kartlade vi istället vilka hjärnområden som bidrar med inflödet av information till Gpr151-cellerna. Inmärkning av dessa nervceller gjordes med hjälp av en nyutvecklad teknik där vi använder ett modifierat rabiesvirus. Således har vi nu en god bild av de nervcellsnätverk som eventuellt kan påverkas vid modulering av Gpr151. Vi har även utfört initiala försök att ta reda på vilka substanser i hjärnan som aktiverar receptorn. Utifrån släktskap mellan olika receptorer identifierade vi olika kandidatmolekyler som vi tillsatte till odlade celler som producerar Gpr151. Dessvärre fann vi inget stöd för att de kandidatmolekyler som vi undersökte kan aktivera Gpr151.

Vi har även i detta arbete tittat närmare på olika nervcellstyper i habenula. En sorts nervceller som verkar hämmande på andra nervceller troddes tills för bara helt nyligen inte existera i habenula. Vi kunde med en känslig metod för att märka in dessa hämmande nervceller beskriva deras utseende. Ökande kunskap kring dessa nervceller kan bidra till förståelsen av hur habenula bearbetar information och hur olika nervceller inom habenula samverkar.

Vi hoppas att en bred karaktärisering av habenula, med avseende på dess struktur och funktion på sikt kan leda till utveckling av nya klasser av läkemedel för behandling av psykiatriska tillstånd.

Introduction

1 Depression

1.1 Clinical presentation and epidemiology

Mood disorders is a category of psychiatric disorders that affects the mood, which may be described as a sustained feeling that tend to influence our decision making, thought processes, motivation and social interactions, among other things. Mood regulation is thus crucial for normal functioning and well-being. Indeed, disorders that cause dysregulation of mood, often have debilitating adverse effects on the life course of the affected individual.

For a patient to be diagnosed with Major Depressive Disorder (MDD) according to the Diagnostic and Statistical Manual of Mental Disorders 5 (DSM-5) a number of criteria must be met (American Psychiatric Association, 2013). The patient must display depressed mood, and/or diminished pleasure or interest in daily life activities. Additional criteria are: change in appetite or body weight; sleep disturbance; psychomotor agitation or retardation; fatigue; feelings of worthlessness or inappropriate guilt; cognitive impairment; and recurrent thoughts of death or suicide. At least five of the criteria above must be met and at least one of the first two criteria must be included. Also, the symptoms must cause clinically significant distress or impairment, and may not be attributable to substance use or psychotic disease. For MDD diagnosis, no manic or hypomanic episodes (abnormally elevated mood) should have been present, which instead implies bipolar disorder.

The life-time prevalence of MDD is around 16% while a much lower prevalence of 4% is observed for bipolar disorder (type I and II) (Kessler et al., 2005). The reported prevalence of depression varies across different countries and cultures (Kessler and Bromet, 2013). In countries with low prevalence, the impairment is often greater, which suggests a culturally determined difference in report threshold rather than true difference in prevalence of depressive symptoms (Simon et al., 2002; Chang et al., 2008).

Severe depression is a life-threatening disease, as many as 60-70% of patients experience sui-

cidal ideas while around 10-15% die as a result of completed suicide (Möller, 2003). Apart from the suffering associated with the condition, depression is also debilitating for personal development and relationships. Being diagnosed with a mood disorder decreases the probability to complete education, increase marital dissatisfaction and risk of divorce, is associated with negative parenting behavior, increase risk of unemployment, and may lead to a lower house-hold income (Kessler and Bromet, 2013). Many of the negative effects of depression are also in themselves risk factors, which may further deepen the severity of the disease.

1.2 Pathogenesis of depression

Explanations exist; they have existed for all time;
there is always a well-known solution to every human problem
— neat, plausible, and wrong.
— H. L. Mencken

The diagnostic criteria for MDD are problematic in the sense that around 1500 combinations of the symptoms above are possible and that two individuals may be diagnosed with the same disorder but not share any symptoms at all (Ostergaard et al., 2011). This indicates that the population of MDD patients is very heterogenous, which should be kept in mind when discussing the cause or causes (etiology) of depression.

Historically and at present, many ideas on what causes depression exist. Does the multitude of hypotheses imply that we are flying blind when we talk about depression or treat people with antidepressive treatment or psychotherapy? It could rather be argued that this is a reflection of the complex nature of depression. Below I will give an account for several hypotheses, that when considered as parts of a broader picture, let you appreciate the heterogenic and multifactorial nature of this psychiatric disorder.

The monoamine hypothesis of depression

Monoamines are a class of neurotransmitters that are derived from aromatic amino acids and include adrenaline, noradrenaline, dopamine, histamine and serotonin. The hypothesis that depression results from imbalances of monoamine signaling dates back almost 60 years (reviewed in Baumeister et al., 2003). It was precipitated by two discoveries during the 1950s. The first was the reported depressogenic effect of *reserpin*, a compound isolated from root of the *Rauvolfia serpentina* plant, which had previously been used traditionally in Indian medicine (Fig. 1). Reserpine inhibit the vesicular monoamine transporters that are responsible for package and storage of monoamines into synaptic vesicles (Henry and

Scherman, 1989). By inhibiting the transporter, the monoamines are instead degraded which cause lasting monoaminergic depletion (Shore et al., 1955; Bertler et al., 1956). Reserpine was being used in the 50-60s for treating hypertension. In several clinical trials, there were reports that some patients developed depression after treatment with reserpine, hence it was for long considered as a depressogenic substance. However, a recent meta-analysis found a depression prevalence of 10% in the reserpine treated population, which is even a bit lower than the prevalence of 16% in the general population (Baumeister et al., 2003), which casts doubt on its depressogenic effects.

The second major contribution to the monoamine hypothesis was the promising antidepressant activity of two newly developed drugs against tuberculosis (Ramachandraih et al., 2011). These drugs were isoniazid (which is still used in clinical practice for treating tuberculosis) and iproniazid. It was shown that iproniazid and (to a lesser extent) isoniazid inhibited the enzyme responsible for breaking down monoamines in the synapse, monoamine oxidase (MAO). When MAO is blocked, the concentration and availability of monoamines thus increase.

This led to the formulation of the monoamine hypothesis of depression, which states that depression is a result of a monoamine deficiency and, in line with this, that a restoration of monoaminergic levels will alleviate depression (Baumeister et al., 2003).

Although it is certainly true that the monoamine hypothesis has spurred research and led to the development of substances that have antidepressant activity, it is at present clear

Figure 1: Rauvolfia serpentina.
Credit: Wellcome Library, London. Wellcome Images images@wellcome.ac.uk http://wellcomeimages.org Rauwolfia serpentina Hortus indicus malabaricus, 12 volumes Hendrik Adriaan Rheede Tot Draakestein, van Published: 1678 - 1703. Copyrighted work available under Creative Commons Attribution only license CC BY 4.0 http://creativecommons.org/licenses/by/4.0/

that the model lacks explanatory power. Depletion of monoamines can be achieved by administration of an amino-acid drink lacking the monoamine precursor tryptophan for serotonin depletion and phenylalanine–tyrosine for noradrenaline and dopamine depletion (Ruhé et al., 2007). The hypothesis predicts that the degree of depressed mood should be proportional to monoamine levels. Indeed, depressed patients in remission tend to relapse when depleted of the monoamine that is targeted by their antidepressive medication (Ruhé et al., 2007). However, depleting serotonin, noradrenalin and dopamine in healthy individuals or currently depressed patients has no effect on mood. A small mood-lowering effect can be observed in healthy individuals with a family history of depression. Given that there is no simple relationship between monoamine levels and depressed mood, this hypothesis is at best an oversimplification. Monoamines are clearly important targets for antidepressive treatment (Hieronymus et al., 2016), but they are not the (only) culprit in causing depression.

Brain reward system

A necessity for all life forms is the ability to adapt their behaviour so that outcomes that increase the chance of survival and reproduction (i.e. food, sex, warmth, social interaction, safe environments) are maximized while outcomes that put survival at risk (i.e. injury, hunger, social isolation) are minimized. In vertebrates, large parts of this evaluation and control is carried out by complex brain circuits that evaluate sensory information and outcomes of actions. This system is often referred to as the *brain reward system*.

The key components of the system are a set of highly interconnected brain areas that respond to salient cues and that may also produce positive or negative experiences when activated. This can be assessed in animals through *intracranial self-stimulation*, which has allowed mapping of the brain areas associated with affective experience. The brain areas that make up the reward system include the nucleus accumbens, VTA, medial prefrontal cortex, lateral hypothalamus, lateral habenula and amygdala. Numerous studies of depressed individuals using non-invasive brain imaging techniques or post-mortem analysis have identified volumetric and functional disturbances in many of these areas (reviewed in Russo and Nestler, 2013). One hypothesis arising from the link between the reward system and depression is that the negative interpretation of experiences that is common in depressed individuals is a result of a dysregulated reward processing (reviewed in Russo and Nestler, 2013). It is possible that this mechanism could account for anhedonia, the inability to experience pleasure, one of the key symptoms of depression (Heshmati and Russo, 2015).

Genes, environment and their interaction

The *stress–vulnerability* model of psychiatric disease was first proposed for conceptualizing the etiology of schizophrenia (Zubin and Spring, 1977) but can be applied to depression as well (McGuffin and Rivera, 2015). According to the model, all individuals exhibit varying sensitivity to challenges arising in the external environment, such as stressful life events, infection, drug use, seasonal variation etc, or from the internal environment, such as metabolic, neurophysiological, biochemical and hormonal changes. When this threshold is surpassed, the homeostatic equilibrium maintaining a healthy mental state is disrupted and a disease episode develops.

Studies of families of depressed individuals have established that the risk of developing depression is increased (odds ratio ~2.8) if a first-degree relative is affected by the disease (reviewed in Sullivan et al., 2000). Similarly, studies comparing identical and non-identical twins have demonstrated a substantial degree of genetic heredity (explaining at least 30% of the variance) (Sullivan et al., 2000). Given the findings above, it is clear that there are genetic factors that influence the risk of developing depression.

Thus, the research on the stress–vulnerability hypothesis has primarily focused on how specific genetic variants in combination with stressful life events may contribute to the development of depression. In 2003, a seminal study on gene–environment interaction was published reporting that a certain genetic variation in the promoter region of the serotonin transporter, designated the serotonin-transporter-linked polymorphic region (5-HTTLPR) genotype, made individuals more susceptible to stressful life events (Caspi et al., 2003). Of importance, the 5-HTTLPR genotype in itself did not increase the risk for depression, but individuals carrying the genotype had a greater risk of developing depression when subjected to stressful life-events.

This finding spurred a huge interest in research in gene–environment interaction in depression. However, replication attempts of the original findings of the Caspi et al. (2003) study have yielded conflicting results (Risch et al., 2009; Karg et al., 2011). Recently, a large collaborative study including 38802 individuals demonstrated a strong effect of stressful life events on the prevalence of depression, but no interaction effect of the 5-HTTLPR genotype could be observed (Culverhouse et al., 2017).

Rather than singling out specific candidate genes, the genetic vulnerability (as demonstrated by the heritability of depression) is likely determined by complex interaction between multiple genes and the detection of such sets of genes requires genome–wide association studies. In order to detect genetic variants that individually contribute very little, huge study samples containing many thousands of study participants are required. Such efforts have recently successfully identified a handful of genes that each contribute very little to the risk of developing depression (Mullins and Lewis, 2017). The CONVERGE consortium,

analyzing more than 5000 Chinese women with recurrent MDD identified two genetic variants that were associated with depression risk, one close to the SIRP1 gene (rs12415800, odds ratio 1.167) and one in an intron of the LHPP gene (rs35936514, odds ratio 0.845) (CONVERGE consortium, 2015). These genetic variants are more common in east Asia but rare (especially for the SIRP1-variant) in other populations rendering these interesting findings non-universal. An estimation of the number of genetic variations needed to explain the heritability of major depressive disorder amounts to around 2500 loci (Flint and Kendler, 2014). A polygenetic disease indeed!

Affective neuroscience

Affective neuroscience is a research field and framework which seeks to identify and investigate primary affect modulating systems in the brain. A primary affect is an instinctual and experienced brain activity. The affective experience may have behavioral, cognitive and physiological consequences for the organism. The role of the primordial subcortical brain for producing emotional affect is emphasized in affective neuroscience, and a lesser role is attributed to the (in humans well-developed) cerebral cortex. It also recognizes that non-human animals are conscious in the sense that they have emotional experiences, as opposed to behavioristic theories of non-humans where the *experiences* of for example pain and pleasure are not emphasised. The main proponent of this view, the late Dr. Jaak Panksepp, identified seven such primary affect systems that are largely conserved in all vertebrate species (Panksepp, 2005). These systems are often denoted in capitals: SEEKING, FEAR, RAGE, LUST, CARE, PANIC, and PLAY.

The primary affects that have been hypothesized to be important for development of depression are the PANIC and the SEEKING systems (Panksepp and Watt, 2011). The PANIC system is activated by social separation, and is thought to mediate isolation-induced distress. The system elicits emotional pain and aids to form and maintain social bonds between individuals. In order to achieve social reunion when isolated, distress calls (crying) are elicited together with a painful experience (most notable in infants isolated from their parents). Endogenous opioids have shown to play an important role in this system, and it appears that drugs targeting opioid receptors may be as effective against psychological pain (resulting from PANIC activation) as for physical pain.

Activation of the SEEKING system is strongly appetitive and drives an energetic motivation to explore the environment and seek resources, i.e. foraging. The SEEKING system is tightly linked with dopamine and dopamine receptors, and incorporates what is known, in behavioristic terminology, as the reward system. The difference between the affective neuroscience view of the SEEKING system and the behavioristic view of the reward system is that affective neuroscience emphasizes subjective experience, where as for a behaviorist the reward system is important for operant conditioning (learning) contexts only. Activation

of the dopaminergic system (i.e. ascending dopaminergic fibers in the medial forebrain bundle) is indeed rewarding, in the sense that animals tend to work for such stimulation. It appears however, that the dopaminergic system is maximally activated during the anticipation of reward rather than during the consummatory phase (Panksepp, 2005).

In order to explain the emotional pathology in depression, Panksepp and Watt (2011) have proposed that a prolonged activation of the PANIC system may lead to a persevering state of distress associated with emotional pain. An accompanying reduction in the activity of the SEEKING system leads to decreased motivation and energy (anhedonia and fatigue) which further decreases the chance of sponteneous reversal of the condition (Panksepp and Watt, 2011). For treating depression, Panksepp proposes that activation of positive primary affects (such the PLAY system which is involved in positive social interactions) may be beneficial.

Adaptive advantages of depression?

From an evolutionary perspective, it is difficult to explain why depression, which is associated with increased morbidity and mortality, is so common in the general population. In order to balance the maladaptive effects of depression, some argue that there must be counterbalancing advantages.

A common view is that depression is the result of dysfunction in systems that otherwise carry adaptive advantages for an organism (Bergstrom and Meacham, 2016). A variation on this theme is the argument that even though the manifestation of depression in itself is evolutionary maladaptive, the alleles that carry genetic *risk* for depression may be adaptive if depression never develops. In the long run, such risk alleles may carry adaptive effects over generations, but lead to dire consequences for some individuals. A well-known example of this is sickle-cell anemia where specific mutations in hemoglobin protects against malaria if present on only one allele, while leading to severe anemia in homozygous individuals. Interestingly, while fecundity rates in depressed individuals are lower (in males) or unchanged (in females), it is increased in non-affected siblings, which completely counterbalances the disadvantage (Power et al., 2013). The increased fecundity of siblings of depressed individuals could explain why risk alleles for depression remain swimming in the gene pool.

2 Habenula

The part of the body in which the soul directly exercises its functions is not the heart at all, or the whole of the brain. It is rather the innermost part of the brain, which is a certain very small [pineal] gland situated in the middle of the brain's substance and suspended above the passage through which the spirits in the brain's anterior cavities communicate with those in its posterior cavities. The slightest movements on the part of this gland may alter very greatly the course of these spirits, and conversely any change, however slight, taking place in the course of the spirits may do much to change the movements of the gland.

— The Passions of the Soul, René Descartes

The habenular nucleus is a paired (bilateral) structure that is situated at the posterodorsal end of the diencephalon, on top of the thalamus. The habenula and pineal gland together form what is known as the *epithalamus* (Fig. 2). The name (*habenularis*, Latin) is the diminutive form of the Latin word *habena*, meaning *strip*, *rein* or *leash*, hinting at its previously considered role as an appendage to the pineal gland. The basic cellular morphology and connectivity of the habenula (Fig. 3) was described more than a century ago (Ramón y Cajal, 1894; Ganser, 1882). The habenula receives the bulk of its input via a fiber tract called *stria medullaris* and the axons of the habenular neurons form the tract known as the *fasciculus retroflexus* (of Meynert) and terminate primarily in mesencephalic and brainstem structures (described in further detail below).

The habenula is present in all vertebrates (Ramón y Cajal, 1894). The basic connections to and from the habenula are similar in primates and in ancient vertebrate species such as the lamprey and hagfish, indicating a strong evolutionary pressure that has conserved the habenular circuitry since its development around 530 million years ago (Stephenson-Jones et al., 2012). Put into evolutionary perspective, the first trees developed around 400 million years ago and flowering plants around 140-250 million years ago, long after the emergence of the habenula in vertebrates.

2.1 Habenular asymmetry

In most species, the habenula displays left–right asymmetry, with regards to its size, connectivity and gene expression patterns (Concha and Wilson, 2001). In mammals this asymmetry is not as striking as in fish, amphibians and reptiles, but recent reports suggest a modest enlargement of the left habenula in humans (Ahumada-Galleguillos et al., 2017). In zebrafish, it has been demonstrated that the left habenula is excited by visual stimuli while the right habenula responds predominantly to odours (Dreosti et al., 2014). The significance of this anatomical and functional lateralization of the habenular circuitry re-

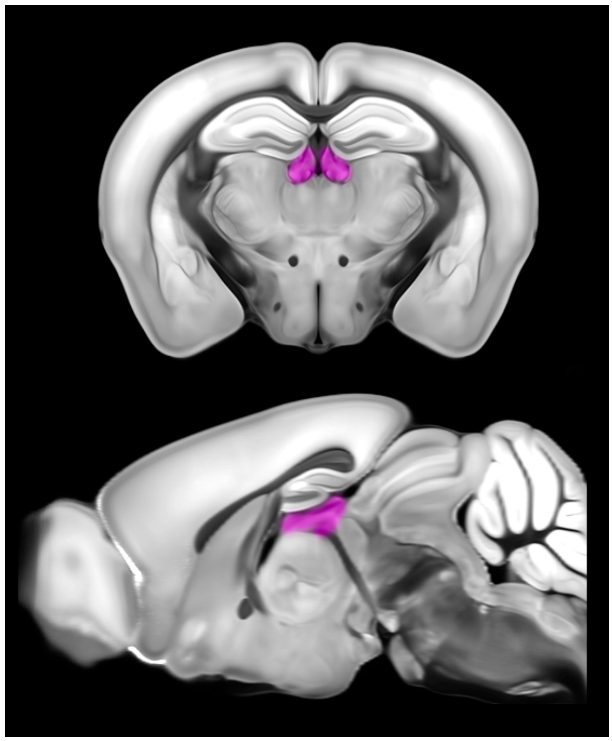

Figure 2: Location of the habenula in the mouse brain
Location of the habenula (magenta) in coronal (top) and sagittal (bottom) sections of a mouse brain. (Image courtesy: Allen Mouse Brain Atlas)

mains unclear, but it should be recognized in future studies so that effects that may only be observed unilaterally are appreciated.

2.2 Sub-nuclear organization and anatomy

It has long been recognized that the habenula consists of two distinct medial and lateral divisions, clearly distinguished by a much higher cellular density in the medial habenula than in the lateral habenula. The connectivity patterns of the two divisions are also distinct. The medial habenula receives input primarily from the bed nucleus of the anterior commissure, septofimbrial nucleus, triangular septum, medial septum and diagonal band of Broca, all located in the forebrain (Qin and Luo, 2009). In some non-mammalian species, the medial habenula receive input directly from primary sensory structures while it appears that a shift towards a more integrated input has occurred in mammals (Grillner et al., 2017; Guglielmotti and Cristino, 2006). The main target of the medial habenula in all vertebrates is the interpeduncular nucleus (IPN) (Grillner et al., 2017; Herkenham and Nauta, 1979; Nauta, 1958). It is a midline structure at the ventral surface of the midbrain rich in inhibitory

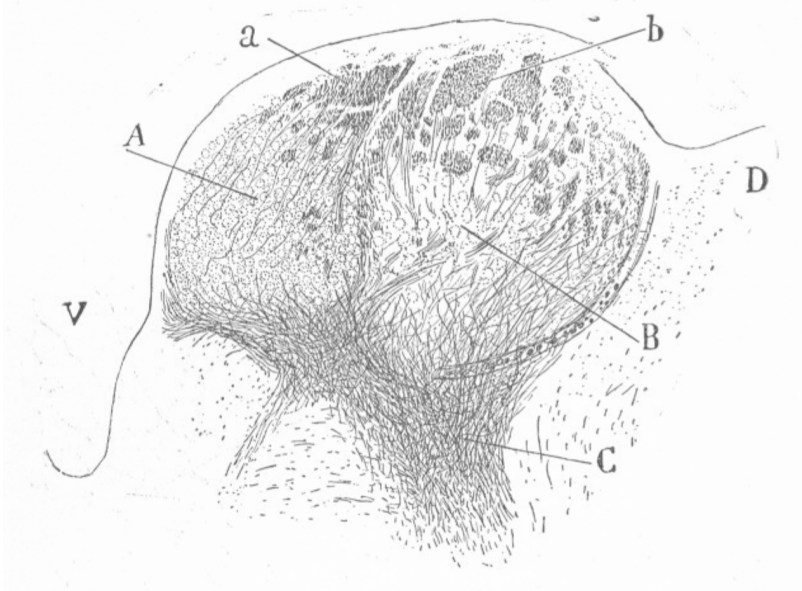

Figure 3: Habenula of the rabbit
Illustration of the habenular nuclei by Ramón y Cajal. The habenula lies lateral to the third ventricle (V) and juxtaposed to the thalamus (D). It consists of a medial (A) and lateral (B) division. The habenula receives its main input via the stria medullaris (a, b) and the axons of the habenular neurons travel towards the ventral midbrain and brainstem via the fasciculus retroflexus (C). (Image courtesy: Ramón y Cajal (1894))

GABAergic neurons. The IPN targets both forebrain areas such as the hippocampus, diagonal band of Broca, septum and preoptic area as well as brainstem areas such as the pontine central grey, dorsal raphe and dorsal tegmentum (Morley, 1986; Shibata and Suzuki, 1984).

Given the small size of the habenula, there is a remarkable number of subdivisions readily distinguishable by differences in gene and protein expression as well as morphological criteria (Andres et al., 1999; Geisler et al., 2003; Pandey et al., 2018). Two major populations of neurons form the majority of the medial habenular cells. The dorsal division can be identified by expression of tachykinin 1 (precursor to substance P) and targets the lateral subnucleus of the IPN (Cuello et al., 1978) (note that the in the reference, the target is misidentified as the ventral tegmental area). The ventral division include a large population of cholinergic neurons producing axons that travel in an enigmatic spiraling pattern through the IPN before terminating in the central subnucleus (Bianco et al., 2008).

Apart from these populations, there are smaller groups of neurons identifiable by expression of interleukin 18 (Sugama et al., 2002) and the μ-opiod receptor (Aizawa et al., 2012).

Most if not all medial habenular neurons produce glutamate and are excitatory (Aizawa et al., 2012). It has been demonstrated that the cholinergic neurons in the habenula co-release acetylcholine and glutamate from the same neurons onto the interpeduncular neu-

rons (Ren et al., 2011). Interestingly, different intensity and pattern of neuronal firing give rise to differences in the transmitters released, implying that the neurochemical phenotypes of habenular neurons are more fluid and dynamic than previously recognized.

The lateral habenula can be subdivided in up to ten subnuclei using morphological and cytochemical criteria (Andres et al., 1999; Geisler et al., 2003; Wagner et al., 2014b). It receives its main input from a continuous band of neurons stretching from the lateral preoptic area to the lateral hypothalamic area (Herkenham and Nauta, 1977; Aizawa et al., 2013; Yetnikoff et al., 2015). Other prominent afferents arise in the basal ganglia (globus pallidus pars interna / entopeduncular nucleus), nucleus of the diagonal band of Broca as well as the ventral tegmental area (VTA) and median raphe nucleus. Most neurons in the lateral habenula appear to be excitatory based on the high expression of the vesicular glutamate transporter 2 and 3 (Aizawa et al., 2012; Herzog et al., 2004). The main efferent connections of lateral habenular neurons target brainstem areas including the rostromedial tegmental nucleus, the median and dorsal raphe and the pontine central grey (Quina et al., 2014). There appears to be a substantial degree of overlap between the brainstem targets of the lateral habenula and the IPN (Oh et al., 2014). The lateral habenula also exhibit minor projections to the VTA and the posterior and lateral hypothalamic areas (Herkenham and Nauta, 1979; Quina et al., 2014).

The complete forebrain-habenular-brainstem circuitry is collectively known as the dorsal diencephalic conduction and constitutes one of the major descending pathways in the brain (Sutherland, 1982).

2.3 Function

The overall inhibitory influence that the habenula exerts on serotonergic, noradrenergic and dopaminergic signaling in the ventral midbrain and the brainstem has long been recognized (Kalén et al., 1989b,a; Nishikawa et al., 1986). These monoaminergic brain stem areas produce projections that terminate in most areas of the brain, thus capable of excerting an (almost) global neuromodulatory influence. The influence that the habenula have on the transmission in the immensely branching monoaminergic systems may be a reason why the habenula can be involved in the multitude of brain functions and behaviors as described below.

Adaptive behavior and reward

Based on self-stimulation experiments in rats, it has long been recognized that the habenula constitutes part of the affective circuitry of the brain (Sutherland and Nakajima, 1981). In 2007, it was shown in single-cell recordings in monkeys that lateral habenular neurons respond to omissions of expected rewards as well as unexpected aversive stimulation,

producing an inverse image of the famous *reward prediction error* responses observed in dopaminergic neurons in the VTA (Matsumoto and Hikosaka, 2007). This finding led to renewed interest in the role of the lateral habenula in reward and adaptive behavior. Subsequently, using a recently developed technique for neuronal stimulation (optogenetics) it was demonstrated that activation of habenular neurons produce strong aversive responses in mice and rats (Stamatakis and Stuber, 2012; Shabel et al., 2012). Similarily, inhibition of the habenula by stimulating inhibitory input from the VTA to the habenula produce the opposite effect (Stamatakis et al., 2013). At least a part of the aversive response produced by habenular stimulation is conveyed by a newly identified nucleus in the brainstem, the rostromedial tegmental nucleus, which receives strong innervation from the lateral habenula (Jhou et al., 2009b; Stamatakis and Stuber, 2012). This nucleus contains inhibitory GABAergic neurons that mainly target midbrain and brainstem areas such as the VTA, medial and laterodorsal tegmental nucleus, dorsal raphe and locus coeruleus.

Experiments imply that the habenula may use this reward information in order to dynamically adapt behavior in response to sub-optimal outcomes, especially in stressful and demanding conditions (Thornton and Davies, 1991; Baker et al., 2015, 2016; Baker and Mizumori, 2017). One function of the lateral habenula may be to compare information about the current response outcome (from prefrontal cortical areas), with information of the current internal state (from subcortical areas) and update behavior accordingly through manipulation of the monoaminergic VTA and dorsal raphe (Thornton and Evans, 1982; Mizumori and Baker, 2017).

Stress

Many acute stressors (restraint stress, swim stress, novel environment, injection of lithium chloride) and chronic stressors (chronic social stress) increase the activity of lateral habenular neurons (Wirtshafter et al., 1994; Chastrette et al., 1991; Matsuda et al., 1996). Activated neurons (as measured by up-regulation of the immediate early gene cFos) are primarily located in the medial part of the lateral habenula, and especially concentrated in the parvocellular subnucleus (Wirtshafter et al., 1994). Chronic treatment with imipramine, a tricyclic antidepressant, does not however antagonize the up-regulation of cFos after acute swim stress (Duncan et al., 1996).

Animals under high cognitive demand show higher stress levels after blocking excitatory input to the lateral habenula (Mathis et al., 2017). This implies that one role of the lateral habenula may be to adapt behavior in stressful situations, rather than just promoting an aversive response. Furthermore it has been shown that cognitive deficits due to habenular lesions are accentuated during stress (Thornton and Evans, 1982; Thornton and Bradbury, 1989; Thornton et al., 1990).

Aggressive behavior

Different subnuclei within the habenular complex of zebrafish regulate behavior in social conflicts differently (Chou et al., 2016). The probability of winning a social conflict was increased by inactivation of the medial dorsal habenula while it was decreased by inactivation of the lateral dorsal habenula.

Aggression-related reward in dominant mice appears to be regulated by a GABAergic projection from the basal forebrain (shell of the nucleus accumbens, diagonal band of Broca and septum) to the lateral habenula (Golden et al., 2016). Inactivation of this pathway increases attack severity in aggressive mice, but also potentiates non-social rewarding experiences such as cocaine administration, indicating a general reward potentiating effect.

Circadian rhythms and sleep

A separate line of research has implicated the habenula in regulation of circadian rhythms and sleep (reviewed in Baño-Otálora and Piggins, 2017). Many organisms dynamically adapt their behavioral repertoar depending on the time of day, i.e physiological and behavioral processes are influenced by the ~24 hour circadian rhythm. The expression of cFos in the medial division of lateral habenula in rats, is highest during the day (inactive period) and subsides during the night (active period) (Chastrette et al., 1991). The same neuronal population appears to express the clock gene PER2 in a circadian pattern that is independent of external cues. The presence of circadian regulated neurons in the lateral habenula indicates that diurnal information might be used by the habenula for optimizing behavior.

Lesions of the habenula or the fasciculus retroflexus disrupts rapid eye-movement sleep (REM), a phenomenon that might be mediated through downstream effects on the serotonergic raphe nuclei (Valjakka et al., 1998; Aizawa et al., 2013). Interestingly, REM sleep disruption is commonly observed in depressed individuals.

2.4 Habenula in depression

The habenula appears to partake in a range of brain functions that are commonly disrupted in depression. Many studies have thus been conducted to investigate if differences in habenula structure and function can be observed in patients suffering from depression. This question has also been addressed in a large number of preclinical studies employing different animal models of depression.

Clinical studies

Volumetric changes of the habenula in depression

The brain is a plastic organ that dynamically adapts to fluctuations in the internal and external environment (McEwen, 2012). Such adaptations include structural modifications of neurons, including dendritic branching, changes in synaptic density and proliferation of neurons, glia and endothelium, which may lead to volumetric changes in specific brain areas. A post-mortem study of volumetric differences between a mixed sample of depressed individuals (bipolar and major depressive disorder) and matched controls found a decreased volume of the medial and lateral habenula in the right hemisphere (Ranft et al., 2010). Using 3T MRI, one study found a decrease in bilateral habenula volumes in non-medicated patients with bipolar depression compared to healthy controls (Savitz et al., 2011). In the same study, a decrease in volume was observed in the right habenula in female patients with MDD. A recent 3T MRI study comparing habenula volumes of healthy volunteers and MDD patients could not reproduce this finding, although no sex-specific stratification was performed (Lawson et al., 2016). A study of habenula volumes at different stages of MDD detected a small increase of habenular white matter volume in medicated female patients with first-episode MDD. Apart from this finding, no other effects could be observed (Carceller-Sindreu et al., 2015). In non-medicated, but not in medicated, patients with MDD, a significant correlation between depressive symptom severity (as measured by HAMD-17 and BDI-II scores) and habenula volume was observed in a study employing high-field (7T) MRI (Schmidt et al., 2017). No group differences could be detected between the MDD patients and the controls however. Another study using 3T MRI detected an increase in left habenular volume in non-medicated MDD patients, and also found a positive association between left habenular volume and anhedonia severity (Liu et al., 2017).

In summary, studies investigating volumetric differences in habenular volume in MDD patients have yielded conflicting results and future studies should be carried out with larger study samples including variables such as disease severity, medication status, sex and brain hemisphere.

Habenular function in depression

As mentioned above, in patients that respond to antidepressive serotonin reuptake inhibitors, tryptophan depletion can elicit depressive symptoms. A small study investigated the effect of tryptophan depletion on habenular blood-flow (using positron emission tomography, PET) in MDD patients in remission (Morris et al., 1999). Habenular blood-flow was negatively correlated with plasma tryptophan levels and positively correlated with severity of depressive symptoms. Covariation between the habenular and the serotonergic dorsal raphe blood-flow was evident in patients with large increases in depressive symptoms after tryptophan depletion. Another study of tryptophan depletion in MDD patients in

remission using functional magnetic resonance imaging (fMRI) did not observe an effect on mood in either patients or controls (Roiser et al., 2009). However, an increase in left habenular blood-oxygen-level dependent (BOLD) signal was observed in MDD patients but not in control subjects.

Using fMRI, an increase was observed in habenular BOLD signal at presentation of a cue signaling an imminent electric shock in healthy volunteers while in MDD patients the BOLD signal instead was decreased (Lawson et al., 2016). This finding implies a disrupted habenular function in MDD patients during processing of aversive information, a dysfunction that could inhibit avoidance of negative stimuli.

Using a task with monetary gain or loss, one study found attenuated BOLD reactivity of the left habenula of MDD patients compared to controls (Furman and Gotlib, 2016). Similarly, in another fMRI study of reward processing, a trend towards blunted response in the left habenular BOLD signal in MDD patients during reward or punishment feedback was observed (Liu et al., 2017).

Patients with treatment resistant depression show decreased white matter integrity (fractional anisotropy) in afferent fibers to the right habenula compared to responders (Gosnell et al., 2018). The same study also reported differences between responders and non-responders in the functional connectivity between the habenula and brain–stem areas including the median raphe and locus coeruleus.

Infusion with ketamine, an NMDA receptor antagonist which has recently gained interest as a rapid acting antidepressant, reduce glucose metabolism in the right habenula of unmedicated treatment resistant MDD patients (Carlson et al., 2013).

In a patient with severe treatment-resistant MDD implanted with bilateral deep brain stimulation electrodes in the habenula, remission was achieved after 4 months of high-voltage stimulation. The patient remained in remission until the stimulation was accidentally discontinued whereupon the patient relapsed. Remission was again achieved after 3 months of continued stimulation (Sartorius et al., 2010). Whether the disease time-course of this patient is best explained by a real antidepressive effect of habenular DBS or the cyclic nature of the disease, remains to be determined.

Most of the studies investigating habenular function in MDD patients have been small, which precludes any definite conclusions to be drawn. Nonetheless, the results of these experiments indicate that the habenular function might be disrupted in MDD and that laterality could be an important factor.

Preclinical studies

In contrast to the meager results obtained from MDD patients, there is strong support of habenular dysfunction in studies employing animal models of depression.

An early study investigating metabolic changes (using ^{14}C-2-deoxyglucose autoradiography) in three different rat models of depression found robust increases of lateral habenular metabolism in all models (Caldecott-Hazard et al., 1988). The increase in metabolism was prevented by pretreatment with tranylcypromine, a monoamine oxidase inhibitor used in the clinical treatment of MDD. Many studies have since replicated the finding of habenular hyperactivity in rodent models of depression.

A common model for depressive–like behavior in rodents is the learned helplessness model. The animals are subjected to uncontrollable and inescapable mild foot-shocks. After this initial conditioning, the animals are again subjected to foot–shocks, but with a possibility to escape. Animals that display learned helplessness do not act on this escape opportunity.

Using PET to measure glucose utilization, an association between habenular metabolism and learned helplessness behavior have been demonstrated (Mirrione et al., 2014).

Similarly, an electrophysiological study investigating the lateral habenular neurons projecting to the VTA, showed an increased spontaneous activity in these cells, that was positively correlated with the degree of helpless behavior (Li et al., 2011). Deep brain stimulation of the lateral habenula was shown to ameliorate helplessness in the learned helplessness paradigm. The deep brain stimulation protocol employed (130Hz bursts) was shown to lead to a suppression of excitatory synaptic activity in these cells that returned to normal levels at cessation of the stimulation.

In a rat strain that have been continuously bred for helpless behavior (congenitally helpless rat), multiple studies have shown an increase in habenular metabolism (Shumake et al., 2003; Shumake and Gonzalez-Lima, 2013). Interestingly, a decreased habenular metabolism was observed in rats treated with the common antidepressive medication fluoxetine (Shumake et al., 2010). In one study of the congenitally helpless rat strain, an up-regulation of the β isoform of Ca^{2+}/calmodulin-dependent protein kinase II (β-CamKII) was observed in the lateral habenula (Li et al., 2013). This finding was reproduced in the acute learned helplessness model as well as in the chronic unpredictable stress model of depression. The protein levels of β-CamKII was reduced after treatment with imipramine, a tricyclic antidepressant. Over-expression of β-CamKII in the lateral habenula of wild-type mice and rats increased spontaneous spiking rates in the habenular neurons and induced depressive-like behavior. Knock-down of β-CamKII produced the opposite effect, leading to reduced depressive-like behavior. The downstream effects of β-CamKII include α-amino-3-hydroxy-5-methyl-4-isoxazolepropionic acid (AMPA) receptor upregulation, which is a

major component in glutamatergic (excitatory) signaling, explaining the potentiation of these neurons. In the congenitally helpless rat strain, a shift towards a more glutamatergic phenotype was observed in glutamate/GABA co-releasing neurons in the entopeduncular nucleus projecting to the lateral habenula (Shabel et al., 2014). This shift could be normalized by administration of the serotonin reuptake inhibitor citalopram.

Neuronal hyper-excitability in the lateral habenula may also be induced by local inhibition of the glial glutamate transporter GLT-1 (Cui et al., 2014). This leads to reduced clearance of glutamate from the synaptic cleft and increased glutamatergic signaling. In mice, this affects various behaviors linked to depressive like behavior, including disrupted rapid-eye movement sleep, which is a symptom commonly observed in patients with MDD.

Mice with learned helplessness exhibit hyper-excitability of lateral habenular neurons (Lecca et al., 2016). This hyper-excitability is partly due to reduced $GABA_B$-receptor signaling, mediated by de-phosphorylation of a serine residue on the receptor. Interestingly, local inhibition of $GABA_B$ de-phosphorylation in the habenula, leads to amelioration of depressive like behavior in this mouse model.

A subset of habenular neurons target the caudal dorsal raphe (Quina et al., 2014), a brain stem area in which the serotonergic signaling increase after in-escapable compared to escapable foot-shocks (Amat et al., 2001). Lesioning the habenula prevents the surge of serotonin in this area.

In conclusion, lateral habenular signaling is potentiated in rodent models of depression, mediated by both increased excitatory (glutamatergic) and decreased inhibitory (GABAergic) tone. The habenular dysfunction in depression appears to affect both serotonergic (caudal dorsal raphe) and dopaminergic (VTA) systems.

3 G protein–coupled receptor 151

G protein–coupled receptors (GPCRs) comprise a large family of transmembrane receptors with around 800 different members in humans (Fredriksson et al., 2003). Although a variety of signaling pathways have been identified in this class of receptors, the principal pathway acts via second messenger systems mediated by interaction between the GPCR and a small protein complex known as the G protein. Upon interaction with an extracellular ligand molecule, the conformation of the GPCR changes which allows activation of intracellular G proteins. The activated G protein mediates downstream effects which range from changes in intracellular ion concentration to regulation of gene expression. Members of the GPCR family are often targeted for drug development, around 34% of drugs approved by the federal drug administration in the US, modulate GPCR activity (Hauser et al., 2017).

For some of the human GPCRs, the endogenous ligands have been identified while the majority remain "orphan".

In 2003 and 2004, three research groups independently discovered a new GPCR in the human, mouse and rat (Berthold et al., 2003; Ignatov et al., 2004; Vassilatis et al., 2003). Although initially assigned different names (Gpr151, PGR7, GALR4, GPCR-2037, and galanin-receptor like), the receptor will in this thesis be referred to as Gpr151 (Fig. 4).

During embryonic development, Gpr151 appears to be expressed in a variety of subcortical brain structures and cranial nerve nuclei but in the adult organism the transcription in the central nervous system is largely restricted to the habenular nucleus (Ignatov et al., 2004) (Fig. 5). Some additional areas, most notably the paraventricular and central thalamic nuclei exhibit a much lower expression in the adult brain. Gpr151 evolved from a common ancestor of allatostatin, kisspeptin and galanin receptors (Liu et al., 2010). In a doctoral thesis of Qin (2011), the first investigation of Gpr151 protein expression was performed in which Gpr151 expression was reported in glutamatergic medial habenular neurons projecting towards the IPN. This pattern of Gpr151 protein expression was confirmed and extended in our work (Broms et al., 2014), described further in this thesis.

The protein sequence of Gpr151 is most similar to that of the members in galanin receptor family, GalR1, GalR2 and GalR3 (~16% identity, ~30% similarity). The similarity to

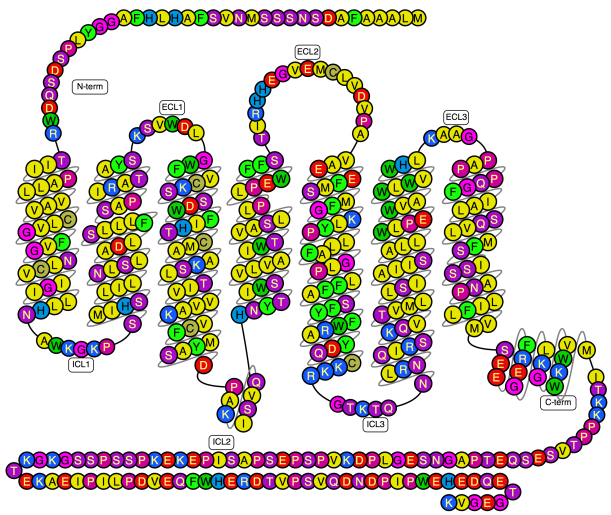

Figure 4: Amino acid sequence of human Gpr151.
The secondary structure of the Gpr151 protein, were the color of each amino acid reflects its chemical property. The protein starts with the amino-terminus (N-term) which is located at the extracellular side of the cell membrane. The amino acid chain then transverses the membrane seven times, forming intracellular (ICL) and extracellular (ECL) loops before terminating intracellularly with the carboxyl-terminus (C-term). (Image courtesy: GPCRdb.org)

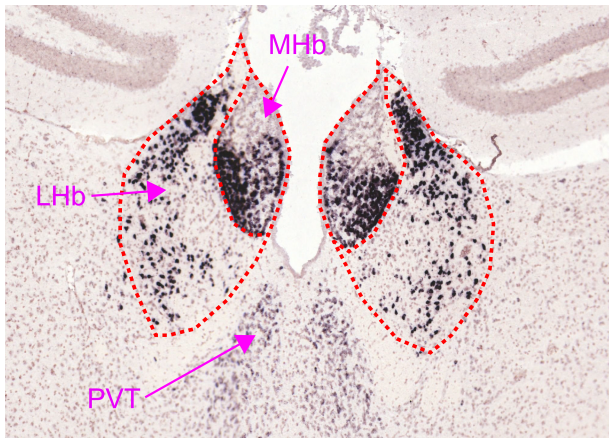

Figure 5: Gpr151 mRNA expression.
Visualization of Gpr151 mRNA using *in situ* hybridization in a coronal section through the diencephalon of an adult mouse. The expression of Gpr151 is enriched in the ventral part of the medial habenula (MHb) and in the lateral habenula (LHb). A weak expression is also detectable in the paraventricular nucleus (PVT). (Image courtesy: Allen Mouse Brain Atlas)

galanin receptors could indicate that the endogenous ligand of Gpr151 is a peptide resembling galanin, which is a neuropeptide involved in diverse functions such as cognition, sleep, nociception, energy metabolism and reproduction (Mechenthaler, 2008). This hypothesis has been explored in assays measuring ligand–induced Gpr151 activation by quantifying induced second messenger production (Ignatov et al., 2004; Qin, 2011; Fontes, 2015). Although Ignatov et al. (2004) observed a weak activation of Gpr151 during incubation with galanin, this was at non-physiological micromolar ligand concentrations. Recently, a large high-throughput screening effort at Scripps Research Institute (Florida, USA) was initiated aiming to find small molecule modulators of this receptor. The interest in this receptor stems from the restricted expression pattern in the habenula, and the potential of serving as a target for treating psychiatric conditions.

Kobayashi et al. (2013) was first to publish a study that investigated the function of the Gpr151 population. They performed selective ablation of Gpr151-expressing neurons in mice and ran an extensive array of behavioral tests in order to detect phenotypic deficits. The ablated mice showed signs of compulsive and impulsive behavior, failure to habituate to repeated exposure to a novel environment, increased anxiety and strong devaluation of rewards that require waiting or physical effort. Additionally, the ablated mice displayed a dampened response to nicotine, which may be attributed to the high concentration of nicotine receptors in the medial habenula.

The sensitivity to nicotine has also been investigated in mice where the *Gpr151* gene has been excised (Fontes, 2015). The Gpr151 knockout mice show a higher sensitivity to nicotine compared to controls, and also exhibit increased anxiety and somatic withdrawal symptoms

at cessation after chronic nicotine administration.

In a study in zebrafish, Chou et al. (2016) investigated how silencing of a Gpr151 expressing population in the medial part of the dorsal habenula (dHbM) influenced aggressive behavior. The dHbM-silenced fish showed increased aggressive behavior and was more likely to win fights.

Outside of the central nervous system, *Gpr151* expression can also be detected in dorsal root ganglia (Ignatov et al., 2004; Holmes et al., 2017). A strong upregulation of *Gpr151* mRNA was observed in a nerve injury model of neuropathic pain (Holmes et al., 2017). However, Gpr151 knockout mice do not display any changes in pain-related behaviors compared to wild-type controls. The significance and function of *Gpr151* expression in the dorsal root ganglia remains to be determined.

A recent study found that a predicted loss-of-function variant in the Gpr151 gene protected against obesity and diabetes in humans (Emdin et al., 2018). This finding indicates a role of Gpr151 in metabolic control.

Aims of the thesis

The general aim of this thesis was to characterize populations of neurons in the habenula that have importance for understanding and treating psychiatric disease, with a special focus on Major Depressive Disorder. Specific aims for each research paper are listed below.

I Characterize the protein expression pattern of Gpr151.

II Map the inputs to the Gpr151-expressing neuronal population.

III Investigate potential neuropeptide ligands to Gpr151.

IV Detect and characterize habenular GABAergic neurons.

Materials and methods

4 Description of materials and methods employed in this thesis

For full details on the experimental procedures, please see the corresponding materials and methods section of each paper.

4.1 Animals

Mice and rats were housed with *ad libitum* access to standard lab chow and water in a room air conditioned at 22°C–23°C with a standard 12 hr light/dark cycle (lights on 7:00 am, off 7:00 pm). A maximum of five mice or three rats were housed per cage. All animals had reached adult age (>8 weeks old) when included in the experiments. Gpr151 knockout mice ($Gpr151^{tm1Dgen}$; paper I), where a lacZ reporter gene was inserted in place of the Gpr151 exon, were obtained from Deltagen (San Mateo, CA, USA). They were backcrossed to C57BL/6J for eight generations. Wild type C57BL/6J mice and Gad2-IRES-Cre mice (paper III) were obtained from The Jackson Laboratory (Bar Harbor, ME, USA). Wild-type Crl:WI Wistar rats were obtained from Charles River (Sulzfeld, Germany)

4.2 Stereotaxic surgery

In two experiments (papers II and IV) we used stereotaxic surgery to make local injections of adenoassociated virus (AAV) in the habenula of mice. Using a three dimensional coordinate system, intracranial injections can be made with high precision. The mice were anesthetized with isoflurane and placed in a stereotaxic frame. The scalp was locally anesthetized with bupivacaine, the scull exposed, and a craniotomy was made using a dental drill. A glass pipette pulled to a small diameter was lowered into the habenula. A small amount (<1µl) of AAV vector was injected. Details about the viral constructs can be found in the papers. The pipette was left in place for three minutes before it was retracted, in order to prevent

backflow. The wound was sealed with tissue adhesive and the mice were returned to their home cages for recovery. The gene construct carried by the AAV vectors are inactivate by default, *i.e* no transcription occurs (Fig. 6). In presence of Cre recombinase, the construct becomes activated and available for constitutive transcription. Since Cre is transcribed under the control of specific promoters (Gpr151 in paper II and Gad2 in paper IV), the gene of interest will only be expressed by neurons in the vicinity of the injection in which these promoters are active. In paper II, the mice were reoperated after 21 days using the same procedure and injected with pseudotyped rabies virus for monosynaptic retrograde tracing.

4.3 Retrograde monosynaptic tracing with pseudotyped rabies virus

Rabies is a viral disease that affects the central nervous system and causes brain inflammation and almost always leads to death (Finke and Conzelmann, 2005). The rabies virus is transmitted by scratches or bites from an infected animal. Once inside the body, the rabies virus enters peripheral nerves and starts to travel in a retrograde fashion towards the central nervous system. A certain membrane protein – rabies glycoprotein (RG) – allows formation of new viral particles and enables it to cross synapses on its way to the brain. The unique characteristics of the rabies virus have been exploited for tracing neuronal circuitry (Etessami et al., 2000; Wall et al., 2010; Wickersham et al., 2007).

By deleting RG from the rabies genome, the rabies virus cannot form new viral particles, since budding from the host cell-membrane requires RG. By replacing RG with another

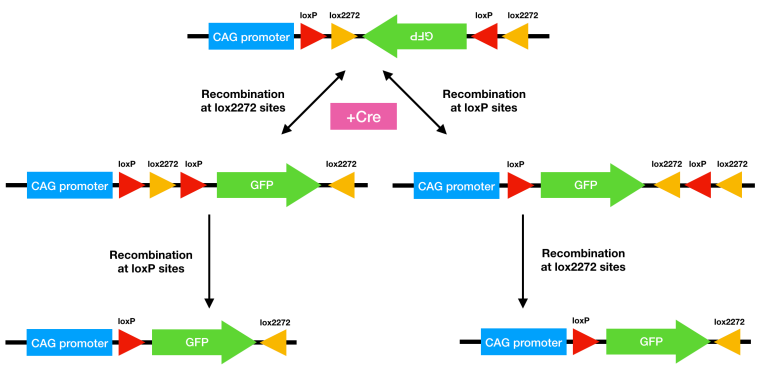

Figure 6: The double-floxed inverse open reading frame (DIO) construct.
The DIO construct has been developed to enable expression of a target gene, only in cells that also express Cre recombinase. The target gene (green fluorescent protein, GFP) is inserted in reverse orientation after a strong promoter (CAG). The target gene is flanked by two recombination sites (LoxP and Lox2272) on each end. Cre is capable of inverting the construct either by recombination between two LoxP sites or between two Lox2272 sites, but not between sites of different identity. After two subsequent recombinations, the resulting construct contains the target gene in forward orientation making it available for transcription.

envelope protein (EnvA) derived from an avian sarcoma leukosis virus, viral particles can again be produced. These modified EnvA-coated viral particles (pseudotyped rabies virus) are only capable of infecting cells expressing the avian sarcoma leukosis virus receptor (TVA receptor). Natively, all mammalian cells lack the TVA receptor, but it may be specifically expressed in certain cells using the Cre-Lox technique as described above (see section 4.2). When pseudotyped rabies virus is injected into the brain, it is thus only capable of infecting Cre-expressing neurons (Fig. 7). By also introducing the gene for RG into the same Cre-expressing neurons, these cells will allow retrograde transport when infected by the pseudotyped rabies virus. The viral particles exit through the dendrites of the Cre-expressing neurons and enter the presynaptic terminals of the afferent neurons. After traveling retrogradely along the axon of the afferent neuron, the viral particle reaches the cytosol where it cannot traverse additional synapses due to lack of RG expression in the afferent neuron. In addition, the pseudotyped rabies virus carries a gene for green fluorescent protein (GFP) which enables detection of the infected neurons. One week after injection of the pseudotyped rabies virus, the brains of the animals are removed and prepared for microscopy as described below (see section 4.4).

Thus, this ingenious method enables Cre-dependent, monosynaptic, retrograde mapping of the neurons that project onto Cre-expressing cells (Wall et al., 2010; Watabe-Uchida et al., 2012). In paper II, we used this technique to find the monosynaptic afferents to Gpr151 expressing neurons, using a Gpr151-Cre mouse line.

4.4 Fixation of mouse and rat brain tissue

Fixation is a (chemical or physical) procedure that terminates ongoing biochemical reactions thereby preventing decay and preserving the tissue. The animals were deeply anesthetized by injection of an overdose of pentobarbital. They were thereafter perfused transcardially with cold isotonic sodium chloride solution followed by buffered paraformaldehyde (PFA, 4%). The brains were then dissected and postfixed in 4% PFA for 24 hours at 4°C. After postfixation, the brains were immersed in sucrose solution (25% in PBS) at 4°C for 2-3 days until osmotic equilibration had occurred. The brains were sectioned in 30-40 µm sections using a sliding microtome (Thermo Scientific HM450), cryoprotected in antifreeze solution, and stored at -20°C until used for immunohistochemistry or *in situ* hybridization.

4.5 In situ hybridization using RNAscope®

In situ hybridization is a method for visualizing specific mRNA molecules in tissues or cells. We used a recently developed (Wang et al., 2012) improved *in situ* hybridization method called RNAscope®that allows specific and sensitive detection of the mRNA of in-

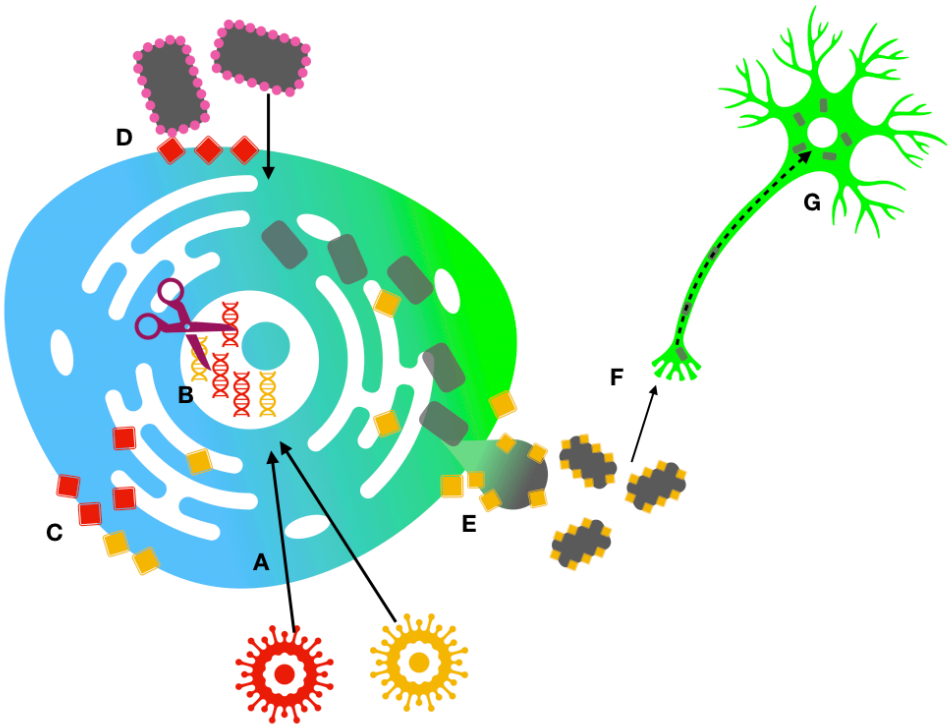

Figure 7: Monosynaptic tracing of afferent neurons using pseudotyped rabies virus.
Adenoassociated viral vectors (AAV) carrying genes for the avian sarcoma leukosis virus receptor (TVA; red) and rabies glycoprotein (RG, yellow) enter nerve cells in the vicinity of the intracranial injection (A). The gene constructs are activated by Cre-recombination (B; purple scissor), thus the expression of TVA and RG is targeted to Cre-expressing neurons only. TVA and RG protein is expressed on the cell surface (C). Two weeks later, a subsequent injection of pseudotyped rabies virus (grey) is made. The pseudotyped rabies virus lacks RG, which renders it incapable of cellular entry. Instead it is coated in a certain envelope protein (EnvA; pink), which allows it to selectively enter cells that express TVA. Upon TVA-mediated entry into the cell (D), the rabies vector starts replicating as well as producing green fluorescent protein (GFP; green). The host cell express RG on its surface and allow budding of new RG-coated rabies viral particles at the postsynaptic membrane (E). These viral particles are taken up into the presynaptic terminal of an afferent neuron (F) and transported retrogradely towards the cell soma. The rabies virus can then not propagate further due to the lack of RG in its genome. The rabies infected afferent neuron starts producing GFP, allowing it to be detected in a microscope (G).

terest (Fig. 8). In brief, either fixed brain sections were mounted directly onto glass during cryosectioning, or previously prepared free floating sections were taken from the freezer, washed in PBS and then mounted onto the glass slides. Pretreatment and amplification in RNAscope®2.5 HD Assay – BROWN or RNAscope®Fluorescent Multiplex Assay was carried out according to the manufacturer's instructions. This *in situ* hybridization assay was used to detect Gpr151 mRNA in paper II, Gpr151 and Spx mRNA in paper III, and Gad2 and Cre mRNA in paper III.

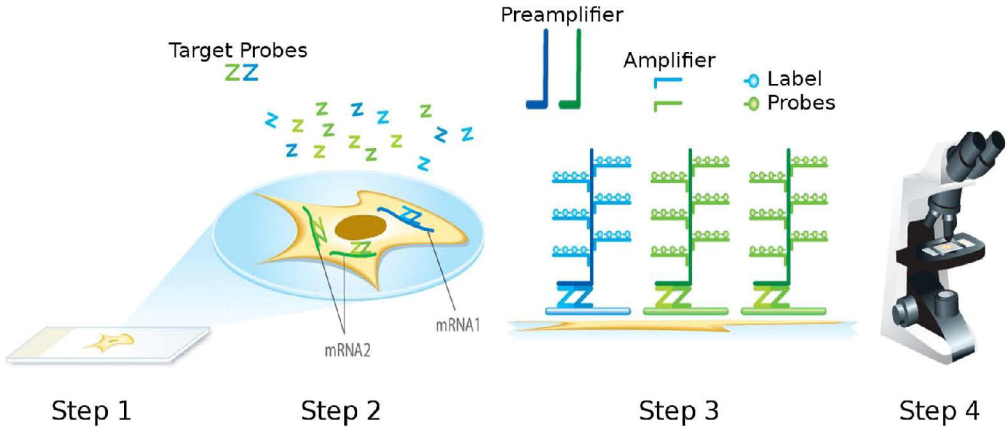

Figure 8: In situ hybridization using RNAscope®.
Step 1: Tissue is fixed and mounted onto microscope glass. Step 2: Specific Z-shaped probe pairs bind to the target mRNA (~20 such pairs are used to provide a strong signal). Step 3: Amplification probes labeled with peroxidase enzyme (for chromogenic detection) or fluorophores (for fluorescent detection) hybridize with the Z-pairs allowing detection of the mRNA. Step 4: The signal is detected using a microscope. Image source: Wang et al. (2012) License: Creative Commons BY-NC-ND 4.0

4.6 Immunohistochemistry of mouse and rat sections

Immunohistochemistry is a method for visualizing proteins in tissue using antibodies. After rinsing in PBS, free floating brain sections were incubated in blocking solution containing serum and detergent for 1 hour. The serum matched the species in which the secondary antibodies were raised. Sections were then incubated overnight at 4°C with primary antibodies diluted in blocking solution. Subsequently, sections were washed with PBS and incubated for 2 hours at room temperature with secondary antibodies (conjugated either with a fluorophore or biotin). Sections were then washed again in PBS and counterstained with the nuclear stain DAPI. The sections were finally mounted on Superfrost Plus glass and coverslipped.

For light microscopy, brain sections were incubated with a biotinylated anti-mouse secondary antibody made in horse (Vector Laboratories, Burlingame, CA, USA), followed by incubation with avidin-biotin-peroxidase complex (VECTASTAIN Elite ABC Kit, Vector Laboratories, Burlingame, CA, USA) and 3,3'-diaminobenzidine (DAB), producing a brown precipitate. Following the DAB reaction, sections were mounted, dehydrated in increasing concentrations of ethanol followed by xylene and finally coverslipped with DPX.

Confocal fluorescent images were acquired with a Zeiss LSM700 (Zeiss, Thornwood, NY; papers I, III) or a Nikon Eclipse Ti (Nikon Instruments Europe BV, Amsterdam, Netherlands; paper II) confocal microscope.

4.7 Preparation of zebrafish brain tissue

In paper I, we performed immunohistochemistry for detecting Gpr151 in zebrafish. Two adult zebrafish (7 months old, AB strain, kindly donated by Dr. Fredrik Ek) were rapidly chilled in ice cold water and subsequently immersed in PFA solution for 24 hours. The brains were then dissected and equilibrated in sucrose solution. Subsequently, the brains were incubated in PBS containing 7.5% gelatin and 20% sucrose at 37°C for 2 hours. The brains were then placed in gelatin-sucrose moulds and cut into blocks. The blocks were frozen and cut in 14 µm sections on a cryomicrotome and mounted on Superfrost Plus glass. Immunohistochemistry was performed as for mouse and rat sections except that incubation with Gpr151 antibodies was performed directly on the glass.

4.8 Colocalization analysis

In paper I, we performed colocalization analysis, to quantify the spatial overlap between different protein molecules. Two measures were used to determine the strength and robustness of colocalization. Manders' colocalization coefficients, M1 and M2, which are proportional to the number of colocalizing pixels in each channel relative to the total number of pixels in that channel were calculated (Manders et al., 1993). Costes' test for statistical significance was used to determine that the colocalization coefficients obtained were not due to random effects (Costes et al., 2004).

4.9 Antibody characterization

The antibodies used in the studies were carefully evaluated. Only antibodies with known specific binding to the protein of interest were chosen (verified in our lab, in prior publications or by the manufacturer). Valid methods for asserting specificity include lack of staining in knock-out animals, detection of the expected band in western blot and co-localization with previously validated antibodies.

Concentrations for optimal signal-to-noise ratio were obtained from the literature or determined by stainings with serial dilutions of the antibody. In all preparations, some sections were prepared identically except for omitting the primary antibody in order to ensure that the observed signal was not due to non-specific binding of the secondary antibody.

4.10 Fluo-4 calcium imaging

In the ligand screening experiments (see section 5.3), Fluo-4 calcium imaging was performed in a cell line expressing Gpr151 together with two G proteins (Gqi5 and G16) to

provide a functional readout for ligand-receptor interaction. Upon stimulation with ligand, a conformational change in the Gpr151 receptor would promote dissociation of the GPCR/G protein complex (by guanine nucleotide exchange). G16 is a G protein that associates non-specifically to a broad range of GPCRs (Offermanns and Simon, 1995), and elicit immobilization of intracellular calcium via the so-called Gq pathway when activated. Gqi5 is a chimeric G protein that allow Gi coupled receptors that normally signals through a cAMP depenedent pathway to instead act via the Gq pathway (Yokoyama et al., 2003). These cells are incubated in an assay solution containing the calcium indicator Fluo-4. The fluorescence of Fluo-4 is proportional to the concentration of intracellular calcium. This allows relative quantification of calcium concentration using a fluorescence microscope or plate reader.

Summary of papers

5 Summary of papers included in the thesis

5.1 Paper I

Conserved expression of the Gpr151 receptor in habenular axonal projections of vertebrates.

The mRNA of the orphan G protein–coupled receptor Gpr151 has been demonstrated to be highly enriched in the habenular nucleus of mice, rats and humans. In this paper the aim was to investigate the protein expression pattern of the Gpr151 receptor using immunohistochemistry to further characterize this population of neurons. Different polyclonal antibodies raised against the Gpr151 protein were obtained from commercial sources. Colocalization analysis with additional immunohistochemical markers was carried out to determine further phenotypical characteristics of the population. In order to assess the evolutionary conservation of the neurocircuitry expressing the receptor, zebrafish (a distant vertebrate relative to rodents and humans) was also investigated. In brief, we found that Gpr151 was heavily expressed in habenular axonal projections targeting midbrain and brainstem structures including the IPN, median and dorsal raphe, rostromedial tegmental nucleus, rhabdoid nucleus (also known as the interpedunculotegmental tract) and the dorsal tegmentum (Fig. 9). Colocalization analysis revealed associations between Gpr151 and choline acetyl transferase (ChAT), vesicular glutamate transporters and substance P in the target areas of the neurons. The Gpr151 protein expression pattern was remarkably similar in zebrafish indicating a strong evolutionary pressure on the conservation of this system in vertebrates.

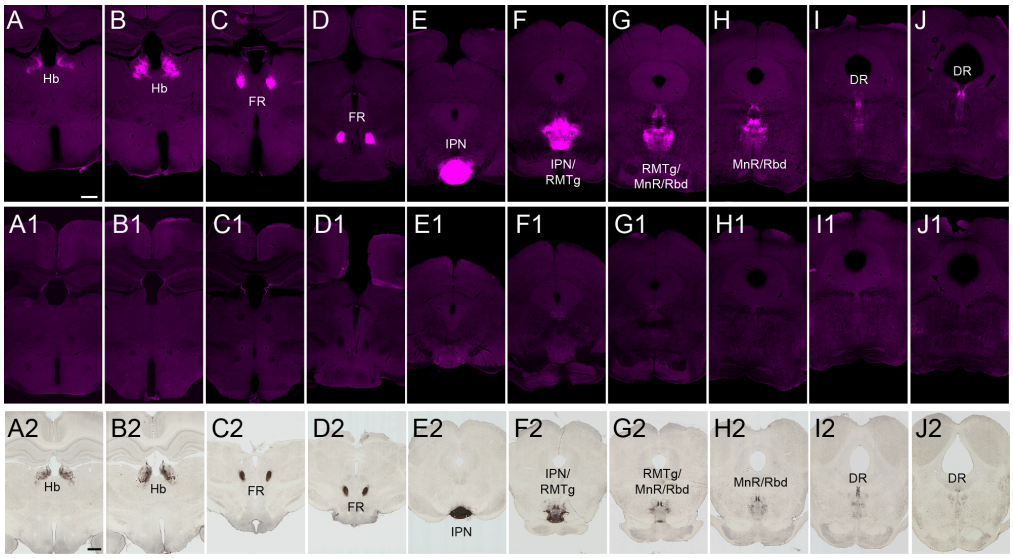

Figure 9: Gpr151 protein expression in the brain.
Immunohistochemical visualization of Gpr151 protein expression in coronal section of a wild-type mouse (A-J), Gpr151 knockout mouse (A1-J1) and Wistar rat (A2-J2).

5.2 Paper II

Monosynaptic retrograde tracing of neurons expressing the G-protein coupled receptor Gpr151 in the mouse brain.

The aim of this study was to extend the mapping of the Gpr151 expressing neurons in the brain to also include the incoming (afferent) connections to these cells. We performed monosynaptic retrograde tracing of Gpr151-expressing neurons using a pseudotyped rabies virus (SADΔG-eGFP(EnvA)). The SADΔG-eGFP(EnvA) vector is capable of transducing neurons expressing the avian sarcoma-leukosis virus receptor (TVA) and being transported retrogradely from these neurons if they also express the rabies virus glycoprotein (RG). Using a transgenic mouse line (Gpr151–Cre) and Cre dependent adenoassociated viral vectors we selectively expressed TVA and RG in Gpr151-expressing neurons. A subsequent injection of SADΔG-eGFP(EnvA) then caused infection of Gpr151 expressing neurons only. The SADΔG-eGFP(EnvA) was then transported monosynaptically to afferent neurons which could be visualized by their production of enhanced green fluorescent protein (eGFP). Using this system, we detected Gpr151 expressing neurons in the habenula, and also a subset of thalamic nuclei. The habenular Gpr151 neurons primarily received input from the diagonal band nucleus, medial septum, bed nucleus of stria terminalis, ventral pallidum, lateral preoptic area, lateral hypothalamic area and entopeduncular nucleus (Fig. 10). A population of Gpr151 expressing neurons in the paraventricular thalamic nucleus received input from many of the areas giving rise to habenular projections, but also some distinct pro-

jections from the zona incerta and medial preoptic area was evident. This population was demonstrated to project to forebrain areas including the medial prefrontal cortex, nucleus accumbens, zona incerta and basolateral amygdala. Third, a population of Gpr151 neurons in the lateral thalamic nucleus received input from areas linked to visual processing including the cingulate cortex, visual cortex, zona incerta and superior colliculus.

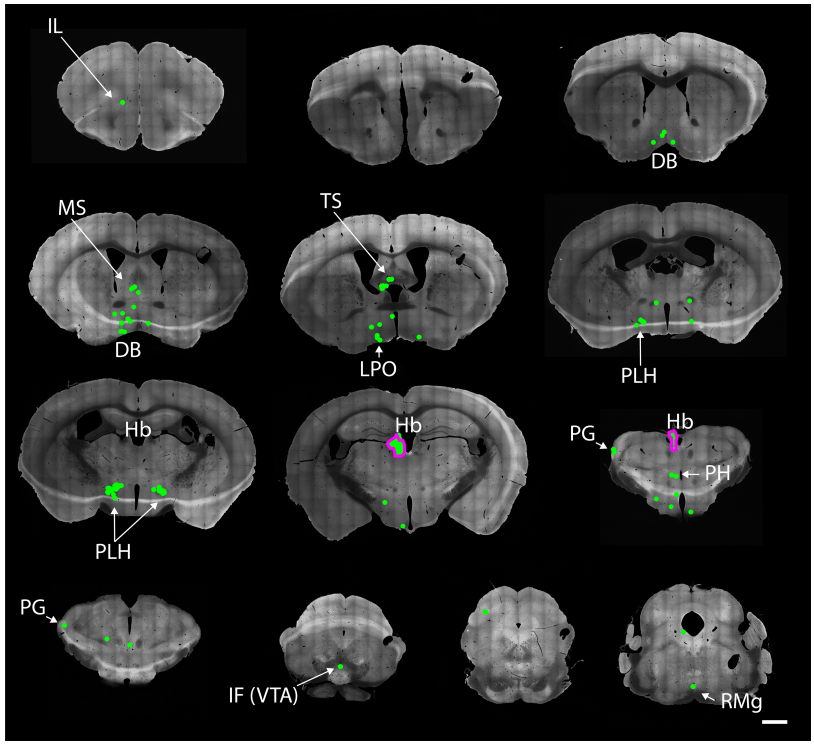

Figure 10: Afferents of habenular Gpr151-Cre neurons.
Coronal brain sections of a Gpr151-Cre mouse where AAV8-Ef1a-FLEX-TVA-mCherry, AAV8-CA-FLEX-RG and SADDG-eGFP(EnvA) was injected unilaterally in the habenula. Neurons coexpressing eGFP and mCherry (starter neurons; magenta outline) were almost exlusively located in the medial and lateral habenula. EGFP positive neurons (green) were found throughout the brain, most notably in the medial septal nucleus, nucleus of the diagonal band, lateral preoptic area, and the lateral hypothalamus (peduncular part). Scale bar = 1000 mm

5.3 Paper III

Investigating spexin and related neuropeptides as possible ligands of Gpr151.

In this work, the aim was to identify potential ligand candidates to Gpr151. Given the that Gpr151 has evolved from a common ancestor to the galanin receptor family (Liu et al., 2010), we focused on peptides which share resemblance with galanin, namely spexin and kisspeptin. Using *in situ* hybridization, we could observe low expression of *Spx* mRNA in *Gpr151* expressing habenular neurons. Receptor activation is usually assessed by measur-

ing the change in concentration of second messengers. However, the signaling pathway of Gpr151 is currently not known. In order to avoid having to guess the second messenger pathway of Gpr151 we took advantage of specific Gα-subunits (G16 and Gqi5) that couple unselectively to most G protein–coupled receptors and lead to activation of the inositol trisphosphate (IP3) / diacylglycerol (DAG) pathway, which ultimately immobilize intracellular calcium. The change in intracellular calcium concentration can then be measured with a calcium sensitive dye (Fluo-4). We thus obtained a commercially available cell line that expressed Gpr151 together with G16 and Gqi5. The cells were cultured on glass slides and incubated with Fluo-4. The fluorescence was monitored in an epifluorescence microscope while peptides of different concentrations were added to the wells. We could reproduce previously reported findings (Ignatov et al., 2004) that micromolar concentrations of galanin activate Gpr151 (Fig. 11). Similarly, spexin and kisspeptin also activated Gpr151 at high concentrations. However, concentrations of this magnitude are unlikely to occur naturally in the synapses were Gpr151 is present, and thus the tested peptides are probably not endogenous ligands to Gpr151.

5.4 Paper IV

***Gad2* expressing interneurons in the mouse habenula.**

In this study, we investigate the presence of GABAergic interneurons in the habenular nucleus of the mouse brain. Previous studies have identified cholinergic, substance P-ergic and glutamatergic projection neurons in the habenula. However, there has been little focus on the intrinsic connectivity in the habenula and the presence of GABAergic interneurons has been largely overlooked. Previous studies on GABAergic interneurons have yielded conflicting results. One study found GABA immunoreactive neurons in the habenula of the Squirrel monkey and another study using the same immunohistochemical technique found only very few GABA neurons in the rat. During the preparation of this manuscript, another research group identified GABA neurons in the lateral habenula by demonstrating co-expression of GABA, Gad65 and vesicular GABA transporter (VGAT) (Zhang et al., 2016, 2018). Using *in situ* hybridization and viral transduction in a knock-in mouse line, we could also observe a rich repertoire of Gad2 (one of two GABA synthesizing isoenzymes) expressing neurons in the lateral habenula, with different morphology and molecular characteristics (Fig. 12). Thus, we could replicate previous findings of the existence of *Gad2* expressing neurons in the habenula, but we also extend the characterization of these neurons to show that these cells may be further divided into sub-classes based on cellular morphology. This finding is important for the understanding of the habenular circuitry and adds to the complexity of this intriguing nucleus.

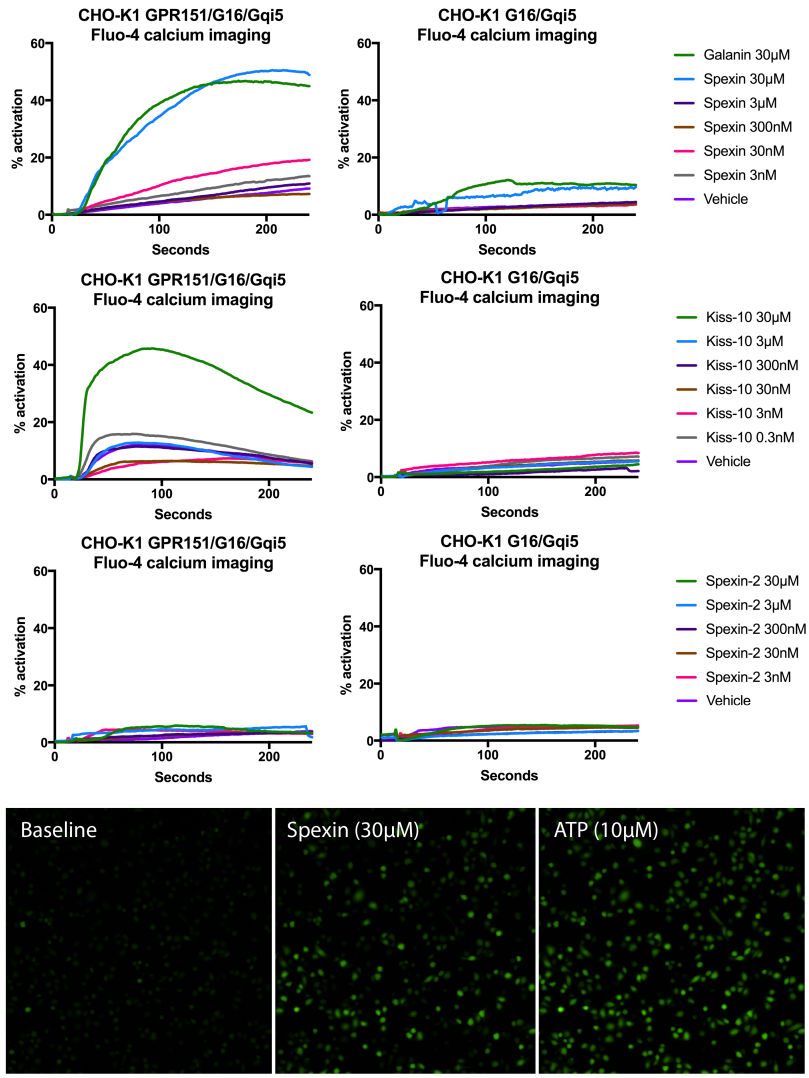

Figure 11: Fluo-4 calcium assay.
Receptor activation was measured as change in fluorescence upon peptide incubation, relative to the maximal response after incubation with 10μM ATP. Galanin, spexin and kisspeptin induced calcium mobilization at high concentrations (30μM) but not at lower concentrations. Spexin-2 did not produce any response.

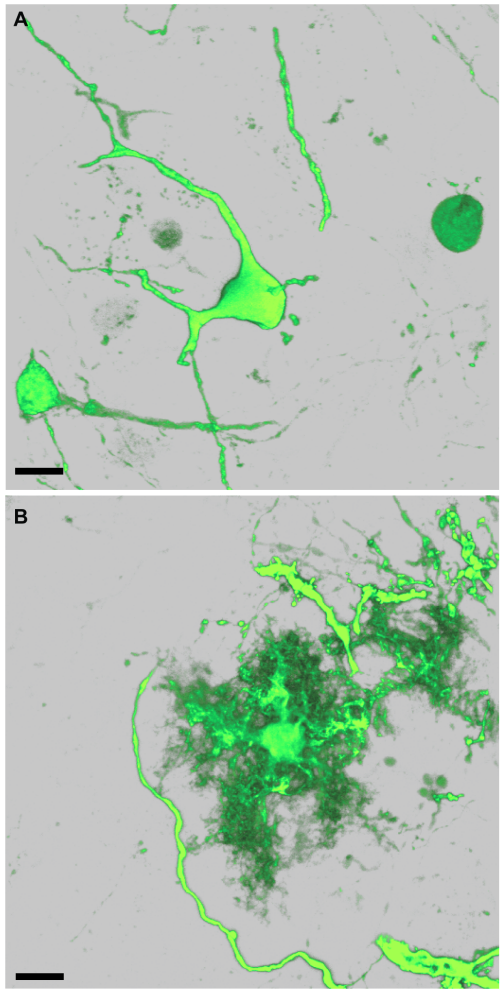

Figure 12: Examples of spherical and neurogliaform habenular interneurons.
3D reconstructions of habenular Gad2 expressing spherical neurons (A) and neurogliaform neurons (B). Scale bar = 10µm.

Discussion

The aim of the work described in this thesis was to extend the characterization of habenular neuronal populations and associated circuitry, with a special focus on the role of the habenula in depression.

6 Gpr151 expression in habenular targets in the midbrain and brainstem

Prior to our research, the orphan receptor Gpr151 was identified and its mRNA was found to be highly enriched in the habenula (Vassilatis et al., 2003; Ignatov et al., 2004; Berthold et al., 2003). The idea of taking advantage of this G protein–coupled receptor to *specifically* modulate habenular activity inspired our first study (see section 5.1) where the protein expression pattern of Gpr151 was investigated. Using a commercially available antibody and conventional immunohistochemistry, the expression of Gpr151 protein was assessed throughout the brain of mouse, rat and zebrafish. This comparative approach was adopted in order to assess the degree of conservation on a neuroanatomical level. In all of the examined species, strong expression of Gpr151 was observed in fibers originating in habenula, that travelled through fasciculus retroflexus and terminated in the IPN and a number of distinct brainstem nuclei (Fig. 13).

IPN

The IPN is one of the areas of the brain with the densest cholinergic innervation (Woolf and Butcher, 1985). These cholinergic fibers originate in the ventral medial habenula, basal forebrain areas including the nucleus of the diagonal band of Broca, preoptic area, medial septal nucleus, substantia innominata and nucleus basalis, as well as hindbrain areas including the laterodorsal- and pendunculopontine tegmentum. In Paper I (see section 5.1), we observed strong Gpr151 immunoreactivity in the cholinergic part of the medial habenula. We also performed colocalization analysis between choline acetyltransferase (ChAT) and Gpr151 immunoreactivity in the IPN, which confirmed the expression of Gpr151 in cholinergic

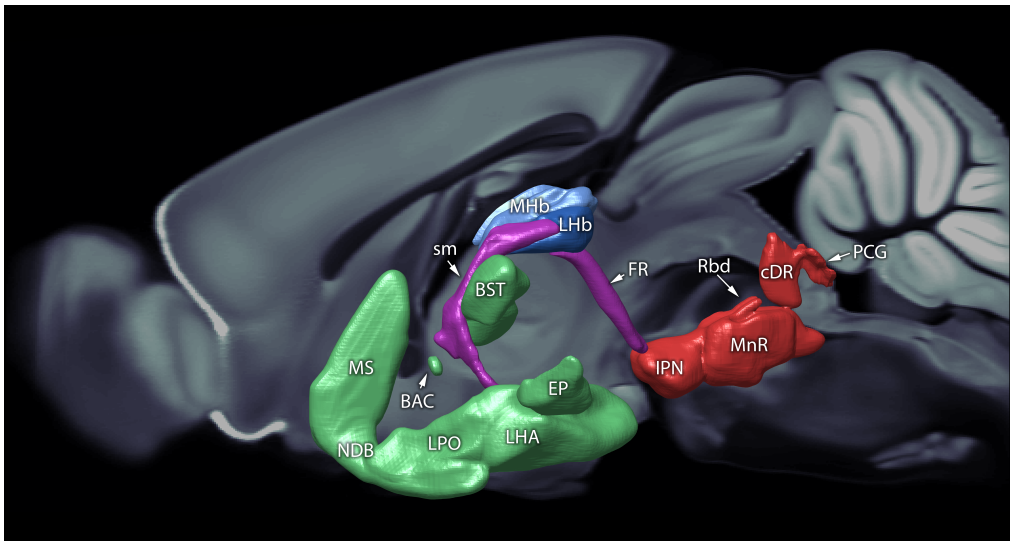

Figure 13: Connections of Gpr151-expressing habenular neurons in rodents.
Brain structures containing neurons that synapses onto Gpr151-expressing habenular neurons (green) include the medial septum (MS), nucleus of the diagonal band of Broca (NDB), lateral preoptic area (LPO), lateral hypothalamic area (LHA), bed nucleus of the anterior commissure (BAC), entopeduncular nucleus (EP) and the bed nucleus of stria terminalis (BST). The afferent fibers travel primarily in the stria medullaris (sm; purple) before reaching the medial and lateral habenula (MHb, LHb; blue). The efferent projections travel through the fasciculus retroflexus (fr; purple) in a ventral-caudal direction towards different brainstem areas (red) including the IPN (IPN), rostromedial tegmental nucleus, rhabdoid nucleus (Rbd), median (MnR) and caudal dorsal raphe (cDR) as well as the pontine central grey (PCG).

fibers. Cholinergic transmission in the IPN has been observed to modulate dopaminergic turnover in the nucleus accumbens and prefrontal cortex, areas highly involved in motivation and reinforcement learning (Nishikawa et al., 1986). Hyperactivity in the cholinergic habenulointerpeduncular pathway could thus be one potential factor contributing to the anhedonia observed in depression. Fontes (2015) observed that shRNA-mediated inhibition of Gpr151 expression in these fibers led to increased sensitivity to nicotine. Whether Gpr151 expression in the habenulointerpeduncular fibers plays any role in depressive like behavior is not known.

Rostromedial tegmental nucleus

The inhibitory influence that the lateral habenular nucleus exerts on dopaminergic neurons in the VTA (Christoph et al., 1986; Ji and Shepard, 2007) was long a mystery since the direct innervation of habenular neurons onto ventral tegmental neurons is quite sparse and mainly excitatory (Omelchenko et al., 2009). The missing link was then found a decade ago: the GABAergic mesopontine rostromedial tegmental nucleus (sometimes refered to as the tail of the VTA) receives its main input from the lateral habenula and sends *inhibitory* projections onto dopaminergic VTA neurons (Jhou et al., 2009b). Functionally, the the rostromedial tegmental nucleus has since been implicated in adaptation to adverse events

and avoidance behavior (Elmer et al., 2018; Stamatakis and Stuber, 2012; Jhou et al., 2009a). In Paper I (see section 5.1) significant protein expression of Gpr151 was observed in axon terminals in the rostromedial tegmental nucleus. This implies that modulation of Gpr151 may influence VTA dopamine circuitry, via this GABAergic relay.

Rhabdoid nucleus / interpedunculotegmental tract of Ganser

In 1882, the psychiatrist and neuroanatomist Dr. Sigbert Ganser, investigated the nervous system of the mole and identified a fiber tract that he named "die Haubenbahn des Ganglion interpedunculare" (Ganser, 1882). This tract, later referred to as the interpedunculotegmental tract of Ganser, displays strong acetylcholinesterase activity as well as substance P immunoreactivity and is nowadays regarded as a pathway between the IPN and the median raphe, dorsal raphe and the caudal central grey (Groenewegen et al., 1986). In our material (see section 5.1), we observed dense expression of Gpr151 in this tract and in the mentioned target areas. Since Gpr151 mRNA is mainly expressed in the habenula and not in the IPN, it can be concluded that some of the fibers of the interpedunculotegmental tract originate in the habenula. Some authors use the name *rhabdoid nucleus*, referring to the elongated (from Greek *rhabdoiedes* – "like a rod") shape of this structure (Paxinos and Watson, 2006). Whether this structure is best described as a proper nucleus or a fiber tract remains an open question. A recent paper suggests that axons from the interpeduncular neurons form synapses in the rhabdoid nucleus (Morton et al., 2018). It would also be interesting to investigate whether Gpr151 axons from the habenula form synapses within this structure.

Raphe nuclei

The median and dorsal raphe contain the majority of the serotonergic neurons in the brain. In the dorsal raphe, both serotonergic and non-serotonergic neurons area activated upon reward (Li et al., 2016). The median raphe has been implicated in anxiety (Andrade et al., 2013) and fear memory consolidation (Wang et al., 2015). The antidepressive class of substances known as the serotonin reuptake inhibitors (SSRIs) targets these systems and the raphe nuclei are thus highly interesting from a psychiatric viewpoint. Gpr151 protein expression was found to be exceptionally high in the median raphe, and to a lesser degree the dorsal raphe (see section 5.1). Additionally, Gpr151-expressing neurons in the habenula appeared to receive reciprocal innervation from these structures (see section 5.2). Recently, a study assessing the resting state functional connectivity between the habenula and raphe nuclei observed greater functional coupling in patients with treatment resistant depression (Gosnell et al., 2018). If Gpr151 is involved in modulating the activity in this circuitry, a Gpr151 ligand could have therapeutic effects for this group of patients, where effective treatment is currently lacking.

7 Convergence of basal forebrain input onto Gpr151 expressing habenular neurons

The retrograde tracing experiment described in paper II (see section5.2) was designed to investigate if Gpr151 positive neurons in the habenula received input from any *specific* brain area. This was however not the case. Instead, all areas that previously have been described as habenular afferent structures (Qin and Luo, 2009; Yetnikoff et al., 2015; Herkenham and Nauta, 1977), were found to contain neurons that contact Gpr151-expressing cells in the habenula.

Basal forebrain

A great number of afferents to the Gpr151-expressing habenular neurons was observed in basal forebrain areas such as the triangular and medial septum, bed nucleus of the anterior commissure and diagonal band of Broca. The triangular septum has long been recognized as one of the main inputs to the medial habenula, and consists of both glutamatergic and purinergic projections (Qin and Luo, 2009; Sperlágh et al., 1998). Ablation of this projection has anxiolytic effects in mice (Yamaguchi et al., 2013). The medial septum and the diagonal band of Broca provide GABAergic innervation to the ventral part of the medial habenula, that is both excitatory (mediated by $GABA_A$-receptors) and inhibitory (mediated by $GABA_B$-receptors) (Choi et al., 2016). This region of the medial habenula, where Gpr151 expression is dense, also receives input from the bed nucleus of the anterior commissure and it has been implicated in fear response and fear learning (Yamaguchi et al., 2013). Gpr151 expression in habenular neurons receiving input from these basal forebrain areas suggest a possible modulatory role of Gpr151 in fear and anxiety related behaviors.

Lateral preoptic – lateral hypothalamic continuum

Herkenham and Nauta (1977) provided a detailed map of habenular afferents in the rat. The authors noted that the majority of the neurons projecting the lateral habenula resided in a continuous band, stretching from the lateral preoptic area to the rostral one third of the lateral hypothalamic area. Injection of anterograde tracer in different parts of this band results in distinctive termination patterns in the lateral habenula, suggesting topographic correspondence between the LPO–LHA continuum and the lateral habenular subnuclei (reviewed in Zahm and Root, 2017). The habenula-projecting neurons in the lateral hypothalamus appears to be of a combined glutamatergic/GABAergic phenotype and capable of modulating feeding and avoidance behavior (Stamatakis et al., 2016). In our material, afferents to Gpr151-expressing habenular neurons were observed in great numbers throughout the LPO–LHA continuum. The functional topography of the LPO–LHA continuum remains one important open research question in habenula research.

Basal ganglia

The globus pallidus interna (corresponding to the entopeduncular nucleus in rodents) provides dense projections to lateral habenular neurons (Herkenham and Nauta, 1977). Stimulation of these projections produce both inhibitory (GABAergic) and excitatory (glutamatergic) currents in lateral habenular neurons. A recent paper dissected this circuitry further showing that the lateral habenula is likely the only target of excitatory neurons in the entopeduncular nucleus (Wallace et al., 2017). Two distinct populations, a somatostatin expressing glutamatergic/GABAergic projection, and a parvalbumin expressing glutamatergic projection was identified. This pallidohabenular projection appears to be inhibited by unexpected rewards and activated by unexpected loss in monkeys (Hong and Hikosaka, 2008). In rodents this projection produce aversive effects when activated (Shabel et al., 2012) and interestingly, the balance of glutamatergic/GABAergic co-release is shifted towards a more glutamatergic phenotype in a model of depression and during cocaine withdrawal (Shabel et al., 2014; Meye et al., 2016). The balance between glutamate and GABA can be restored by administration of citalopram, a common SSRI antidepressant. The habenular neurons receiving input from the entopeduncular nucleus project to the rostromedial tegmental nucleus, an area rich in Gpr151 immunoreactivity (Meye et al., 2016).

8 Gpr151 expression in the paraventricular thalamic nucleus and its targets

Although Gpr151 *protein* expression was only detectable in habenular axons in Paper I (see section 5.1), we subsequently identified thalamic neuronal populations that may exhibit low or transient mRNA expression of Gpr151 (see section 5.2). Gpr151 mRNA expression in the paraventricular thalamic (PV) nucleus has previously been reported (Ignatov et al., 2004; Wagner et al., 2014a) which prompted us to investigate the connectivity of this population. The afferent input to the Gpr151-expressing neurons in the paraventricular thalamic nucleus was in part similar to the input to the habenular population as afferent neurons were observed in the LPO–LHA continuum and in the diagonal band of Broca. The major inputs to the Gpr151-expressing PV population however, was observed throughout the medial hypothalamus and the zona incerta. The efferent connectivity of the Gpr151-expressing PV population was strikingly different from the habenular population. Four major projection targets were identified: the prelimbic cortex, basolateral amygdala, nucleus accumbens and zona incerta. These ascending projections are not shared with the habenular Gpr151 population which instead projects exclusively towards the ventral midbrain and brainstem. The PV has recently been implicated in opiate addiction and withdrawal (Matzeu et al., 2014; Zhu et al., 2016), and given that Gpr151 appears to mediate sensitivity to nicotine it is tempting to speculate that this receptor may play a broader role in addiction.

9 Endogenous ligand of Gpr151

Neuroanatomical studies of the afferent and efferent projections of Gpr151-expressing neurons may only provide hints to what functions this receptor might be involved in. Identifying molecules that can modulate the signaling of the receptor (so called ligands), would allow a much more detailed functional characterization of Gpr151 in normal physiology and disease.

Several efforts to identify such ligands to Gpr151 have been performed (Ignatov et al., 2004; Qin, 2011; Fontes, 2015; Holmes et al., 2017). Galanin was observed to activate Gpr151 (at high concentrations) in one heterologous cell assay (Ignatov et al., 2004). However, this finding could not be confirmed using a different cell line (Holmes et al., 2017). Some peptide fractions of porcine brain extracts were also observed to activate Gpr151, although the identity of the peptides in these fractions were never reported (Qin, 2011).

Given that Gpr151 shows structural similarities to members of the galanin receptor family and that galanin is the only identified peptide that to this date have been shown to be capable of activating Gpr151 we chose to investigate close relatives to this neuropeptide. Spexin and kisspeptin are two peptides that co-evolved with galanin (Kim et al., 2014). Two cleavage products, called spexin (or spexin-1) and spexin-2 can be derived from the spexin prohormone. Interestingly, we observed a weak expression of spexin mRNA in most Gpr151-expressing habenular neurons (see section 5.3). Spexin and kisspeptin was found to elicit functional activation of Gpr151 in a heterologous cell assay, but only at non-physiological micromolar concentrations. Incubation with spexin-2 did not result in any observable effect at any concentration.

The results from our pilot study thus suggest that Gpr151 has lost affinity to the peptides in the galanin/spexin/kisspeptin family during the evolutionary history of the receptor.

A recent study mapping the neuropeptidome of the rat habenular nucleus has compiled a list of neuropeptides present in the habenula (Yang et al., 2018). Applying similar methods to areas enriched in Gpr151 protein expression, for example the IPN, could lead to the discovery of new ligand candidates.

Fontes (2015) quantified cyclic adenosine monophosphate (cAMP) in the IPN of Gpr151 knockout mice. An increase in cAMP was observed, indicating that Gpr151 may be coupled to a G protein of the Gi class. Using an online tool (PRED-COUPLE 2.00) for predicting coupling specificity between a GPCR and four different G protein classes (Gs, Gq, Gi and G12/13) using Hidden Markov Models, we analyzed the Gpr151 protein sequence in 12 vertebrate species (Sgourakis et al., 2005). An association between Gpr151 and the Gi class of G proteins was consistently predicted (Fig. 14).

It is thus possible that an assay measuring activation of the Gi-pathway could be a better

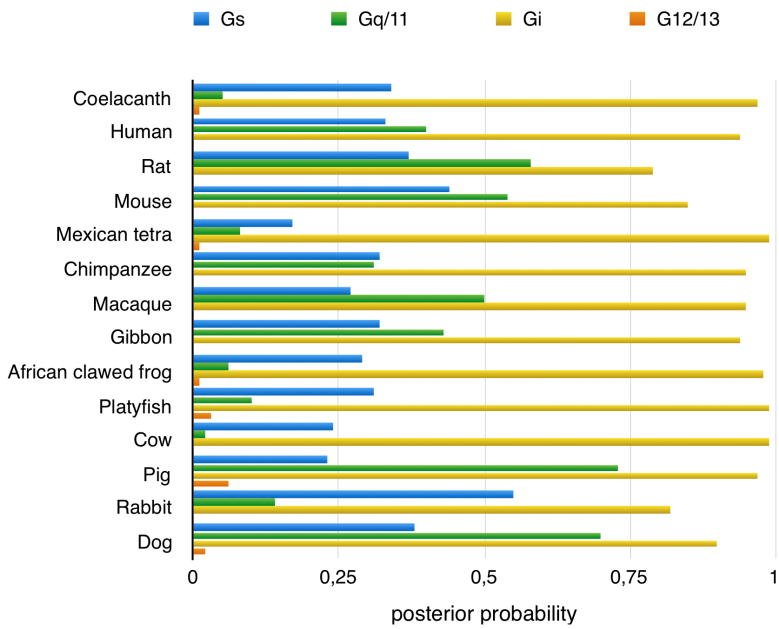

Figure 14: Prediction of the G protein coupling of Gpr151.
PRED-COUPLE2 generated posterior probability (0 to 1) that Gpr151 couples to the four G protein classes.

choice as a functional readout for this receptor than the calcium immobilization assay used in our work (see section 5.4). The expression of specific G protein subunits or other factors that could impact the intracellular signaling cascade may also be needed in future assays in order to reliably query the signaling mechanisms of Gpr151.

10 Characterization of GABAergic interneurons in the habenula

There have been conflicting reports about the presence of GABAergic interneurons in the habenula. The combination of a knock-in mouse strain expressing Cre recombinase under control of the Gad2 promoter and adenoassociated virus mediated expression of a Cre-dependent fluorescent reporter provided a sensitive method of labeling Gad2 expressing neurons in the habenula. Using this approach we could identify different classes of (presumably) GABAergic neurons in the lateral habenula, based on morphological and neurochemical characteristics (see section 5.4). Synaptic boutons observed within the lateral habenular nucleus indicated that at least a part of the Gad2-expressing neurons were interneurons. This picture gets more complicated by the findings of two recent papers. Zhang et al. (2018) demonstrated that lateral habenular GABAergic neurons can produce branching axons both terminating in the habenula itself but also leaving the habenula through the

fasciculus retroflexus. A paper investigating neurons with mixed glutamatergic/GABAergic phenotypes showed that most Gad-expressing neurons in the lateral habenula also express VGlut2, a marker expressed by some glutamatergic neurons (Root et al., 2018). How the GABAergic neuronal population in the lateral habenula modulate the activity within and outside the habenula, and the impact of the balance between glutamate and GABA, remains an intriguing open research question.

Concluding remarks and future perspectives

Numerous studies have demonstrated dysfunction and alterations in volume of the habenula in patients with depression, leading to the idea that the habenula and its related neurocircuitry could provide a promising target for novel treatment strategies. Around 8 years ago initial pilot experiments of directly modulating the habenula in human patients using deep brain stimulation (DBS) was performed and yielded promising results, but since then there have been no follow-up studies of this sort (Sartorius et al., 2010).

The need of less invasive techniques for modulating habenular activity sparked our interest in an orphan G protein–coupled receptor known as Gpr151, which exhibits a remarkably high and almost exclusive expression in the habenula. We performed a careful characterization of the connections of the Gpr151 expressing neurons and could thus provide a map of the brain areas that are likely modulated by the Gpr151 receptor (see sections 5.1 and 5.2). However, this map can only provide hints to what functions Gpr151 may have in normal physiology and disease. A limiting factor in studying Gpr151 function is that no ligands have been identified. To this end, we investigated the functional activation of Gpr151 after incubation with a few neuropeptides similar to galanin, the only molecule that have been demonstrated to activate Gpr151 (Ignatov et al., 2004). Unfortunately, neither galanin, nor its relatives spexin and kisspeptin appears to activate Gpr151 at physiological concentrations (see section 5.3).

The presence of GABAergic interneurons in the habenula has been disputed. In this thesis, we provide evidence of Gad2-expressing neurons in the lateral habenula and show that this set of neurons may be further subclassified using neurochemical and morphological criteria (see section 5.4). A recent set of papers, supports our findings of GABAergic interneurons in the lateral habenula, but also indicate a great complexity in that some of these neurons may produce both local and long-range projections (Zhang et al., 2018, 2016) and that some are of a mixed inhibitory/excitatory phenotype (Root et al., 2018). How these differents GABAergic habenular populations modulate habenular activity and if these neurons have

any role in psychiatric disease remain unexplored.

The work described in this thesis is a small contribution to the understanding of the intriguingly complex habenular nucleus. Whether the habenula may provide a future target for treating depression is an open question, but as our knowledge about the habenula is extending at an accelerating pace, the answer may be within reach.

References

11 Bibliography

Ahumada-Galleguillos, P., Lemus, C. G., Díaz, E., Osorio-Reich, M., Härtel, S., and Concha, M. L. (2017). Directional asymmetry in the volume of the human habenula. *Brain structure & function*, 222(2):1087–1092.

Aizawa, H., Kobayashi, M., Tanaka, S., Fukai, T., and Okamoto, H. (2012). Molecular characterization of the subnuclei in rat habenula. *The Journal of comparative neurology*, 520(18):4051–4066.

Aizawa, H., Yanagihara, S., Kobayashi, M., Niisato, K., Takekawa, T., Harukuni, R., McHugh, T. J., Fukai, T., Isomura, Y., and Okamoto, H. (2013). The synchronous activity of lateral habenular neurons is essential for regulating hippocampal theta oscillation. *The Journal of Neuroscience*, 33(20):8909–8921.

Amat, J., Sparks, P. D., Matus-Amat, P., Griggs, J., Watkins, L. R., and Maier, S. F. (2001). The role of the habenular complex in the elevation of dorsal raphe nucleus serotonin and the changes in the behavioral responses produced by uncontrollable stress. *Brain research*, 917(1):118–126.

American Psychiatric Association (2013). *Diagnostic and Statistical Manual of Mental Disorders (DSM-5®)*. American Psychiatric Pub.

Andrade, T. G., Zangrossi, H., and Graeff, F. G. (2013). The median raphe nucleus in anxiety revisited. *Journal of psychopharmacology (Oxford, England)*, 27(12):1107–1115.

Andres, K. H., von Düring, M., and Veh, R. W. (1999). Subnuclear organization of the rat habenular complexes. *The Journal of comparative neurology*, 407(1):130–150.

Baker, P. M. and Mizumori, S. J. Y. (2017). Control of behavioral flexibility by the lateral habenula. *Pharmacology, biochemistry, and behavior*, 162:62–68.

Baker, P. M., Oh, S. E., Kidder, K. S., and Mizumori, S. J. Y. (2015). Ongoing behavioral state information signaled in the lateral habenula guides choice flexibility in freely moving rats. *Frontiers in Behavioral Neuroscience*, 9:295.

Baker, P. M., Raynor, S. A., Francis, N. T., and Mizumori, S. J. Y. (2016). Lateral habenula integration of proactive and retroactive information mediates behavioral flexibility. *Neuroscience*.

Baño-Otálora, B. and Piggins, H. D. (2017). Contributions of the lateral habenula to circadian timekeeping. *Pharmacology, biochemistry, and behavior*.

Baumeister, A. A., Hawkins, M. F., and Uzelac, S. M. (2003). The myth of reserpine-induced depression: role in the historical development of the monoamine hypothesis. *Journal of the history of the neurosciences*, 12(2):207–220.

Bergstrom, C. T. and Meacham, F. (2016). Depression and anxiety: maladaptive byproducts of adaptive mechanisms. *Evolution, medicine, and public health*, 2016(1):214–218.

Berthold, M., Collin, M., Sejlitz, T., Meister, B., and Lind, P. (2003). Cloning of a novel orphan G protein-coupled receptor (GPCR-2037): in situ hybridization reveals high mRNA expression in rat brain restricted to neurons of the habenular complex. *Brain research. Molecular brain research*, 120(1):22–29.

Bertler, Å., Carlsson, A., and Rosengren, E. (1956). Release by reserpine of catechol amines from rabbits' hearts. *Die Naturwissenschaften*, 43(22):521–521.

Bianco, I. H., Carl, M., Russell, C., Clarke, J. D. W., and Wilson, S. W. (2008). Brain asymmetry is encoded at the level of axon terminal morphology. *Neural development*, 3(1):9.

Broms, J., Antolin-Fontes, B., Tingström, A., and Ibañez-Tallon, I. (2014). Conserved expression of the GPR151 receptor in habenular axonal projections of vertebrates. *Journal of Comparative Neurology*, 523(3):359–380.

Caldecott-Hazard, S., Mazziotta, J., and Phelps, M. (1988). Cerebral correlates of depressed behavior in rats, visualized using 14C-2-deoxyglucose autoradiography. *The Journal of Neuroscience*, 8(6):1951–1961.

Carceller-Sindreu, M., de Diego-Adeliño, J., Serra-Blasco, M., Vives-Gilabert, Y., Martí, A., n-Blanco, Puigdemont, D., Álvarez, E., Pérez, V., and Portella, M. J. (2015). Volumetric MRI study of the habenula in first episode, recurrent and chronic major depression. *European neuropsychopharmacology : the journal of the European College of Neuropsychopharmacology*, 25(11):2015–2021.

Carlson, P. J., Diazgranados, N., Nugent, A. C., Ibrahim, L., Luckenbaugh, D. A., Brutsche, N., Herscovitch, P., Manji, H. K., Zarate, C. A., and Drevets, W. C. (2013). Neural correlates of rapid antidepressant response to ketamine in treatment-resistant unipolar depression: a preliminary positron emission tomography study. *Biological psychiatry*, 73(12):1213–1221.

Caspi, A., Sugden, K., Moffitt, T. E., Taylor, A., Craig, I. W., Harrington, H., McClay, J., Mill, J., Martin, J., Braithwaite, A., and Poulton, R. (2003). Influence of life stress on depression: moderation by a polymorphism in the 5-HTT gene. *Science (New York, NY)*, 301(5631):386–389.

Chang, S. M., Hahm, B.-J., Lee, J.-Y., Shin, M. S., Jeon, H. J., Hong, J.-P., Lee, H. B., Lee, D.-W., and Cho, M. J. (2008). Cross-national difference in the prevalence of depression caused by the diagnostic threshold. *Journal of affective disorders*, 106(1-2):159–167.

Chastrette, N., Pfaff, D. W., and Gibbs, R. B. (1991). Effects of daytime and nighttime stress on Fos-like immunoreactivity in the paraventricular nucleus of the hypothalamus, the habenula, and the posterior paraventricular nucleus of the thalamus. *Brain research*, 563(1-2):339–344.

Choi, K., Lee, Y., Lee, C., Hong, S., Lee, S., Kang, S. J., and Shin, K. S. (2016). Optogenetic activation of septal GABAergic afferents entrains neuronal firing in the medial habenula. *Scientific reports*, 6:34800.

Chou, M.-Y., Amo, R., Kinoshita, M., Cherng, B.-W., Shimazaki, H., Agetsuma, M., Shiraki, T., Aoki, T., Takahoko, M., Yamazaki, M., Higashijima, S.-i., and Okamoto, H. (2016). Social conflict resolution regulated by two dorsal habenular subregions in zebrafish. *Science (New York, NY)*, 352(6281):87–90.

Christoph, G. R., Leonzio, R. J., and Wilcox, K. S. (1986). Stimulation of the lateral habenula inhibits dopamine-containing neurons in the substantia nigra and ventral tegmental area of the rat. *The Journal of Neuroscience*, 6(3):613–619.

Concha, M. L. and Wilson, S. W. (2001). Asymmetry in the epithalamus of vertebrates. *Journal of anatomy*, 199(Pt 1-2):63–84.

CONVERGE consortium (2015). Sparse whole-genome sequencing identifies two loci for major depressive disorder. *Nature*, 523(7562):588–591.

Costes, S. V., Daelemans, D., Cho, E. H., Dobbin, Z., Pavlakis, G., and Lockett, S. (2004). Automatic and quantitative measurement of protein-protein colocalization in live cells. *Biophysical journal*, 86(6):3993–4003.

Cuello, A. C., Emson, P. C., Paxinos, G., and Jessell, T. (1978). Substance P containing and cholinergic projections from the habenula. *Brain research*, 149(2):413–429.

Cui, W., Mizukami, H., Yanagisawa, M., Aida, T., Nomura, M., Isomura, Y., Takayanagi, R., Ozawa, K., Tanaka, K., and Aizawa, H. (2014). Glial dysfunction in the mouse habenula causes depressive-like behaviors and sleep disturbance. *The Journal of Neuroscience*, 34(49):16273–16285.

Culverhouse, R. C., Saccone, N. L., Horton, A. C., Ma, Y., Anstey, K. J., Banaschewski, T., Burmeister, M., Cohen-Woods, S., Etain, B., Fisher, H. L., Goldman, N., Guillaume, S., Horwood, J., Juhasz, G., Lester, K. J., Mandelli, L., Middeldorp, C. M., Olié, E., Villafuerte, S., Air, T. M., Araya, R., Bowes, L., Burns, R., Byrne, E. M., Coffey, C., Coventry, W. L., Gawronski, K. A. B., Glei, D., Hatzimanolis, A., Hottenga, J.-J., Jaussent, I., Jawahar, C., Jennen-Steinmetz, C., Kramer, J. R., Lajnef, M., Little, K., Zu Schwabedissen, H. M., Nauck, M., Nederhof, E., Petschner, P., Peyrot, W. J., Schwahn, C., Sinnamon, G., Stacey, D., Tian, Y., Toben, C., Van der Auwera, S., Wainwright, N., Wang, J.-C., Willemsen, G., Anderson, I. M., Arolt, V., Åslund, C., Bagdy, G., Baune, B. T., Bellivier, F., Boomsma, D. I., Courtet, P., Dannlowski, U., de Geus, E. J. C., Deakin, J. F. W., Easteal, S., Eley, T., Fergusson, D. M., Goate, A. M., Gonda, X., Grabe, H. J., Holzman, C., Johnson, E. O., Kennedy, M., Laucht, M., Martin, N. G., Munafò, M. R., Nilsson, K. W., Oldehinkel, A. J., Olsson, C. A., Ormel, J., Otte, C., Patton, G. C., Penninx, B. W. J. H., Ritchie, K., Sarchiapone, M., Scheid, J. M., Serretti, A., Smit, J. H., Stefanis, N. C., Surtees, P. G., Völzke, H., Weinstein, M., Whooley, M., Nurnberger, J. I., Breslau, N., and Bierut, L. J. (2017). Collaborative meta-analysis finds no evidence of a strong interaction between stress and 5-HTTLPR genotype contributing to the development of depression. *Molecular psychiatry*.

Dreosti, E., Vendrell Llopis, N., Carl, M., Yaksi, E., and Wilson, S. W. (2014). Left-right asymmetry is required for the habenulae to respond to both visual and olfactory stimuli. *Current biology : CB*, 24(4):440–445.

Duncan, G. E., Knapp, D. J., Johnson, K. B., and Breese, G. R. (1996). Functional classification of antidepressants based on antagonism of swim stress-induced fos-like immunoreactivity. *The Journal of pharmacology and experimental therapeutics*, 277(2):1076–1089.

Elmer, G. I., Palacorolla, H., Mayo, C. L., Brown, P. L., Jhou, T. C., Brady, D., and Shepard, P. D. (2018). The rostromedial tegmental nucleus modulates the development of stress-induced helpless behavior. *Behavioural brain research*.

Emdin, C. A., Khera, A. V., Chaffin, M., Klarin, D., Natarajan, P., Aragam, K., Haas, M., Bick, A., Zekavat, S. M., Nomura, A., Ardissino, D., Wilson, J. G., Schunkert, H., McPherson, R., Watkins, H., Elosua, R., Bown, M. J., Samani, N. J., Baber, U., Erdmann, J., Gupta, N., Danesh, J., Chasman, D., Ridker, P., Denny, J., Bastarache, L., Lichtman, J. H., D'Onofrio, G., Mattera, J., Spertus, J. A., Sheu, W. H. H., Taylor, K. D., Psaty, B. M., Rich, S. S., Post, W., Rotter, J. I., Chen, Y.-D. I., Krumholz,

H., Saleheen, D., Gabriel, S., and Kathiresan, S. (2018). Analysis of predicted loss-of-function variants in UK Biobank identifies variants protective for disease. *Nature communications*, 9(1):1613.

Etessami, R., Conzelmann, K. K., Fadai-Ghotbi, B., Natelson, B., Tsiang, H., and Ceccaldi, P. E. (2000). Spread and pathogenic characteristics of a G-deficient rabies virus recombinant: an in vitro and in vivo study. *The Journal of general virology*, 81(Pt 9):2147–2153.

Finke, S. and Conzelmann, K.-K. (2005). Replication strategies of rabies virus. *Virus research*, 111(2):120–131.

Flint, J. and Kendler, K. S. (2014). The Genetics of Major Depression. *Neuron*, 81(5):1214.

Fontes, B. A. (2015). *Identification of a novel synaptic G protein-coupled receptor controlling nicotine dependence and withdrawal*. PhD thesis, Department of Biology, Chemistry and Pharmacy of the Freie Universität Berlin.

Fredriksson, R., Lagerström, M. C., Lundin, L.-G., and Schiöth, H. B. (2003). The G-Protein-Coupled Receptors in the Human Genome Form Five Main Families. Phylogenetic Analysis, Paralogon Groups, and Fingerprints. *Molecular pharmacology*, 63(6):1256–1272.

Furman, D. J. and Gotlib, I. H. (2016). Habenula responses to potential and actual loss in major depression: preliminary evidence for lateralized dysfunction. *Social cognitive and affective neuroscience*, 11(5):843–851.

Ganser, S. (1882). Vergleichend-anatomische Studien über das Gehirn des Maulwurfs. *Morphologisches Jahrbuch*, 7:591–725.

Geisler, S., Andres, K. H., and Veh, R. W. (2003). Morphologic and cytochemical criteria for the identification and delineation of individual subnuclei within the lateral habenular complex of the rat. *The Journal of comparative neurology*, 458(1):78–97.

Golden, S. A., Heshmati, M., Flanigan, M., Christoffel, D. J., Guise, K., Pfau, M. L., Aleyasin, H., Menard, C., Zhang, H., Hodes, G. E., Bregman, D., Khibnik, L., Tai, J., Rebusi, N., Krawitz, B., Chaudhury, D., Walsh, J. J., Han, M.-H., Shapiro, M. L., and Russo, S. J. (2016). Basal forebrain projections to the lateral habenula modulate aggression reward. *Nature*, 534(7609):688–692.

Gosnell, S. N., Curtis, K. N., Velasquez, K., Fowler, J. C., Madan, A., Goodman, W., and Salas, R. (2018). Habenular Connectivity May Predict Treatment Response in Depressed Psychiatric Inpatients. *Journal of affective disorders*.

Grillner, S., von Twickel, A., and Robertson, B. (2017). The blueprint of the vertebrate forebrain - With special reference to the habenulae. *Seminars in cell & developmental biology*.

Groenewegen, H. J., Ahlenius, S., Haber, S. N., Kowall, N. W., and Nauta, W. J. (1986). Cytoarchitecture, fiber connections, and some histochemical aspects of the interpeduncular nucleus in the rat. *The Journal of comparative neurology*, 249(1):65–102.

Guglielmotti, V. and Cristino, L. (2006). The interplay between the pineal complex and the habenular nuclei in lower vertebrates in the context of the evolution of cerebral asymmetry. *Brain research bulletin*, 69(5):475–488.

Hauser, A. S., Attwood, M. M., Rask-Andersen, M., Schiöth, H. B., and Gloriam, D. E. (2017). Trends in GPCR drug discovery: new agents, targets and indications. *Nature reviews. Drug discovery*, 16(12):829–842.

Henry, J. P. and Scherman, D. (1989). Radioligands of the vesicular monoamine transporter and their use as markers of monoamine storage vesicles. *Biochemical pharmacology*, 38(15):2395–2404.

Herkenham, M. and Nauta, W. J. (1977). Afferent connections of the habenular nuclei in the rat. A horseradish peroxidase study, with a note on the fiber-of-passage problem. *The Journal of comparative neurology*, 173(1):123–146.

Herkenham, M. and Nauta, W. J. (1979). Efferent connections of the habenular nuclei in the rat. *The Journal of comparative neurology*, 187(1):19–47.

Herzog, E., Gilchrist, J., Gras, C., Muzerelle, A., Ravassard, P., Giros, B., Gaspar, P., and El Mestikawy, S. (2004). Localization of VGLUT3, the vesicular glutamate transporter type 3, in the rat brain. *Neuroscience*, 123(4):983–1002.

Heshmati, M. and Russo, S. J. (2015). Anhedonia and the brain reward circuitry in depression. *Current behavioral neuroscience reports*, 2(3):146–153.

Hieronymus, F., Emilsson, J. F., Nilsson, S., and Eriksson, E. (2016). Consistent superiority of selective serotonin reuptake inhibitors over placebo in reducing depressed mood in patients with major depression. *Molecular psychiatry*, 21(4):523–530.

Holmes, F. E., Kerr, N., Chen, Y.-J., Vanderplank, P., McArdle, C. A., and Wynick, D. (2017). Targeted disruption of the orphan receptor Gpr151 does not alter pain-related behaviour despite a strong induction in dorsal root ganglion expression in a model of neuropathic pain. *Molecular and cellular neurosciences*, 78:35–40.

Hong, S. and Hikosaka, O. (2008). The globus pallidus sends reward-related signals to the lateral habenula. *Neuron*, 60(4):720–729.

Ignatov, A., Hermans-Borgmeyer, I., and Schaller, H. C. (2004). Cloning and characterization of a novel G-protein-coupled receptor with homology to galanin receptors. *Neuropharmacology*, 46(8):1114–1120.

Jhou, T. C., Fields, H. L., Baxter, M. G., Saper, C. B., and Holland, P. C. (2009a). The rostromedial tegmental nucleus (RMTg), a GABAergic afferent to midbrain dopamine neurons, encodes aversive stimuli and inhibits motor responses. *Neuron*, 61(5):786–800.

Jhou, T. C., Geisler, S., Marinelli, M., Degarmo, B. A., and Zahm, D. S. (2009b). The mesopontine rostromedial tegmental nucleus: A structure targeted by the lateral habenula that projects to the ventral tegmental area of Tsai and substantia nigra compacta. *The Journal of comparative neurology*, 513(6):566–596.

Ji, H. and Shepard, P. D. (2007). Lateral habenula stimulation inhibits rat midbrain dopamine neurons through a GABA(A) receptor-mediated mechanism. *The Journal of Neuroscience*, 27(26):6923–6930.

Kalén, P., Lindvall, O., and Björklund, A. (1989a). Electrical stimulation of the lateral habenula increases hippocampal noradrenaline release as monitored by in vivo microdialysis. *Experimental brain research Experimentelle Hirnforschung Expérimentation cérébrale*, 76(1):239–245.

Kalén, P., Strecker, R. E., Rosengren, E., and Björklund, A. (1989b). Regulation of striatal serotonin release by the lateral habenula-dorsal raphe pathway in the rat as demonstrated by in vivo microdialysis: role of excitatory amino acids and GABA. *Brain research*, 492(1-2):187–202.

Karg, K., Burmeister, M., Shedden, K., and Sen, S. (2011). The Serotonin Transporter Promoter Variant (5-HTTLPR), Stress, and Depression Meta-analysis Revisited: Evidence of Genetic Moderation. *Archives of general psychiatry*, 68(5):444–454.

Kessler, R. C., Berglund, P., Demler, O., Jin, R., Merikangas, K. R., and Walters, E. E. (2005). Lifetime prevalence and age-of-onset distributions of DSM-IV disorders in the National Comorbidity Survey Replication. *Archives of general psychiatry*, 62(6):593–602.

Kessler, R. C. and Bromet, E. J. (2013). The epidemiology of depression across cultures. *Annual review of public health*, 34:119–138.

Kim, D.-K., Yun, S., Son, G. H., Hwang, J.-I., Park, C. R., Kim, J. I., Kim, K., Vaudry, H., and Seong, J. Y. (2014). Coevolution of the spexin/galanin/kisspeptin family: Spexin activates galanin receptor type II and III. *Endocrinology*, 155(5):1864–1873.

Kobayashi, Y., Sano, Y., Vannoni, E., Goto, H., Suzuki, H., Oba, A., Kawasaki, H., Kanba, S., Lipp, H.-P., Murphy, N. P., Wolfer, D. P., and Itohara, S. (2013). Genetic dissection of medial habenula-interpeduncular nucleus pathway function in mice. *Frontiers in Behavioral Neuroscience*, 7:17.

Lawson, R. P., Nord, C. L., Seymour, B., Thomas, D. L., Dayan, P., Pilling, S., and Roiser, J. P. (2016). Disrupted habenula function in major depression. *Molecular psychiatry*, 22(2):202–208.

Lecca, S., Pelosi, A., Tchenio, A., Moutkine, I., Lujan, R., Hervé, D., and Mameli, M. (2016). Rescue of GABAB and GIRK function in the lateral habenula by protein phosphatase 2A inhibition ameliorates depression-like phenotypes in mice. *Nature medicine*, 22:254–261.

Li, B., Piriz, J., Mirrione, M., Chung, C., Proulx, C. D., Schulz, D., Henn, F., and Malinow, R. (2011). Synaptic potentiation onto habenula neurons in the learned helplessness model of depression. *Nature*, 470(7335):535–539.

Li, K., Zhou, T., Liao, L., Yang, Z., Wong, C., Henn, F., Malinow, R., Yates, J. R., and Hu, H. (2013). βCaMKII in lateral habenula mediates core symptoms of depression. *Science (New York, NY)*, 341(6149):1016–1020.

Li, Y., Zhong, W., Wang, D., Feng, Q., Liu, Z., Zhou, J., Jia, C., Hu, F., Zeng, J., Guo, Q., Fu, L., and Luo, M. (2016). Serotonin neurons in the dorsal raphe nucleus encode reward signals. *Nature communications*, 7:10503.

Liu, W.-H., Valton, V., Wang, L.-Z., Zhu, Y.-H., and Roiser, J. P. (2017). Association between habenula dysfunction and motivational symptoms in unmedicated major depressive disorder. *Social cognitive and affective neuroscience*, 12(9):1520–1533.

Liu, Z., Xu, Y., Wu, L., and Zhang, S. (2010). Evolution of galanin receptor genes: insights from the deuterostome genomes. *Journal of biomolecular structure & dynamics*, 28(1):97–106.

Manders, E. M. M., Verbeek, F. J., and Aten, J. A. (1993). Measurement of co-localization of objects in dual-colour confocal images. *Journal of microscopy*, 169(3):375–382.

Mathis, V., Cosquer, B., Barbelivien, A., Herbeaux, K., Bothorel, B., Sage-Ciocca, D., Poirel, V.-J., Mathis, C., and Lecourtier, L. (2017). The lateral habenula interacts with the hypothalamo-pituitary adrenal axis response upon stressful cognitive demand in rats. *Behavioural brain research*, 341:63–70.

Matsuda, S., Peng, H., Yoshimura, H., Wen, T. C., Fukuda, T., and Sakanaka, M. (1996). Persistent c-fos expression in the brains of mice with chronic social stress. *Neuroscience research*, 26(2):157–170.

Matsumoto, M. and Hikosaka, O. (2007). Lateral habenula as a source of negative reward signals in dopamine neurons. *Nature*, 447(7148):1111–1115.

Matzeu, A., Zamora-Martinez, E. R., and Martin-Fardon, R. (2014). The paraventricular nucleus of the thalamus is recruited by both natural rewards and drugs of abuse: recent evidence of a pivotal role for orexin/hypocretin signaling in this thalamic nucleus in drug-seeking behavior. *Frontiers in Behavioral Neuroscience*, 8:117.

McEwen, B. S. (2012). The ever-changing brain: cellular and molecular mechanisms for the effects of stressful experiences. *Developmental neurobiology*, 72(6):878–890.

McGuffin, P. and Rivera, M. (2015). The interaction between stress and genetic factors in the etiopathogenesis of depression. *World psychiatry : official journal of the World Psychiatric Association (WPA)*, 14(2):161–163.

Mechenthaler, I. (2008). Galanin and the neuroendocrine axes. *Cellular and molecular life sciences : CMLS*, 65(12):1826–1835.

Meye, F. J., Soiza-Reilly, M., Smit, T., Diana, M. A., Schwarz, M. K., and Mameli, M. (2016). Shifted pallidal co-release of GABA and glutamate in habenula drives cocaine withdrawal and relapse. *Nature neuroscience*, 19(8):1019–1024.

Mirrione, M. M., Schulz, D., Lapidus, K. A. B., Zhang, S., Goodman, W., and Henn, F. A. (2014). Increased metabolic activity in the septum and habenula during stress is linked to subsequent expression of learned helplessness behavior. *Frontiers in human neuroscience*, 8:29.

Mizumori, S. J. Y. and Baker, P. M. (2017). The Lateral Habenula and Adaptive Behaviors. *Trends in neurosciences*, 40(8):481–493.

Möller, H. J. (2003). Suicide, suicidality and suicide prevention in affective disorders. *Acta psychiatrica Scandinavica. Supplementum*, (418):73–80.

Morley, B. J. (1986). The interpeduncular nucleus. *International review of neurobiology*, 28:157–182.

Morris, J. S., Smith, K. A., Cowen, P. J., Friston, K. J., and Dolan, R. J. (1999). Covariation of activity in habenula and dorsal raphé nuclei following tryptophan depletion. *Neuroimage*, 10(2):163–172.

Morton, G., Nasirova, N., Sparks, D. W., Brodsky, M., Sivakumaran, S., Lambe, E. K., and Turner, E. E. (2018). Chrna5-expressing neurons in the interpeduncular nucleus mediate aversion primed by prior stimulation or nicotine exposure. *The Journal of neuroscience : the official journal of the Society for Neuroscience*, 38(31):6900–6920.

Mullins, N. and Lewis, C. M. (2017). Genetics of Depression: Progress at Last. *Current psychiatry reports*, 19(8):43.

Nauta, W. J. (1958). Hippocampal projections and related neural pathways to the midbrain in the cat. *Brain : a journal of neurology*, 81(3):319–340.

Nishikawa, T., Fage, D., and Scatton, B. (1986). Evidence for, and nature of, the tonic inhibitory influence of habenulointerpeduncular pathways upon cerebral dopaminergic transmission in the rat. *Brain research*, 373(1-2):324–336.

Offermanns, S. and Simon, M. I. (1995). G alpha 15 and G alpha 16 couple a wide variety of receptors to phospholipase C. *The Journal of biological chemistry*, 270(25):15175–15180.

Oh, S. W., Harris, J. A., Ng, L., Winslow, B., Cain, N., Mihalas, S., Wang, Q., Lau, C., Kuan, L., Henry, A. M., Mortrud, M. T., Ouellette, B., Nguyen, T. N., Sorensen, S. A., Slaughterbeck, C. R., Wakeman, W., Li, Y., Feng, D., Ho, A., Nicholas, E., Hirokawa, K. E., Bohn, P., Joines, K. M., Peng, H., Hawrylycz, M. J., Phillips, J. W., Hohmann, J. G., Wohnoutka, P., Gerfen, C. R., Koch, C., Bernard, A., Dang, C., Jones, A. R., and Zeng, H. (2014). A mesoscale connectome of the mouse brain. *Nature*, 508(7495):207–214.

Omelchenko, N., Bell, R., and Sesack, S. R. (2009). Lateral habenula projections to dopamine and GABA neurons in the rat ventral tegmental area. *The European journal of neuroscience*, 30(7):1239–1250.

Ostergaard, S. D., Jensen, S. O. W., and Bech, P. (2011). The heterogeneity of the depressive syndrome: when numbers get serious. *Acta Psychiatrica Scandinavica*, 124(6):495–496.

Pandey, S., Shekhar, K., Regev, A., and Schier, A. F. (2018). Comprehensive Identification and Spatial Mapping of Habenular Neuronal Types Using Single-Cell RNA-Seq. *Current biology : CB*, 28(7):1052–1065.e7.

Panksepp, J. (2005). Affective consciousness: Core emotional feelings in animals and humans. *Consciousness and cognition*, 14(1):30–80.

Panksepp, J. and Watt, D. (2011). Why does depression hurt? Ancestral primary-process separation-distress (PANIC/GRIEF) and diminished brain reward (SEEKING) processes in the genesis of depressive affect. *Psychiatry*, 74(1):5–13.

Paxinos, G. and Watson, C. (2006). *The Rat Brain in Stereotaxic Coordinates*. Elsevier / Academic Press, New York, 6th edition edition.

Power, R. A., Kyaga, S., Uher, R., MacCabe, J. H., Långström, N., Landen, M., McGuffin, P., Lewis, C. M., Lichtenstein, P., and Svensson, A. C. (2013). Fecundity of patients with schizophrenia, autism, bipolar disorder, depression, anorexia nervosa, or substance abuse vs their unaffected siblings. *JAMA psychiatry*, 70(1):22–30.

Qin, C. (2011). *Neurochemical Phenotypes of the Afferent and Efferent Projections of the Mouse Medial Habenula*. PhD thesis, Peking Union Medical College.

Qin, C. and Luo, M. (2009). Neurochemical phenotypes of the afferent and efferent projections of the mouse medial habenula. *Neuroscience*, 161(3):827–837.

Quina, L. A., Tempest, L., Ng, L., Harris, J., Ferguson, S., Jhou, T., and Turner, E. E. (2014). Efferent pathways of the mouse lateral habenula. *Journal of Comparative Neurology*, 523(1):32–60.

Ramachandraih, C. T., Subramanyam, N., Bar, K. J., Baker, G., and Yeragani, V. K. (2011). Antidepressants: From MAOIs to SSRIs and more. *Indian journal of psychiatry*, 53(2):180–182.

Ramón y Cajal, S. (1894). Estructura del ganglio de la habénula de los mamíferos. *Anales de la Sociedad Española de Historia Natural*, XXIII:9.

Ranft, K., Dobrowolny, H., Krell, D., Bielau, H., Bogerts, B., and Bernstein, H.-G. (2010). Evidence for structural abnormalities of the human habenular complex in affective disorders but not in schizophrenia. *Psychological medicine*, 40(4):557–567.

Ren, J., Qin, C., Hu, F., Tan, J., Qiu, L., Zhao, S., Feng, G., and Luo, M. (2011). Habenula "cholinergic" neurons co-release glutamate and acetylcholine and activate postsynaptic neurons via distinct transmission modes. *Neuron*, 69(3):445–452.

Risch, N., Herrell, R., Lehner, T., Liang, K.-Y., Eaves, L., Hoh, J., Griem, A., Kovacs, M., Ott, J., and Merikangas, K. R. (2009). Interaction between the serotonin transporter gene (5-HTTLPR), stressful life events, and risk of depression: a meta-analysis. *JAMA : the journal of the American Medical Association*, 301(23):2462–2471.

Roiser, J. P., Levy, J., Fromm, S. J., Nugent, A. C., Talagala, S. L., Hasler, G., Henn, F. A., Sahakian, B. J., and Drevets, W. C. (2009). The effects of tryptophan depletion on neural responses to emotional words in remitted depression. *Biological psychiatry*, 66(5):441–450.

Root, D. H., Zhang, S., Barker, D. J., Miranda-Barrientos, J., Liu, B., Wang, H.-L., and Morales, M. (2018). Selective Brain Distribution and Distinctive Synaptic Architecture of Dual Glutamatergic-GABAergic Neurons. *Cell reports*, 23(12):3465–3479.

Ruhé, H. G., Mason, N. S., and Schene, A. H. (2007). Mood is indirectly related to serotonin, norepinephrine and dopamine levels in humans: a meta-analysis of monoamine depletion studies. *Molecular psychiatry*, 12(4):331–359.

Russo, S. J. and Nestler, E. J. (2013). The brain reward circuitry in mood disorders. *Nature reviews Neuroscience*, 14(9):609–625.

Sartorius, A., Kiening, K. L., Kirsch, P., von Gall, C. C., Haberkorn, U., Unterberg, A. W., Henn, F. A., and Meyer-Lindenberg, A. (2010). Remission of major depression under deep brain stimulation of the lateral habenula in a therapy-refractory patient. *Biological psychiatry*, 67(2):e9–e11.

Savitz, J. B., Nugent, A. C., Bogers, W., Roiser, J. P., Bain, E. E., Neumeister, A., Zarate, C. A., Manji, H. K., Cannon, D. M., Marrett, S., Henn, F. A., Charney, D. S., and Drevets, W. C. (2011). Habenula volume in bipolar disorder and major depressive disorder: a high-resolution magnetic resonance imaging study. *Biological psychiatry*, 69(4):336–343.

Schmidt, F. M., Schindler, S., Adamidis, M., Strauß, M., Tränkner, A., Trampel, R., Walter, M., Hegerl, U., Turner, R., Geyer, S., and Schönknecht, P. (2017). Habenula volume increases with disease severity in unmedicated major depressive disorder as revealed by 7T MRI. *European archives of psychiatry and clinical neuroscience*, 267(2):107–115.

Sgourakis, N. G., Bagos, P. G., Papasaikas, P. K., and Hamodrakas, S. J. (2005). A method for the prediction of GPCRs coupling specificity to G-proteins using refined profile Hidden Markov Models. *BMC bioinformatics*, 6(1):104.

Shabel, S. J., Proulx, C. D., Piriz, J., and Malinow, R. (2014). Mood regulation. GABA/glutamate co-release controls habenula output and is modified by antidepressant treatment. *Science (New York, NY)*, 345(6203):1494–1498.

Shabel, S. J., Proulx, C. D., Trias, A., Murphy, R. T., and Malinow, R. (2012). Input to the lateral habenula from the basal ganglia is excitatory, aversive, and suppressed by serotonin. *Neuron*, 74(3):475–481.

Shibata, H. and Suzuki, T. (1984). Efferent projections of the interpeduncular complex in the rat, with special reference to its subnuclei: a retrograde horseradish peroxidase study. *Brain research*, 296(2):345–349.

Shore, P. A., Silver, S. L., and Brodie, B. B. (1955). Interaction of reserpine, serotonin, and lysergic acid diethylamide in brain. *Science (New York, NY)*, 122(3163):284–285.

Shumake, J., Colorado, R. A., Barrett, D. W., and Gonzalez-Lima, F. (2010). Metabolic mapping of the effects of the antidepressant fluoxetine on the brains of congenitally helpless rats. *Brain research*, 1343:218–225.

Shumake, J., Edwards, E., and Gonzalez-Lima, F. (2003). Opposite metabolic changes in the habenula and ventral tegmental area of a genetic model of helpless behavior. *Brain research*, 963(1-2):274–281.

Shumake, J. and Gonzalez-Lima, F. (2013). Functional opposition between habenula metabolism and the brain reward system. *Frontiers in human neuroscience*, 7:662.

Simon, G. E., Goldberg, D. P., Von Korff, M., and Ustün, T. B. (2002). Understanding cross-national differences in depression prevalence. *Psychological medicine*, 32(4):585–594.

Sperlágh, B., Maglóczky, Z. S., Vizi, E. S., and Freund, T. F. (1998). The triangular septal nucleus as the major source of ATP release in the rat habenula: A combined neurochemical and morphological study. *Neuroscience*, 86(4):1195–1207.

Stamatakis, A. M., Jennings, J. H., Ung, R. L., Blair, G. A., Weinberg, R. J., Neve, R. L., Boyce, F., Mattis, J., Ramakrishnan, C., Deisseroth, K., and Stuber, G. D. (2013). A unique population of ventral tegmental area neurons inhibits the lateral habenula to promote reward. *Neuron*, 80(4):1039–1053.

Stamatakis, A. M. and Stuber, G. D. (2012). Activation of lateral habenula inputs to the ventral midbrain promotes behavioral avoidance. *Nature neuroscience*, 15(8):1105–1107.

Stamatakis, A. M., Van Swieten, M., Basiri, M. L., Blair, G. A., Kantak, P., and Stuber, G. D. (2016). Lateral Hypothalamic Area Glutamatergic Neurons and Their Projections to the Lateral Habenula Regulate Feeding and Reward. *The Journal of neuroscience : the official journal of the Society for Neuroscience*, 36(2):302–311.

Stephenson-Jones, M., Floros, O., Robertson, B., and Grillner, S. (2012). Evolutionary conservation of the habenular nuclei and their circuitry controlling the dopamine and 5-hydroxytryptophan (5-HT) systems. *Proceedings of the National Academy of Sciences of the United States of America*, 109(3):E164–73.

Sugama, S., Cho, B. P., Baker, H., Joh, T. H., Lucero, J., and Conti, B. (2002). Neurons of the superior nucleus of the medial habenula and ependymal cells express IL-18 in rat CNS. *Brain research*, 958(1):1–9.

Sullivan, P. F., Neale, M. C., and Kendler, K. S. (2000). Genetic epidemiology of major depression: review and meta-analysis. *The American journal of psychiatry*, 157(10):1552–1562.

Sutherland, R. J. (1982). The dorsal diencephalic conduction system: a review of the anatomy and functions of the habenular complex. *Neuroscience and biobehavioral reviews*, 6(1):1–13.

Sutherland, R. J. and Nakajima, S. (1981). Self-stimulation of the habenular complex in the rat. *Journal of comparative and physiological psychology*, 95(5):781–791.

Thornton, E. W. and Bradbury, G. E. (1989). Effort and stress influence the effect of lesion of the habenula complex in one-way active avoidance learning. *Physiology & behavior*, 45(5):929–935.

Thornton, E. W., Bradbury, G. E., and Davies, C. (1990). Increased immobility in an automated forced swimming test following lesion of the habenula in rats: absence of evidence for a contribution from motor impairment. *Behavioral neuroscience*, 104(1):37–43.

Thornton, E. W. and Davies, C. (1991). A water-maze discrimination learning deficit in the rat following lesion of the habenula. *Physiology & behavior*, 49(4):819–822.

Thornton, E. W. and Evans, J. C. (1982). The role of habenular nuclei in the selection of behavioral strategies. *Physiological Psychology*, 10(3):361–367.

Valjakka, A., Vartiainen, J., Tuomisto, L., Tuomisto, J. T., Olkkonen, H., and Airaksinen, M. M. (1998). The fasciculus retroflexus controls the integrity of REM sleep by supporting the generation of hippocampal theta rhythm and rapid eye movements in rats. *Brain research bulletin*, 47(2):171–184.

Vassilatis, D. K., Hohmann, J. G., Zeng, H., Li, F., Ranchalis, J. E., Mortrud, M. T., Brown, A., Rodriguez, S. S., Weller, J. R., Wright, A. C., Bergmann, J. E., and Gaitanaris, G. A. (2003). The G protein-coupled receptor repertoires of human and mouse. *Proceedings of the National Academy of Sciences of the United States of America*, 100(8):4903–4908.

Wagner, F., French, L., and Veh, R. W. (2014a). Transcriptomic-anatomic analysis of the mouse habenula uncovers a high molecular heterogeneity among neurons in the lateral complex, while gene expression in the medial complex largely obeys subnuclear boundaries. *Brain structure & function*, pages 1–20.

Wagner, F., Stroh, T., and Veh, R. W. (2014b). Correlating habenular subnuclei in rat and mouse using topographical, morphological and cytochemical criteria. *The Journal of comparative neurology*, 522(11):2650–62.

Wall, N. R., Wickersham, I. R., Cetin, A., De La Parra, M., and Callaway, E. M. (2010). Monosynaptic circuit tracing in vivo through Cre-dependent targeting and complementation of modified rabies virus. *Proceedings of the National Academy of Sciences of the United States of America*, 107(50):21848–21853.

Wallace, M. L., Saunders, A., Huang, K. W., Philson, A. C., Goldman, M., Macosko, E. Z., McCarroll, S. A., and Sabatini, B. L. (2017). Genetically Distinct Parallel Pathways in the Entopeduncular Nucleus for Limbic and Sensorimotor Output of the Basal Ganglia. *Neuron*, 94(1):138–152.e5.

Wang, D. V., Yau, H.-J., Broker, C. J., Tsou, J.-H., Bonci, A., and Ikemoto, S. (2015). Mesopontine median raphe regulates hippocampal ripple oscillation and memory consolidation. *Nature neuroscience*, 18(5):728–735.

Wang, F., Flanagan, J., Su, N., Wang, L.-C., Bui, S., Nielson, A., Wu, X., Vo, H.-T., Ma, X.-J., and Luo, Y. (2012). RNAscope: a novel in situ RNA analysis platform for formalin-fixed, paraffin-embedded tissues. *The Journal of molecular diagnostics : JMD*, 14(1):22–29.

Watabe-Uchida, M., Zhu, L., Ogawa, S. K., Vamanrao, A., and Uchida, N. (2012). Whole-brain mapping of direct inputs to midbrain dopamine neurons. *Neuron*, 74(5):858–873.

Wickersham, I. R., Lyon, D. C., Barnard, R. J. O., Mori, T., Finke, S., Conzelmann, K.-K., Young, J. A. T., and Callaway, E. M. (2007). Monosynaptic restriction of transsynaptic tracing from single, genetically targeted neurons. *Neuron*, 53(5):639–647.

Wirtshafter, D., Asin, K. E., and Pitzer, M. R. (1994). Dopamine agonists and stress produce different patterns of Fos-like immunoreactivity in the lateral habenula. *Brain research*, 633(1-2):21–26.

Woolf, N. J. and Butcher, L. L. (1985). Cholinergic systems in the rat brain: II. Projections to the interpeduncular nucleus. *Brain research bulletin*, 14(1):63–83.

Yamaguchi, T., Danjo, T., Pastan, I., Hikida, T., and Nakanishi, S. (2013). Distinct roles of segregated transmission of the septo-habenular pathway in anxiety and fear. *Neuron*, 78(3):537–544.

Yang, N., Anapindi, K. D. B., Rubakhin, S. S., Wei, P., Yu, Q., Li, L., Kenny, P. J., and Sweedler, J. V. (2018). Neuropeptidomics of the Rat Habenular Nuclei. *Journal of proteome research*, 17(4):1463–1473.

Yetnikoff, L., Cheng, A. Y., Lavezzi, H. N., Parsley, K. P., and Zahm, D. S. (2015). Sources of input to the rostromedial tegmental nucleus, ventral tegmental area, and lateral habenula compared: A study in rat. *Journal of Comparative Neurology*, 523(16):2426–2456.

Yokoyama, T., Kato, N., and Yamada, N. (2003). Development of a high-throughput bioassay to screen melatonin receptor agonists using human melatonin receptor expressing CHO cells. *Neuroscience letters*, 344(1):45–48.

Zahm, D. S. and Root, D. H. (2017). Review of the cytology and connections of the lateral habenula, an avatar of adaptive behaving. *Pharmacology, biochemistry, and behavior*.

Zhang, L., Hernández, V. S., Swinny, J. D., Verma, A. K., Giesecke, T., Emery, A. C., Mutig, K., Garcia-Segura, L. M., and Eiden, L. E. (2018). A GABAergic cell type in the lateral habenula links hypothalamic homeostatic and midbrain motivation circuits with sex steroid signaling. *Translational psychiatry*, 8(1):50.

Zhang, L., Hernández, V. S., Vázquez-Juárez, E., Chay, F. K., and Barrio, R. A. (2016). Thirst Is Associated with Suppression of Habenula Output and Active Stress Coping: Is

there a Role for a Non-canonical Vasopressin-Glutamate Pathway? *Frontiers in neural circuits*, 10:13.

Zhu, Y., Wienecke, C. F. R., Nachtrab, G., and Chen, X. (2016). A thalamic input to the nucleus accumbens mediates opiate dependence. *Nature*, 530(7589):219–222.

Zubin, J. and Spring, B. (1977). Vulnerability–a new view of schizophrenia. *Journal of abnormal psychology*, 86(2):103–126.

Scientific publications

Author contributions

Co-authors are abbreviated as follows:
Jonas Jester-Broms (**JJB**), Anders Tingström (AT), Beatriz Antolin-Fontes (BAF), Ines Ibanez-Tallon (IIT), Matilda Grahm (MG), Matilda Grahm (MG), Lea D. Haugegaard (LDH), Konstantinos Meletis (KM), Joakim Ekstrand (JE), Thomas Blom (TB).

Paper I: Conserved expression of the Gpr151 receptor in habenular axonal projections of vertebrates.

Study concept and design: AT and IIT. Acquisition of data: **JJB**, BAF. Analysis and interpretation of data: **JJB**, BAF, AT, IIT. Writing of the manuscript: **JJB**, BAF, AT, IIT. Conceptualization and critical revision of the manuscript for intellectual content: AT, IIT. Obtained funding: AT, IIT. Study supervision: AT, IIT.

Paper II: Monosynaptic retrograde tracing of neurons expressing the G-protein coupled receptor Gpr151 in the mouse brain.

Study concept and design: **JJB**, MG, TB, and AT. Acquisition of data: **JJB**, MG, and LDH. Analysis and interpretation of data: **JJB**, LDH, and AT. Writing of the manuscript: **JJB** and AT. Conceptualization and critical revision of the manuscript for intellectual content: AT and KM. Obtained funding: **JJB** and AT. Study supervision: AT.

Paper III: Investigating spexin and related neuropeptides as possible ligands of Gpr151.

Study concept and design: AT and **JJB**. Acquisition of data: **JJB**, LDH. Analysis and interpretation of data: **JJB**, AT. Writing of the manuscript: **JJB**, AT. Conceptualization and critical revision of the manuscript for intellectual content: AT. Obtained funding: **JJB** and AT. Study supervision: AT.

Paper IV: *Gad2* expressing interneurons in the mouse habenula.

Study concept and design: AT and **JJB**. Acquisition of data: **JJB**, MG, LDH. Analysis and interpretation of data: **JJB**, LDH, MG, AT. Writing of the manuscript: **JJB**, LDH, JE, AT. Conceptualization and critical revision of the manuscript for intellectual content: JE, AT. Obtained funding: **JJB** and AT. Study supervision: AT.

Paper 1

Published in final edited form as:
J Comp Neurol. 2015 February 15; 523(3): 359–380. doi:10.1002/cne.23664.

Conserved expression of the GPR151 receptor in habenular axonal projections of vertebrates

Jonas Broms[1,*], **Beatriz Antolin-Fontes**[2,*], **Anders Tingström**[1,#], and **Ines Ibañez-Tallon**[2,#]

[1]Psychiatric Neuromodulation Unit, Clinical Sciences, Lund University, Lund, Sweden

[2]Laboratory of Molecular Biology, The Rockefeller University, New York, U.S.A

Abstract

The habenula is a phylogenetically conserved brain structure in the epithalamus. It is a major node in the information flow between fronto-limbic brain regions and monoaminergic brainstem nuclei, thus anatomically and functionally ideally positioned to regulate emotional, motivational and cognitive behaviors. Consequently, the habenula may be critically important in the pathophysiology of psychiatric disorders such as addiction and depression. Here we investigated the expression pattern of GPR151, a G coupled-protein receptor (GPCR), whose mRNA has been identified as highly and specifically enriched in habenular neurons by in situ hybridization and Translating Ribosome Affinity Purification (TRAP). In the present immunohistochemical study we demonstrate a pronounced and highly specific expression of the GPR151 protein in the medial and lateral habenula of rodent brain. Specific expression was also seen in efferent habenular fibers projecting to the interpeduncular nucleus, the rostromedial tegmental area, the rhabdoid nucleus, the mesencephalic raphe nuclei and the dorsal tegmental nucleus. Using confocal microscopy and quantitative colocalization analysis we found that GPR151 expressing axons and terminals overlap with cholinergic, substance P-ergic and glutamatergic markers. Virtually identical expression pattern was observed in rat, mouse and zebrafish brains. Our data demonstrate that GPR151 is highly conserved, specific for a subdivision of the habenular neurocircuitry, and constitutes a promising novel target for psychiatric drug development.

Keywords

G protein-coupled receptor; fasciculus retroflexus; interpeduncular nucleus; rostromedial tegmental nucleus; rhabdoid nnucleus; raphe nucleus; MGI_MGI:3606630; RGD_737929; ZIRC_ZL1; AB_10743815; AB_10608138; AB_307210; AB_887876; AB_887878; AB_887883;

[#]Corresponding authors: Anders Tingström, M.D., Ph.D., Psychiatric Neuromodulation Unit, Biomedical Center, D11, Klinikgatan 30, 222 42 Lund, Sweden, anders.tingstrom@med.lu.se, Phone: +46-46-2220611. Ines Ibañez-Tallon, Ph.D., Laboratory of Molecular Biology, The Rockefeller University, 1230 York Avenue, Box 260, New York, NY 10065, USA, iibanez@rockefeller.edu, Phone: 1-212-327-7989.
[*]These authors contributed equally to this work

CONFLICT OF INTEREST STATEMENT
The authors declare no conflicts of interest.

ROLE OF AUTHORS
All authors had full access to all the data in the study and take responsibility for the integrity and presentation of the data. Study concept and design: AT and IIT. Acquisition of data: JB, BAF. Analysis and interpretation of data: JB, BAF, AT, IIT. Writing of the manuscript: JB, BAF, AT, IIT. Conceptualization and critical revision of the manuscript for intellectual content: AT, IIT. Obtained funding: AT, IIT. Study supervision: AT, IIT.

AB_887884; AB_2079751; AB_10123643; AB_477560; AB_261587; AB_90754; AB_572266; AB_628299; SciRes_000137

INTRODUCTION

The habenula is an ancient, highly conserved brain structure present throughout the vertebrate lineage. The habenula is a bilateral diencephalic structure that modulates brainstem monoaminergic and cholinoreceptive nuclei (Lecourtier and Kelly, 2007; Bianco and Wilson, 2009). In lower vertebrates (such as fish and amphibians) the habenula is asymmetric. In contrast, the mammalian habenula shows no lateralization. It is divided in medial (MHb) and lateral (LHb) nuclei that are readily distinguishable in Nissl preparations. In addition, as many as 15 subnuclei have been described using ultrastructural, morphological and cytochemical criteria (Andres et al., 1999; Geisler et al., 2003; Aizawa et al., 2012; Wagner et al., 2014). The habenula is thus a highly heterogeneous structure, and this is also reflected by its diverse connectivity. The habenula receives inputs primarily via the stria medullaris and sends outputs via the fasciculus retroflexus. The MHb receives afferents from the septum and the diagonal band of Broca and projects to the interpeduncular nucleus (IPN) (Herkenham and Nauta, 1977; 1979), while the LHb receives input from large portions of the ventral forebrain, including the lateral preoptic area, lateral hypothalamus and basal ganglia as well as the serotonergic dorsal raphe and the dopaminergic ventral tegmental area (VTA) (Herkenham and Nauta, 1977; Sim and Joseph, 1993). In turn, the LHb projects mainly to the VTA, the median and dorsal raphe, and the recently described rostromedial tegmental nucleus (RMTg) (Herkenham and Nauta, 1979; Jhou et al., 2009b; Kim, 2009).

The behavioral contributions of the LHb and MHb have traditionally been reported as segregated, despite the fact that these nuclei are adjacent to each other and that intra-habenular connectivity has been described (Kim and Chang, 2005). The MHb and its major target, the IPN, have emerged as key regions in the regulation of nicotine consumption and withdrawal (Fowler et al., 2011; Frahm et al., 2011; Salas et al., 2009). The MHb shows the highest concentration of nicotinic acetylcholine receptors (nAChRs) in the brain (90–100% of the neurons in the MHb express α3, α4, β2, β3 or β4 nAChRs) (Görlich et al., 2013; Hsu et al., 2013; Sheffield et al., 2000). Importantly genetic variants in the *CHRNA5-CHRNA3-CHRNB4* gene cluster encoding α5, α3 and β4 nAChR subunits have been linked to nicotine dependence and smoking related diseases in humans (Berrettini et al., 2008; Bierut et al., 2008; Lips et al., 2010; Liu JZ et al., 2010; Ware et al., 2011). Functional studies have shown that α5 and β4 nAChRs in the MHb-IPN pathway regulate nicotine intake and withdrawal (Fowler et al., 2011, Frahm et al., 2011, Zhao-Shea et al., 2013) and that MHb neurons display spontaneous phasic activity that is enhanced upon nicotine withdrawal (Görlich et al., 2013).

On the other hand the LHb has been shown to play a crucial role in negative reward and decision-making (Hikosaka, 2010; Stopper and Floresco, 2013). Phasic activation of LHb neurons occurs during aversive stimulation or when a less-than-expected reward is presented (Matsumoto and Hikosaka, 2007; 2009). When unexpected negative events occur, activation of LHb causes inhibition of dopaminergic neurons in the VTA. This inhibition, mediated

mainly via a GABAergic relay in the RMTg, gives rise to the reward-prediction error response of VTA neurons (Balcita-Pedicino et al., 2011). LHb neurons also display slow, tonic responses encoding temporal proximity to future rewards (Bromberg-Martin et al., 2010). Optogenetic stimulation of excitatory synapses in the LHb, as well as stimulation of axon terminals of LHb neurons in the RMTg, produce an avoidance response (Shabel et al., 2012; Stamatakis and Stuber, 2012). Investigations of human brain activity using fMRI have found increased BOLD responses in the habenula to negative feedback and negative reward prediction error (Ullsperger and Cramon, 2003; Salas et al., 2010) as well as when cues associated with painful stimulation are presented (Lawson et al., 2014). Based on these findings, it has been proposed that the LHb does not merely encode disappointment, but that it provides information about cost and uncertainty in order to facilitate optimal decision-making and learning (Stopper and Floresco, 2013).

Both the LHb and MHb show reduced volume in people affected with depression (Ranft et al., 2010), thus implicating both nuclei in the pathophysiology of this disorder. Serotonergic neurons in the dorsal raphe, known to be involved in depression, are inhibited by stimulation of the habenula (Wang and Aghajanian, 1977; Reisine et al., 1982; Park, 1987). In agreement, increased LHb metabolism and reduced brain serotonin levels have been observed in several animal models of depression. This effect can be reversed with antidepressant drugs (Caldecott-Hazard et al., 1988; Shumake and Gonzalez-Lima, 2013) or lesions of the LHb (Yang et al., 2008). In fact, inactivation of the habenula by deep brain stimulation has been used in the treatment of major depressive disorder (Sartorius and Henn, 2007; Sartorius et al., 2010). Moreover, neuroimaging studies have identified heightened habenula activity in depressed patients (Morris et al., 1999; Roiser et al., 2009). However, determining the specific functional contribution of MHb versus LHb in human in vivo studies will require higher fMRI resolution than the currently commonly used 7 Tesla scanners allow for (Viswanath et al., 2013).

One gene that has been found to be highly expressed in both the MHb and the LHb is *GPR151* whose mRNA has been detected by in situ hybridization in the cell bodies of habenular neurons in the ventral MHb and in sparse neurons of the LHb (Berthold et al., 2003; Aizawa et al., 2012; Quina et al., 2009). GPR151, also known as PGR7, GALR4, GPCR-2037 and GALRL, belongs to the A type of G protein-coupled receptor (GPCR) and shows the highest homology to the galanin receptors 2 and 3 but responds only very weakly to the neuropeptide galanin (Ignatov et al., 2004). To this date, no endogenous or synthetic ligand for this receptor has been reported and its function is still largely unknown. The *GPR151* gene is conserved in mammals (~83% identity in human versus rodent and ~89% in rat versus mouse) and has orthologs in chicken and zebrafish (NCBI HomoloGene). The zebrafish genome contains two nearly identical copies of the *probable gpr151-like* gene (LOC100538082 and LOC565170), which share homology with human *GPR151* (54% DNA sequence identity). While the in situ hybridization mRNA pattern of *Gpr151* has been reported in rodents (Berthold et al., 2003, Aizawa et al., 2012, Quina et al., 2003) and Translating Ribosome Affinity Purification (TRAP) assay, identified *Gpr151* mRNA as highly and specifically enriched in mouse habenular neurons (Görlich et al., 2013), no studies have addressed the localization of the GPR151 receptor protein.

The present study therefore sought to investigate the protein expression pattern of GPR151 in rats, mice and zebrafish. Given the homologous organization of habenular subnuclei between mice and rat (Wagner et al., 2014), and the similar habenular neurocircuitry in fish (Amo et al., 2010), we compared the GPR151 immunoreactivity between these species, to determine whether GPR151 could be used as a marker for a conserved population of medial and lateral habenular neurons, that could further facilitate functional studies in all three model organisms. In order to characterize the GPR151 expressing neurons we used a combination of markers for known habenular neurotransmitters such as acetylcholine, substance P and glutamate, as well as markers for dopamine and serotonin to identify monoaminergic neuronal populations innervated by GPR151 positive projections.

MATERIALS AND METHODS

Animals

Mice and rats were housed with *ad libitum* access to standard lab chow and water in a room air conditioned at 22°C–23°C with a standard 12 hr light/dark cycle (lights on 7:00 am, off 7:00 pm), with a maximum of five mice or three rats per cage. GPR151 knockout mice (GPR151^{tm1Dgen}, RRID:MGI_MGI:3606630), where a *lacZ* reporter gene was inserted in place of the *Gpr151* exon, were obtained from Deltagen. They were backcrossed to C57BL/6J for eight generations. Six wild type C57BL/6J mice (The Jackson Laboratory, RRID:IMSR_JAX:000664), three *Gpr151*$^{-/-}$ mice and six Crl:WI Wistar rats (Charles River, Germany, RRID:RGD_737929) aged 8–12 weeks were used for experiments and were perfused between 10am and 2pm.

Fixation of mouse and rat brain tissue

The animals were deeply anesthetized by injecting an overdose of pentobarbital and perfused transcardially with 100 ml of cold isotonic NaCl solution (0.9%) followed by 200 ml of cold sodium phosphate buffered saline (PBS) containing 4% paraformaldehyde (PFA). The brains were then dissected and post fixed in 4% PFA for 24 hours at 4°C. A shorter post fixation time of 2 hours yielded uneven and weak immunostaining, especially in rat tissue. After post fixation, the brains were immersed in sucrose solution (25% in PBS) at 4°C for 2–3 days until equilibration had occurred (i.e. the brains sank to the bottom of the vial). The brains were sectioned in 40 μm sections using a sliding microtome (Thermo Scientific HM450), cryoprotected in antifreeze solution (30% glycerol, 30% ethylene glycol, 40% 0.5M PBS), and stored at −20°C until commencing immunohistochemistry.

Immunohistochemistry of mouse and rat sections

After rinsing in sodium phosphate buffered saline solution (PBS), free-floating brain sections were blocked in PBS containing normal serum (10% in mouse, 5% in rat) and 0.3% TritonX-100 for 1 hour. The normal serum matched the species in which the secondary antibodies were raised. Sections were then incubated overnight at 4°C with primary antibodies (Table 1) diluted in blocking solution. Subsequently, sections were washed with PBS and incubated for 2 hours at room temperature with secondary antibodies (Table 2). Sections were then washed twice for 15 minutes in PBS and counterstained with the nuclear stain DAPI at 1 μg/ml in PBS for 10 minutes. The sections were then mounted on Superfrost

Plus glass (Menzel-Gläser, Germany) and coverslipped with ImmuMount™ (Thermo Scientific).

For visualization of immunoreactivity for light microscopy, brain sections were incubated with a biotinylated anti-mouse secondary antibody made in horse (Vector Laboratories), followed by incubation with avidin-biotin-peroxidase complex (diluted 1:125 in PBS) (VECTASTAIN Elite ABC Kit, Vector Laboratories) and 3,3′-diaminobenzidine (DAB). Following the DAB reaction, sections were mounted, dehydrated in increasing concentrations of ethanol followed by xylene and finally coverslipped with DPX (Fisher Scientific).

The primary antibodies used in the experiment are listed in Table 1. When using VGLUT1 and VGLUT2 antibodies, TritonX-100 was omitted in order to preserve synaptic membranes. Heat mediated antigen retrieval, 15 minutes at 95°C in citric acid (pH 6.0), was performed prior to incubation with the ChAT antibody to enhance immunostaining.

Confocal fluorescent images were acquired with a Zeiss LSM700 confocal microscope. Brightness and contrast of the images was adjusted with Adobe Photoshop CS6.

Preparation of zebrafish brain tissue

Two adult zebrafish (7 months old, AB strain, RRID:ZIRC_ZL1) were rapidly chilled in ice cold water and subsequently immersed in PFA solution (4% in PBS) for 24 hours. The brains were then dissected and equilibrated in sucrose (20% in PBS). Subsequently, the brains were incubated in PBS containing 7.5% gelatin and 20% sucrose at 37°C for 2 hours. The brains were then put in to fresh gelatin-sucrose molds and cut into blocks. The blocks were cut in 14 μm transverse sections on a cryomicrotome and mounted on Superfrost Plus glass (Menzel-Gläser, Germany). Immunohistochemistry was performed as for mouse and rat sections except that incubation with GPR151 antibodies was performed directly on the glass instead of free-floating. Two polyclonal antibodies (raised in mouse and rabbit) against human GPR151 were used (described below).

Colocalization analysis

Images that were used for colocalization analysis were acquired with a 63x oil immersion objective on a Zeiss LSM700 confocal microscope. The detection pinhole was set to 1 Airy unit in order to maximize signal-to-noise. The channels where captured in sequence to minimize the risk of bleed-through. The intensity gain was adjusted for each channel before capture in order to avoid saturated pixels, and the intensity range of the images was left untouched to preserve linearity. Colocalization analysis was performed with the Coloc 2 plugin in the Fiji image processing package (v. 1.48, RRID:SciRes_000137). Background was eliminated by median subtraction (Dunn et al., 2011). Manders' colocalization coefficients, M1 and M2, which are proportional to the number of colocalizing pixels in each channel relative to the total number of pixels in that channel were calculated (Manders et al., 1994). M1 or M2 > 0.55 indicates colocalization (Zinchuk and Grossenbacher-Zinchuk, 2014). In the present study, only M1 is presented and refers to the proportion of pixels with Gpr151 immunoreactivity that colocalize with a second marker. Costes' test for statistical significance was used to determine that the colocalization coefficients obtained

where not due to random effects (Costes et. al., 2004). In the test, one channel is scrambled repeatedly (n=100) and correlated with the other channel, which results in a Costes' P-value where P is the proportion of random images that are less correlated than the original. A P-value > 0.95 indicates statistically significant correlation.

Antibody characterization

The antibodies used in the study are indicated below. Concentrations for optimal signal-to-noise ratio were determined for each antibody based on literature and serial dilution of the antibody. In all preparations, some sections were prepared identically except for omitting the primary antibody in order to ensure that the observed signal was not due to non-specific binding of the secondary antibody. Working concentrations (for purified antibodies) or dilutions (for non-purified antibodies) of primary antibodies are provided in Table 1.

1. Rabbit GPR151 polyclonal antibody (SAB4500418, Sigma-Aldrich) is raised against a synthetic peptide containing amino acids 370–419 (*EKEKPSSPSSGKGKTEKAEIPILPDVEQFWHERDTVPSVQDNDPIPWEHEDQETGEGVK)* of the C-terminal of human GPR151. It recognizes a single band of 46 kDa on western blots of K562 cell lysate. The specificity was confirmed by pre-adsorption with the immunogen peptide (according to manufacturer's technical information). Antibody specificity was in the present study verified using *Gpr151*$^{-/-}$ mice (see below).
2. Mouse GPR151 polyclonal antibody (SAB1402000, Sigma-Aldrich) is raised against full-length human GPR151 protein. Western blots of GPR151 transfected HEK293T lysate shows a band at ~46 kDa, which was not present in lysate of non-transfected cells (according to manufacturer's technical information). This antibody produce the same pattern of staining as the rabbit anti GPR151 polyclonal and is discussed below.
3. Rabbit VGLUT1 polyclonal antibody (135 303, Synaptic Systems) is generated against Strep-Tag® fusion protein of rat VGLUT1, containing amino acid residues 456–560 (*TLSGMVCPIIVGAMT)*. The antibody is affinity purified using the immunogen. Immunoreactivity in brain sections was abolished by pre-adsorption with the immunogen (Zhou et al., 2007). Western blot of lysate of cerebellum and cochlear nucleus in guinea pig detects a band at ~60 kDa. The molecular weight corresponds to what has previously been reported for the VGLUT1 protein (Takamori et al., 2000). No staining was observed in VGLUT1$^{-/-}$ mice (Wojcik et al., 2004).
4. Guinea pig VGLUT1 polyclonal antibody (135 304, Synaptic Systems) is generated against a purified recombinant protein of rat VGLUT 1, containing amino acid residues 456–560 (*TLSGMVCPIIVGAMT)*. The antibody recognizes one major broad band of the expected molecular weight (50–60 kDa) on western blots of a synaptic vesicle fraction of rat brain (LP2) and immunostaining is absent in VGLUT1$^{-/-}$ mice (according to the manufacturer). The antibody has been shown to produce an identical immunostaining pattern as the rabbit VGLUT1 polyclonal antibody in rat striatum and cortex (Wouterlood et al., 2012).

5. Rabbit VGLUT2 polyclonal antibody (135 403, Synaptic Systems) is raised against Strep-Tag® fusion protein of rat VGLUT2, containing amino acid residues 510–582 (*EKQPWADPEETSEEKCGFIHEDELDEETGDITQNYINYGTTKSYGATSQENGG WPNGEKKEEFVQESAQDAYSYKDRDDYS)*. Selective immunoreactivity in brain sections has been demonstrated by pre-adsorption with the immunogen (Zhou et al., 2007). Western blot of lysate of cerebellum and cochlear nucleus detects a band at ~65 kDa which corresponds to previous reports (Takamori et al., 2001).

6. Guinea pig VGLUT2 polyclonal antibody (135 404, Synaptic Systems) is generated against a purified recombinant protein of rat VGLUT2, containing amino acid residues 510–582 (*EKQPWADPEETSEEKCGFIHEDELDEETGDITQNYINYGTTKSYGATSQENGG WPNGEKKEEFVQESAQDAYSYKDRDDYS)*. The antibody recognizes one major broad band of the expected molecular weight (65 kDa) on western blots of a synaptic vesicle fraction of rat brain and immunostaining was abolished by pre-adsorption with the immunogen (according to the manufacturer). No cross-reactivity against VGLUT1 or VGLUT3 was observed.

7. Goat choline acetyltransferase (ChAT) polyclonal antibody (AB144P, Millipore) is raised against human placental choline acetyltransferase enzyme. The antibody recognizes a single band of 68–70 kDa on western blots of mouse brain (according to the manufacturer). This antibody has previously been used to investigate the expression of ChAT in the rat habenula (Aizawa et al., 2012) and yields the same pattern of expression as other ChAT antibodies (Contestabile et al., 1987).

8. Mouse neurofilament H monoclonal antibody (SMI-32R, clone SMI-32, Covance) is raised against homogenized hypothalami from Fischer 344 rat brain (Sternberger et al., 1982). This antibody recognizes a non-phosphorylated epitope on the neurofilament heavy polypeptide in human and monkey brain lysate (Campbell and Morrison, 1989). The antibody has previously been used to differentiate between different subnuclei in the rat and mouse LHb (Geisler et al., 2003; Wagner et al., 2014).

9. Mouse monoclonal tyrosine hydroxylase (TH) antibody (T1299, clone TH-2, Sigma-Aldrich) is derived from a hybridoma produced by the fusion of mouse myeloma cells and splenocytes from a mouse immunized against whole-rat TH protein (Haycock et al., 1993). The antibody recognizes an epitope (amino acids 9–16) present in the N-terminal region of both rodent (~60 kDa) and human (62–68 kDa) TH (Haycock et al., 1993). Its specificity for dopaminergic neurons was demonstrated by the topographic distribution of immunoreactive TH cell bodies and axon terminals in different brain regions and by their near total disappearance from mesencephalon and striatum after neonatal 6-OHDA lesion (Bérubé-Carrière et al., 2009).

10. Mouse tryptophan hydroxylase (TPH) monoclonal antibody (T0678, clone WH-3, Sigma-Aldrich) is raised against recombinant rabbit TPH. The antibody detects a band at 55 kDa on western blot of rabbit pineal gland (according to the

manufacturer). The pattern of immunoreactive cells marked by this antibody corresponded well to known serotonergic nuclei and has been used extensively as a marker of serotonergic neurons (Liu and Wong-Riley, 2010; Sevigny et al., 2012).

11. Sheep TPH polyclonal antibody (AB1541, Chemicon) is raised against a recombinant rabbit TPH, isolated as inclusion bodies from E. coli and purified by preparative SDS-PAGE. It recognizes a major band of 55 kDa molecular weight on western blot from rat dorsal raphe that corresponds to TPH; a less intense band can be observed at 62–65 kDa, indicating a partial cross-reactivity with TH (Chemicon datasheet). The cross-reactivity with TH did not affect our conclusions since we used the antibody only to localize the TPH-positive cell bodies present in the raphe nuclei. The antibody produces an identical pattern of staining as the mouse TPH monoclonal antibody and has previously been used to identify TPH expressing neurons in the raphe nuclei (Kaufling et al., 2009).

12. Rabbit substance P polyclonal antibody (20064, Immunostar) is raised against synthetic substance P coupled to keyhole limpet hemocyanin with carbodiimide. Immunolabeling was significant in rat dorsal horn and substantia nigra (according to the manufacturer). Pre-adsorption with substance P (10μg/ml) completely abolishes immunolabeling while incubation with neurokinin A, neurokinin B, somatostatin or neuropeptide K did not affect immunolabeling (manufacturer's specification; Weissner et al., 2006).

13. Rat substance P monoclonal antibody (sc-21715, Santa Cruz) is raised against eight-amino acids of the COOH-terminal fragment of substance P (NC1/34HL). The antibody does not cross react with β-endorphin, somatostatin, leu-enkephalin, or met-enkephalin. The specificity was verified by pre-adsorption with synthetic substance P (220μg/ml) (Cuello et al., 1979).

14. Chicken β-galactosidase polyclonal antibody (AB9361, Abcam) is raised against the purified full length native Escherichia coli (E. coli) protein and immunoaffinity purified using purified β-galactosidase immobilized on a solid phase. The antibody specificity was confirmed by the absence of staining in wild-type animals.

RESULTS

Comparable expression of GPR151 in habenular axonal projections in rat and mouse brain

To begin to assess the expression pattern of GPR151 we analyzed serial brain section of mouse and rat using two different antibodies against GPR151. Both antibodies yielded robust and comparable immunoreactivity in habenular axons, and no signal was detected in brain sections of *Gpr151*$^{-/-}$ mice (Fig. 1 A1–J1) confirming the antibody specificity. GPR151 immunoreactivity was detected in axonal fibers originating in the habenula (Fig. 1 A,B), continuing through the fasciculus retroflexus (FR) (Fig. 1 C,D) and contacting the IPN (Fig. 1 E,F). Caudal to the IPN, GPR151 immunoreactive fibers continued in a dorsocaudal direction through the RMTg (Fig. 1 F,G), rhabdoid nucleus (Fig. 1 G,H), median and paramedian raphe (Fig. 1G,H) and dorsal raphe nucleus (Fig. 1 I,J). Comparative analyses of mouse and rat brains at similar section planes revealed a strikingly high similarity in the

pattern of GPR151-immunoreactive neuronal projections between mouse (Fig. 1 A–J) and rat (Fig. 1 A2–J2)

Conserved GPR151 immunoreactivity in the habenular circuitry of zebrafish

Interestingly the human *GPR151* gene shows 54% identity with two loci in the zebrafish genome that may encode two probable Gpr151-like receptors, which only differ between each other in one amino acid residue (NCBI HomoloGene). These two loci LOC100538082 and LOC565170 are in very close proximity to each other in chromosome 14 of *D. rerio* adjacent to two genes (tcerg1 and ppp2r2), which are also neighboring *GPR151* in chromosome 5 in the human genome. This raises the possibility that the genomic locus containing *GPR151* has been preserved during evolution but that one copy of the probable *Gpr151-like* receptor gene in zebrafish has been lost in higher vertebrates.

We wanted to test whether antibodies raised against the human GPR151 protein could recognize the zebrafish putative Gpr151-like receptor, which shows 45% identity at the protein level. As shown in figure 2, a remarkably similar and selective immunoreactivity for habenular circuitry as found in rat and mouse brain was also seen in the zebrafish with strong expression in axonal projections originating in the habenula (Fig. 2A), and coursing via the FR (Fig. 2B) to the IPN (Fig. 2C) and ventral median raphe (Fig. 2D). Double immunofluorescence staining using rabbit and mouse polyclonal antibodies resulted in completely overlapping labeling (data not shown). Tracing and immunostaining studies in zebrafish have determined that the dorsal habenula is asymmetric, projects to the IPN and corresponds to the MHb of mammals, while the ventral habenula is homologous to the LHb in mammals, projects to the median raphe and is not lateralized (Amo et al., 2010). Thus, consistent with GPR151 expression in MHb and LHb projections in rodents, Gpr151 is present in the homologous habenular axonal projections to the IPN and raphe in zebrafish. Dense immunoreactivity was observed in fibers in the dorsal habenula while the ventral habenula was only very sparsely labeled. This pattern was also reflected in the strong Gpr151 positive innervation of the interpeduncular nucleus, while only a few axon terminals were observed in the ventral median raphe (Fig. 2). Altogether, these results show that the protein expression pattern of GPR151 is highly conserved.

Expression of GPR151 in habenular subnuclei

We next examined in detail the expression of GPR151 in the habenula. To this end we compared the GPR151 immunoreactivity to the *lacZ* reporter signal in *Gpr151*$^{-/-}$ mice (Fig. 3A) and to different markers that have been employed to subdivide the habenular subnuclei in mouse and rat (Fig. 3B–U). The MHb can be subdivided in a ventral (vMHb) and a dorsal (dMHb) part. Neurons in the dMHb express substance P (SP) (Contestabile et al., 1987; Cuello et al., 1978) and project to the rostral and lateral subnuclei of the IPN (Contestabile et al., 1987). Neurons in the vMHb express the ACh synthesizing enzyme choline acetyltransferase (ChAT) (Aizawa et al., 2012) and project to the central and intermediate subnuclei of IPN (Contestabile et al., 1987). In the MHb, GPR151 was detected in the cholinergic vMHb (Fig. 3C–E, M–O), but not in the SP expressing dMHb (Fig. 3B, F–H, P–R). In *Gpr151*$^{-/-}$ mice, where the bacterial *lacZ* reporter gene is expressed under the control of the *Gpr151* gene regulatory sequences, βGal immunoreactivity was confined to habenular

cell bodies (Fig. 3A). In the MHb βGal-positive cells were only detected in vMHb, consistent with in situ hybridization reports for *Gpr151* mRNA (Aizawa et al., 2012).

In addition GPR151 was also present in the LHb. To evaluate the localization of GPR151 within subnuclei of the LHb, we used the delineation of habenular subdivisions in rat and mouse proposed by Wagner and colleagues (Wagner et al., 2014). The LHb is composed of a medial and a lateral subregion. The medial LHb is further subdivided into the superior (LHbMS), parvocellular (LHbMPc), central (LHbMC), marginal (LHbMMg) subnuclei (Fig. 3A,B,L). The lateral LHb is subdivided into the parvocellular (LHbLPc), magnocellular (LHbLMc), oval (LHbLO), basal (LHbLB), and marginal (LHbLMg) subnuclei (Fig. 3A,B,L). Consistent with the previously reported expression of *Gpr151* mRNA (Aizawa et al., 2012), βGal-positive cells in *Gpr151*$^{-/-}$ mice were scattered throughout the LHb with a tendency for a more marked expression in the dorsal part (containing the LHbMS and LHbLPc) (Fig. 3A). In addition, given that neurofilament H (NF-H) has been used as a marker to delineate the LHb subnuclei of rat and mouse brain sections (Geisler et al., 2003; Wagner et al., 2014), we performed colabeling of GPR151 and NF-H. As observed in figure 3, LHbMPc and LHbMC are completely devoid of NF-H immunoreactivity. In contrast, GPR151 immunoreactivity is strongly expressed in these subnuclei (Fig. 3I–K, L, S–U).

GPR151 expression in habenular efferents projecting to the IPN and not the VTA

Given that Gpr151 mRNA and βGal reporter expression is highly concentrated in the MHb (Fig 3A; Görlich et al., 2013) and that the major output of the MHb is the IPN, we next investigated the expression of GPR151 in habenular axons that innervate the IPN. GPR151 expression was extremely prominent in the rostral (IPR), dorsomedial (IPDM), dorsolateral (IPDL) and apical subnuclei (IPA) but immunoreactivity in the central (IPC), intermediate (IPI) and lateral IPN (IPL) was also observed (Fig. 4,5,6). It has been shown that the vesicular glutamate transporter VGLUT1 is expressed in MHb neurons but not in LHb neurons (Aizawa et al., 2012) and that within the MHb, cholinergic neurons in the ventral part co-release ACh and glutamate (Ren et al., 2011). Therefore we performed double staining of GPR151 with ChAT (Fig. 4A–H) and VGLUT1 (Fig. 4I–P) antibodies to evaluate whether GPR151 is specifically expressed in cholinergic and/or glutamatergic terminals. In order to quantify the degree of overlap we calculated Manders' colocalization coefficient. The statistical significance of this colocalization was given by the Costes' P-value. Colocalization between GPR151 and VGLUT1 was statistically significant (mouse, P=1.0; rat, P=1.0) and moderately overlapping (Fig. 4I–P; mouse M1=0.71; rat M1=0.88). A significant and more pronounced colocalization of GPR151 and ChAT was observed in the rostral subnucleus and in the dorsal part of the central subnucleus (Fig. 4A–H; mouse M1=0.83, P=1.0; rat M1=0.99, P=1.0). These results indicate that a major proportion of GPR151 habenular fibers projecting to the IPN are glutamatergic and that a high number are cholinergic. Possibly, those GPR151-fibers are both glutamatergic and cholinergic (Ren et al., 2011).

The VTA is adjacent to the IPN and innervated by LHb (Herkenham and Nauta, 1979). To evaluate whether GPR151 positive axonal fibers innervate this region, we performed

immunostaining for the dopaminergic marker tyrosine hydroxylase (TH). This marker delineates the sharp boundary between the IPN and the VTA (Fig. 5B,E). Colabeling with GPR151 and TH in mouse and rat brain section clearly show that LHb neurons that express GPR151 do not terminate in the VTA region (Fig. 5A–F).

GPR151 expression in habenular neurons projecting to the RMTg and rhabdoid nucleus

In addition to the VTA, the LHb has been shown to project to forebrain areas including the ventrolateral septum and the substantia innominata, to midbrain areas including the RMTg, to the median and dorsal raphe nuclei and to hindbrain areas, including the laterodorsal and dorsal tegmental nucleus, the locus coeruleus (Herkenham and Nauta, 1979; Jhou et al., 2009b; Lecourtier and Kelly, 2007) and the nucleus incertus (Goto et al., 2001; Olucha-Bordonau et al., 2003). We analyzed sagittal sections including forebrain, midbrain and hindbrain regions and detected habenular GPR151 fibers continuing caudally through the IPN, via the rhabdoid nucleus reaching mesencephalic raphe nuclei and the dorsal tegmental nucleus (Fig. 6). However, no immunoreactivity was observed in the forebrain, indicating that GPR151 positive neurons of the habenula do not project to forebrain areas. The rhabdoid nucleus is a bilateral structure extending from the IPN to the dorsal raphe nucleus and the dorsal tegmentum (Fig. 6). To examine whether GPR151 immunoreactive projections in the rhabdoid nucleus originated from glutamatergic LHb neurons, we performed double immunolabeling of GPR151 and VGLUT2 (Fig. 7A–J). A statistically significant colocalization of GPR151 and VGLUT2 was observed in the rhabdoid nucleus (Fig. 7A–J; mouse M1=0.82, P=1.0; rat M1=0.59, P=1.0). This finding supports that at least part of the GPR151 positive neurons may be glutamatergic. Since previous studies have demonstrated dense SP immunoreactivity in the rhabdoid nucleus (Paxinos, 2004), we next carried out GPR151 and SP double immunofluorescence stainings. Even though partial colocalization of SP and GPR151 in the rhabdoid nucleus was revealed (Fig. 7K–T; mouse M1=0.65, P=1.0; rat M1=0.84, P=1.0), we cannot conclude whether GPR151 projections from the LHb are also SP-ergic or whether GPR151 projections from LHb are travelling together with SP fibers originating elsewhere.

Furthermore, the LHb has been shown to send glutamatergic projections to the RMTg which acts as an inhibitory center of the midbrain dopaminergic cells (Balcita-Pedicino et al., 2011; Ferreira et al., 2008; Geisler and Zahm, 2005; Jhou et al., 2009a). The RMTg, also known as the tail of the VTA, extends from the caudal pole of the VTA into the mesopontine tegmentum (Jhou et al., 2009a,b; Bourdy and Barrot, 2012). GPR151 immunofluorescence staining on mouse and rat coronal sections showed heavy GPR151 expression in RMTg (Fig. 8). Since most LHb neurons are glutamatergic and known to express the vesicular glutamate transporter 2 (VGLUT2) (Aizawa et al., 2012), we performed double labeling for this transporter and GPR151. Colocalization was indeed observed in terminals located in the RMTg (Fig. 8; mouse M1=0.72, P=1.0; rat M1=0.62, P=1.0), indicating the existence of glutamatergic GPR151 positive neurons projecting from the LHb to the RMTg.

GPR151 immunoreactive projections to the mesencephalic raphe nuclei and the dorsal tegmental nucleus

We next analyzed GPR151 immunoreactive projections to the mesencephalic raphe nuclei. Results from previous anterograde tracing studies targeting the LHb show labeling at the median, paramedian and dorsal raphe nucleus (Gonçalves et al., 2012; Kim, 2009; Sego et al., 2014). In agreement with these studies, we observed GPR151 positive fibers (presumably originating in the LHb) in the median, paramedian and dorsal raphe (Fig. 6 and 9).

GPR151 immunostaining in coronal rat and mouse brain sections at the level of the dorsal raphe showed GPR151 expression particularly in the interfascicular and caudal subnucleus (Fig. 9). Some GPR151 positive fibers appear to make contact with serotonergic neurons positive for the tryptophan hydroxylase (TPH) serotonergic marker (Fig. 9D–F,J–L, arrows), suggesting that LHb GPR151 expressing neurons may be implicated in dorsal raphe functions such as motivation and reward seeking.

In addition to GPR151 expression in the dorsal raphe, we also observed sparse GPR151 immunoreactivity in the dorsal tegmental nucleus in both sagittal (Fig. 6) and coronal rodent brain sections (Fig. 9A–C,G–I). Projections from LHb to the dorsal tegmental nucleus have been previously documented (Liu et al., 1984; Kim, 2009).

DISCUSSION

In the present study we investigated the anatomical and subcellular protein localization of the G protein-coupled receptor GPR151 in the brain of mammals and fish. We show that this receptor marks a specific and conserved subset of habenular axonal projections in vertebrates. GPR151 is not expressed in the soma of habenular neurons, but in their axonal projections. GPR151 immunoreactivity in selective habenular axonal projections and colocalization with neurotransmitter marker proteins, establish that GPR151 positive neurons in habenula project to the IPN, the RMTg, the rhabdoid nucleus, the mesencephalic raphe nuclei and the dorsal tegmentum (Fig. 10). Below we discuss the conservation of habenular nuclei in mouse and rat evidenced by GPR151 topographic distribution, and the specific axonal projections to discrete nuclei in the midbrain.

GPR151 immunoreactivity highlights the conservation of habenula subnuclear architecture

In the present study, we investigated the expression of GPR151 by immunohistochemical analysis of rat and mouse brain sections and confirmed the specificity of the antibodies using *Gpr151*$^{-/-}$ mice. Consistent with *Gpr151* mRNA expression (Aizawa et al., 2012) we observed immuno βGal staining in *Gpr151*$^{-/-}$ mice containing the lacZ reporter in the ventral MHb and scattered throughout the LHb with a marked expression in LHbMS (Fig. 3A).

We found that GPR151 immunoreactivity is not localized to neuronal cell bodies, but to their axonal projections. Within the habenula, GPR151 positive neurites are especially enriched in the parvocellular subnucleus LHbMPc (Fig. 3), a subnucleus in the LHb reliably

detected because it is largely devoid of neurofilament-H (NF-H) both in rat and mouse. Nissl staining of this area shows densely packed small neurons in agreement with its designation as the parvocellular subnucleus (Wagner et al., 2014). Interestingly this subnucleus has very weak *Gpr151* in situ hybridization signal (Aizawa et al., 2012) and lacks βGal immunoreactivity in *Gpr151*$^{-/-}$ mice (Fig. 3A), indicating that cell bodies in the LHbMPc do not express the GPR151 protein. However, it is remarkable that LHbMPc is transversed by very few fibers positive for NF-H and Kir2.3 which both label dense fiber complexes in other habenula subnuclei (Geisler et al., 2003; Wagner et al., 2014). Kir2.3 channel subunits are expressed in dendrites in many types of neurons (Inanobe et al., 2002), while NF-H is abundant in large dendritic trees (Kong et al., 1998) but also expressed in axons (Marszalek et al., 1996). Given the dense network of GPR151-positive fibers in the LHbMPc, and the lack of Kir2.3 and NF-H in this subnucleus, it is tempting to speculate that these fibers are indeed habenular axons converging at this site and continuing through the FR to target areas in the brainstem. Although topographically organized commissural projections from the LHb to the contralateral LHb have been described (Kim, 2009), these do not seem to project to the LHbMPc but to more central and lateral LHb subnuclei. In conclusion, GPR151 is a valuable marker to identify and correlate several subnuclei in rat and mice habenula including the cholinergic ventral medial habenula and the conspicuous LHbMPc.

Habenular GPR151 positive projections to the IPN

While it is established that the major input to the IPN originates in the MHb and that these projections are organized in a dorso-ventral to latero-central topographic manner (i.e. substance P projections from the dorsal MHb to the IPL and cholinergic projections from the ventral MHb to the IPC), it has been controversial and much more difficult to visualize whether the lateral habenula also sends projections to the IPN (Kim, 2009). In the present study we detected very intense GPR151 immunoreactivity in habenular axons terminating in the IPN. In the IPC, GPR151 immunoreactivity colocalized with ChAT and the glutamatergic marker VGLUT1 (Fig. 4). This is consistent with the fact that GPR151 is highly enriched in cholinergic neurons located in the ventral medial habenula (Görlich et al., 2013; Aizawa et al., 2012; Fig. 3) that project mainly to the IPC and co-release glutamate (Ren et al., 2011). However GPR151 was also present in non-cholinergic habenular terminals in the IPL (Fig. 4A,E), which is mostly innervated by substance P projections form the dorsal MHb. Since GPR151 is not expressed in the dorsal MHb (Fig. 3), these results indicate that the GPR151 positive projections that we detect in the IPL might in fact originate from the lateral habenula. Such projections to the IPL have been visualized using anterograde tracers injected in the central and medial subregions of the lateral habenula (Kim, 2009).

This is interesting as it indicates that GPR151-positive projections from both the lateral and medial habenula terminate in the IPN. Given that the cholinergic MHb-IPN circuit has emerged as key pathway in the regulation of nicotine reinforcement, dependence and withdrawal (Fowler et al., 2011; Frahm et al., 2011; Glick et al., 2011; Salas et al., 2009), it is tempting to hypothesize that GPR151 modulates nicotine-mediated behaviors.

Habenular GPR151 positive projections to the RMTg

The LHb has been shown to project predominantly to the substantia nigra, VTA, raphe nuclei (Herkenham and Nauta, 1979) and RMTg (Gonçalves et al., 2012; Jhou et al., 2009b; Kaufling et al., 2009). Interestingly we did not observe GPR151 staining in the substantia nigra or in the VTA (Fig. 5), indicating that GPR151 is not expressed in the subpopulation of LHb neurons that directly innervate these dopaminergic areas. However we detected strong immunoreactivity in the RMTg (Fig. 8) and since the RMTg acts as an inhibitory center of the substantia nigra and VTA (Balcita-Pedicino et al., 2011; Ferreira et al., 2008; Geisler and Zahm, 2005; Jhou et al., 2009a), it is possible that GPR151 positive habenular efferents to the RMTg indirectly modulate dopaminergic neurons in the midbrain, and thereby the motivational aspects of reinforcement learning and decision-making. In fact, specific (diphtheria toxin-mediated) ablation of neurons expressing *Gpr151* caused a broad range of cognitive deficits, including delay and effort aversion in a decision-making test (Kobayashi et al., 2013). RMTg neurons also project to the dorsal raphe where they terminate mainly on glutamatergic neurons (Lavezzi et al., 2011; Sego et al., 2014). Further studies are needed to determine if the neurons in the RMTg innervated by GPR151 habenular axons, preferentially target VTA, substantia nigra or the dorsal raphe.

Habenular GPR151 positive projections to the rhabdoid nucleus

In addition we observed strong GPR151 immunolabeling in the rhabdoid nucleus (Figure 6–8). The rhabdoid nucleus is a bilateral structure dorsal to the median raphe nucleus that stretches from the IPN to the dorsal raphe nucleus (Fig. 6), and is readily visible in acetylcholine esterase histochemical preparations (Paxinos and Watson, 2006). The nucleus has previously been reported to exhibit rich substance P immunoreactivity (Paxinos, 2004), which was confirmed in our study (Fig. 7). Projections from habenula to the rhabdoid nucleus have not previously been described. In fact, the connectivity and function of the rhabdoid nucleus is poorly understood. One study showed substance P containing axons that appeared to originate from the dorsal rhabdoid nucleus and terminate primarily on dendrites of serotonergic neurons (Lacoste et al., 2009). Bilateral lesioning of the habenula abolished substance P immunoreactivity in this region. Habenular lesions also decreased the concentration of substance P in the dorsal raphe (Neckers et al., 1979; Vincent et al., 1980). Given that substance P has been reported to have both excitatory and inhibitory effects on neurons in the dorsal raphe (Valentino et al., 2003), and that these terminals coexpress GPR151, it could be hypothesized that GPR151 regulates substance P neurotransmission in the dorsal raphe and thereby modulating serotonergic neuronal activity. The origin of the substance P in the rhabdoid nucleus, is not clear. We detected substance P neurons in the dorsal MHb, but this region is devoid of *Gpr151* expressing neurons (Fig. 3A; Aizawa et al., 2012). However, we also observed substance P immunoreactivity in neurons of the medial part of the LHb which show scattered expression of *Gpr151* (Fig. 3A). Further studies at electronmicroscopic level are needed to clarify the details of substance P and GPR151 expression in the rhabdoid nucleus. Nonetheless the studies presented here demonstrate that GPR151 can be used as a marker to localize the rhabdoid nucleus, which could facilitate further studies to gain insight into the biological role of this brain area.

GPR151 habenular projections to brainstem serotonergic nuclei

We also detected GPR151 positive fibers in the serotonergic median, paramedian and dorsal raphe nuclei (Fig. 9). Both indirect and direct habenular projections to serotonergic neurons in the dorsal raphe have previously been reported. In the present study, we observed GPR151 positive fibers making contact to serotonergic neurons in the dorsal raphe (Fig. 9, arrows). Electrical stimulation of the LHb decreases serotonin release in the caudate nucleus and substantia nigra, an effect that could be blocked by infusion of the $GABA_A$ receptor antagonist picrotoxin in the dorsal raphe (Reisine et al., 1982). Stimulation of the LHb also modulates serotonin release in the hippocampus, mediated through both direct and indirect projections to the dorsal raphe (Ferraro et al., 1997). The presence of GPR151 in axonal terminals innervating serotonergic neurons, raises the possibility that GPR151 could modulate serotonin release, which in turn would have implications for pain, stress, sleep and depressive-like behavior.

GPR151 habenular projections to the dorsal tegmental nucleus

Finally, we observed GPR151 immunoreactive axons projecting to the dorsal tegmental nucleus, mainly to the central part (DTgC) (Fig. 6 and 9). This is in agreement with previous reports describing the projections from LHb to the dorsal tegmental nucleus (Liu et al., 1984). The dorsal tegmental nucleus contains cells that signal the animal's momentary directional heading and thus it is thought to be involved in navigation. Moreover, Sharp et al. reported that activity of 10% of the LHb neurons correlated with angular head motion (Sharp et al., 2006). In summary, GPR151 may possibly modulate these functions controlled by the dorsal tegmental nucleus.

CONCLUDING REMARKS

In summary, GPR151 expression in the rat, mouse and zebrafish brain is restricted to habenular neurons projecting to the IPN, RMTg, rhabdoid nucleus, mesencephalic raphe nuclei and dorsal tegmental nucleus. The medial and lateral habenula have traditionally been considered as functionally segregated. However GPR151 expression in both habenular subdivisions raises the possibility that GPR151 projection targets may constitute a functional system. Through modulation of cholinergic, serotonergic and peptidergic neuronal circuits in the brainstem, GPR151 may coordinate functions related to addiction, reinforcement learning, decision-making, pain processing and depression. For instance, can addiction be considered an impairment in decision-making, or is withdrawal a form of unexpected negative reward, and how can these behaviors relate to pain processing and depression? Altogether, the fact that GPR151 is highly conserved from lower vertebrates to mammals, including humans (Hawrylycz et al., 2012), and that it belongs to the highly druggable Class A of GPCRs, makes it a potential target for novel treatment modalities for common and devastating psychiatric maladies such as mood disorders and drug dependence.

Acknowledgments

This work was supported by the Bror Gadelius memorial fund (JB and AT) and the NIH/NIDA grant 1P30 DA035756-01 (BAF and IIT).

The authors thank Madeleine Åberg Andersson, Fredrik Ek and Sylvia Lipford for their technical assistance. This work was supported by the NIH/NIDA grant 1P30 DA035756-01 (II-T), and a grant from the Bror Gadelius memorial fund.

Glossary

3V	Third ventricle
4V	Fourth ventricle
CLi	Central linear nucleus of the raphe
dIPN	Dorsal part of the interpeduncular nucleus
dMHb	Dorsal part of the medial habenula
DRC	Caudal part of the dorsal raphe
DRD	Dorsal part of the dorsal raphe
DRI	Interfascicular part of the dorsal raphe
DRV	Ventral part of the dorsal raphe
DTg	Dorsal tegmental nucleus
DTgC	Central part of the dorsal tegmental nucleus
DTgP	Pericent part of the dorsal tegmental nucleus
FR	Fasciculus retroflexus
IPA	Apical part of the interpeduncular nucleus
IPC	Central part of the interpeduncular nucleus
IPDL	Dorsolateral part of the interpeduncular nucleus
IPDM	Dorsomedial part of the interpeduncular nucleus
IPI	Intermediate part of the interpeduncular nucleus
IPL	Lateral part of the interpeduncular nucleus
IPN	Interpeduncular nucleus
IPR	Rostral part of the interpeduncular nucleus
IPRL	Rostrolateral part of the interpeduncular nucleus
LDTg	Laterodorsal tegmental nucleus
LHb	Lateral habenula
LHbLB	Basal subnucleus of the lateral part of the LHb
LHbLMc	Magnocellular subnucleus of the lateral part of the LHb
LHbLMg	Marginal subnucleus of the lateral part of the LHb
LHbLO	Oval subnucleus of the lateral part of the LHb
LHbLPc	Parvocellular subnucleus of the lateral part of the LHb

LHbMC	Central subnucleus of the medial part of the LHb
LHbMMg	Marginal subnucleus of the medial part of the LHb
LHbMPc	Parvocellular subnucleus of the medial part of the LHb
LHbMS	Superior subnucleus of the medial part of the LHb
MHb	Medial habenula
mlf	Medial longitudinal fasciculus
MnR	Median raphe nucleus
PDTg	Posterodorsal tegmental nucleus
PMnR	Paramedian raphe nucleus
Rbd	Rhabdoid nucleus
RMTg	Rostromedial tegmental nucleus
scp	Superior cerebellar peduncle
vIPN	Ventral part of the interpeduncular nucleus
vMHb	Ventral part of the medial habenula
VTA	Ventral tegmental area

LITERATURE CITED

Aizawa H, Kobayashi M, Tanaka S, Fukai T, Okamoto H. Molecular characterization of the subnuclei in rat habenula. J Comp Neurol. 2012; 520:4051–4066. [PubMed: 22700183]

Amo R, Aizawa H, Takahoko M, Kobayashi M, Takahashi R, Aoki T, Okamoto H. Identification of the zebrafish ventral habenula as a homolog of the mammalian lateral habenula. J Neurosci. 2010; 30:1566–1574. [PubMed: 20107084]

Andres KH, von Düring M, Veh RW. Subnuclear organization of the rat habenular complexes. J Comp Neurol. 1999; 407:130–150. [PubMed: 10213193]

Balcita-Pedicino JJ, Omelchenko N, Bell R, Sesack SR. The inhibitory influence of the lateral habenula on midbrain dopamine cells: Ultrastructural evidence for indirect mediation via the rostromedial mesopontine tegmental nucleus. J Comp Neurol. 2011; 519:1143–1164. [PubMed: 21344406]

Berrettini W, Yuan X, Tozzi F, Song K, Francks C, Chilcoat H, Waterworth D, Muglia P, Mooser V. Alpha-5/alpha-3 nicotinic receptor subunit alleles increase risk for heavy smoking. Mol Psychiatry. 2008; 13:368–373. [PubMed: 18227835]

Berthold M, Collin M, Sejlitz T, Meister B, Lind P. Cloning of a novel orphan G protein-coupled receptor (GPCR-2037): in situ hybridization reveals high mRNA expression in rat brain restricted to neurons of the habenular complex. Brain Res Mol Brain Res. 2003; 120:22–29. [PubMed: 14667573]

Bérubé-Carrière N, Riad M, Dal Bo G, Lévesque D, Trudeau L-E, Descarries L. The dual dopamine-glutamate phenotype of growing mesencephalic neurons regresses in mature rat brain. J Comp Neurol. 2009; 517:873–891. [PubMed: 19844994]

Bérubé-Carrière N, Guay G, Fortin GM, Kullander K, Olson L, Wallén-Mackenzie Å, Trudeau L-E, Descarries L. Ultrastructural characterization of the mesostriatal dopamine innervation in mice, including two mouse lines of conditional VGLUT2 knockout in dopamine neurons. Eur J Neurosci. 2012; 35:527–538. [PubMed: 22330100]

Bianco IH, Wilson SW. The habenular nuclei: a conserved asymmetric relay station in the vertebrate brain. Philos Trans R Soc Lond, B, Biol Sci. 2009; 364:1005–1020. [PubMed: 19064356]

Bierut LJ, Stitzel JA, Wang JC, Hinrichs AL, Grucza RA, Xuei X, Saccone NL, Saccone SF, Bertelsen S, Fox L, Horton WJ, Breslau N, Budde J, Cloninger CR, Dick DM, Foroud T, Hatsukami D, Hesselbrock V, Johnson EO, Kramer J, Kuperman S, Madden PAF, Mayo K, Nurnberger J, Pomerleau O, Porjesz B, Reyes O, Schuckit M, Swan G, Tischfield JA, Edenberg HJ, Rice JP, Goate AM. Variants in nicotinic receptors and risk for nicotine dependence. Am J Psychiatry. 2008; 165:1163–1171. [PubMed: 18519524]

Bromberg-Martin ES, Matsumoto M, Hikosaka O. Distinct tonic and phasic anticipatory activity in lateral habenula and dopamine neurons. Neuron. 2010; 67:144–155. [PubMed: 20624598]

Caldecott-Hazard S, Mazziotta J, Phelps M. Cerebral correlates of depressed behavior in rats, visualized using 14C-2-deoxyglucose autoradiography. J Neurosci. 1988; 8:1951–1961. [PubMed: 3385484]

Campbell MJ, Morrison JH. Monoclonal antibody to neurofilament protein (SMI-32) labels a subpopulation of pyramidal neurons in the human and monkey neocortex. J Comp Neurol. 1989; 282:191–205. [PubMed: 2496154]

Contestabile A, Villani L, Fasolo A, Franzoni MF, Gribaudo L, Oktedalen O, Fonnum F. Topography of cholinergic and substance P pathways in the habenulo-interpeduncular system of the rat. An immunocytochemical and microchemical approach. Neuroscience. 1987; 21:253–270. [PubMed: 2439945]

Costes SV, Daelemans D, Cho EH, Dobbin Z, Pavlakis G, Lockett S. Automatic and quantitative measurement of protein-protein colocalization in live cells. Biophys J. 2004; 86:3993–4003. [PubMed: 15189895]

Cuello AC, Emson PC, Paxinos G, Jessell T. Substance P containing and cholinergic projections from the habenula. Brain Res. 1978; 149:413–429. [PubMed: 352479]

Cuello AC, Galfre G, Milstein C. Detection of substance P in the central nervous system by a monoclonal antibody. Proc Natl Acad Sci USA. 1979; 76:3532–3536. [PubMed: 386341]

Dunn KW, Kamocka MM, McDonald JH. A practical guide to evaluating colocalization in biological microscopy. Am J Physiol, Cell Physiol. 2011; 300:C723–42. [PubMed: 21209361]

Ferraro G, Montalbano ME, Sardo P, La Grutta V. Lateral habenula and hippocampus: a complex interaction raphe cells-mediated. Journal of neural transmission (Vienna, Austria: 1996). 1997; 104:615–631.

Ferreira JGP, Del-Fava F, Hasue RH, Shammah-Lagnado SJ. Organization of ventral tegmental area projections to the ventral tegmental area-nigral complex in the rat. Neuroscience. 2008; 153:196–213. [PubMed: 18358616]

Fowler CD, Lu Q, Johnson PM, Marks MJ, Kenny PJ. Habenular α5 nicotinic receptor subunit signalling controls nicotine intake. Nature. 2011; 471:597–601. [PubMed: 21278726]

Frahm S, Slimak MA, Ferrarese L, Santos-Torres J, Antolin-Fontes B, Auer S, Filkin S, Pons S, Fontaine J-F, Tsetlin V, Maskos U, Ibañez-Tallon I. Aversion to nicotine is regulated by the balanced activity of β4 and α5 nicotinic receptor subunits in the medial habenula. Neuron. 2011; 70:522–535. [PubMed: 21555077]

Geisler S, Andres KH, Veh RW. Morphologic and cytochemical criteria for the identification and delineation of individual subnuclei within the lateral habenular complex of the rat. J Comp Neurol. 2003; 458:78–97. [PubMed: 12577324]

Geisler S, Zahm DS. Afferents of the ventral tegmental area in the rat-anatomical substratum for integrative functions. J Comp Neurol. 2005; 490:270–294. [PubMed: 16082674]

Gonçalves L, Sego C, Metzger M. Differential projections from the lateral habenula to the rostromedial tegmental nucleus and ventral tegmental area in the rat. J Comp Neurol. 2012; 520:1278–1300. [PubMed: 22020635]

Goto M, Swanson LW, Canteras NS. Connections of the nucleus incertus. J Comp Neurol. 2001; 438:86–122. [PubMed: 11503154]

Görlich A, Antolin-Fontes B, Ables JL, Frahm S, Slimak MA, Dougherty JD, Ibañez-Tallon I. Reexposure to nicotine during withdrawal increases the pacemaking activity of cholinergic habenular neurons. Proc Natl Acad Sci USA. 2013; 110:17077–17082. [PubMed: 24082085]

Hawrylycz MJ, Lein ES, Guillozet-Bongaarts AL, Shen EH, Ng L, Miller JA, van de Lagemaat LN, Smith KA, Ebbert A, Riley ZL, Abajian C, Beckmann CF, Bernard A, Bertagnolli D, Boe AF, Cartagena PM, Chakravarty MM, Chapin M, Chong J, Dalley RA, Daly BD, Dang C, Datta S, Dee N, Dolbeare TA, Faber V, Feng D, Fowler DR, Goldy J, Gregor BW, Haradon Z, Haynor DR, Hohmann JG, Horvath S, Howard RE, Jeromin A, Jochim JM, Kinnunen M, Lau C, Lazarz ET, Lee C, Lemon TA, Li L, Li Y, Morris JA, Overly CC, Parker PD, Parry SE, Reding M, Royall JJ, Schulkin J, Sequeira PA, Slaughterbeck CR, Smith SC, Sodt AJ, Sunkin SM, Swanson BE, Vawter MP, Williams D, Wohnoutka P, Zielke HR, Geschwind DH, Hof PR, Smith SM, Koch C, Grant SGN, Jones AR. An anatomically comprehensive atlas of the adult human brain transcriptome. Nature. 2012; 489:391–399. [PubMed: 22996553]

Haycock JW. Multiple forms of tyrosine hydroxylase in human neuroblastoma cells: quantitation with isoform-specific antibodies. J Neurochem. 1993; 60:493–502. [PubMed: 8093479]

Herkenham M, Nauta WJ. Afferent connections of the habenular nuclei in the rat. A horseradish peroxidase study, with a note on the fiber-of-passage problem. J Comp Neurol. 1977; 173:123–146. [PubMed: 845280]

Herkenham M, Nauta WJ. Efferent connections of the habenular nuclei in the rat. J Comp Neurol. 1979; 187:19–47. [PubMed: 226566]

Hikosaka O. The habenula: from stress evasion to value-based decision-making. Nat Rev Neurosci. 2010; 11:503–513. [PubMed: 20559337]

Hsu Y-WA, Tempest L, Quina LA, Wei AD, Zeng H, Turner EE. Medial habenula output circuit mediated by α5 nicotinic receptor-expressing GABAergic neurons in the interpeduncular nucleus. J Neurosci. 2013; 33:18022–18035. [PubMed: 24227714]

Ignatov A, Hermans-Borgmeyer I, Schaller HC. Cloning and characterization of a novel G-protein-coupled receptor with homology to galanin receptors. Neuropharmacology. 2004; 46:1114–1120. [PubMed: 15111018]

Inanobe A, Fujita A, Ito M, Tomoike H, Inageda K, Kurachi Y. Inward rectifier K+ channel Kir2.3 is localized at the postsynaptic membrane of excitatory synapses. Am J Physiol, Cell Physiol. 2002; 282:C1396–403. [PubMed: 11997254]

Jhou TC, Fields HL, Baxter MG, Saper CB, Holland PC. The rostromedial tegmental nucleus (RMTg), a GABAergic afferent to midbrain dopamine neurons, encodes aversive stimuli and inhibits motor responses. Neuron. 2009a; 61:786–800. [PubMed: 19285474]

Jhou TC, Geisler S, Marinelli M, Degarmo BA, Zahm DS. The mesopontine rostromedial tegmental nucleus: A structure targeted by the lateral habenula that projects to the ventral tegmental area of Tsai and substantia nigra compacta. J Comp Neurol. 2009b; 513:566–596. [PubMed: 19235216]

Kaufling J, Veinante P, Pawlowski SA, Freund-Mercier M-J, Barrot M. Afferents to the GABAergic tail of the ventral tegmental area in the rat. J Comp Neurol. 2009; 513:597–621. [PubMed: 19235223]

Kim U, Chang S-Y. Dendritic morphology, local circuitry, and intrinsic electrophysiology of neurons in the rat medial and lateral habenular nuclei of the epithalamus. J Comp Neurol. 2005; 483:236–250. [PubMed: 15678472]

Kim U. Topographic commissural and descending projections of the habenula in the rat. J Comp Neurol. 2009; 513:173–187. [PubMed: 19123238]

Kobayashi Y, Sano Y, Vannoni E, Goto H, Suzuki H, Oba A, Kawasaki H, Kanba S, Lipp HP, Murphy NP, Wolfer DP, Itohara S. Genetic dissection of medial habenula–interpeduncular nucleus pathway function in mice. Frontiers in Behavioral Neuroscience. 2013; 7:17. [PubMed: 23487260]

Kong J, Tung VW, Aghajanian J, Xu Z. Antagonistic roles of neurofilament subunits NF-H and NF-M against NF-L in shaping dendritic arborization in spinal motor neurons. J Cell Biol. 1998; 140:1167–1176. [PubMed: 9490729]

Lacoste B, Riad M, Ratté MO, Boye SM, Lévesque D, Descarries L. Trafficking of neurokinin-1 receptors in serotonin neurons is controlled by substance P within the rat dorsal raphe nucleus. Eur J Neurosci. 2009; 29:2303–2314. [PubMed: 19490080]

Lavezzi HN, Parsley KP, Zahm DS. Mesopontine rostromedial tegmental nucleus neurons projecting to the dorsal raphe and pedunculopontine tegmental nucleus: psychostimulant-elicited Fos

expression and collateralization. Brain structure & function. 2011; 217:719–734. [PubMed: 22179106]

Lawson RP, Seymour B, Loh E, Lutti A, Dolan RJ, Dayan P, Weiskopf N, Roiser JP. The habenula encodes negative motivational value associated with primary punishment in humans. Proc Natl Acad Sci USA. 2014:201323586.

Lecourtier L, Kelly PH. A conductor hidden in the orchestra? Role of the habenular complex in monoamine transmission and cognition. Neurosci Biobehav Rev. 2007; 31:658–672. [PubMed: 17379307]

Lips EH, Gaborieau V, McKay JD, Chabrier A, Hung RJ, Boffetta P, Hashibe M, Zaridze D, Szeszenia-Dabrowska N, Lissowska J, Rudnai P, Fabianova E, Mates D, Bencko V, Foretova L, Janout V, Field JK, Liloglou T, Xinarianos G, McLaughlin J, Liu G, Skorpen F, Elvestad MB, Hveem K, Vatten L, Study E, Benhamou S, Lagiou P, Holcátová I, Merletti F, Kjaerheim K, Agudo A, Castellsagué X, Macfarlane TV, Barzan L, Canova C, Lowry R, Conway DI, Znaor A, Healy C, Curado MP, Koifman S, Eluf-Neto J, Matos E, Menezes A, Fernandez L, Metspalu A, Heath S, Lathrop M, Brennan P. Association between a 15q25 gene variant, smoking quantity and tobacco-related cancers among 17 000 individuals. Int J Epidemiol. 2010; 39:563–577. [PubMed: 19776245]

Liu R, Chang L, Wickern G. The dorsal tegmental nucleus: an axoplasmic transport study. Brain Res. 1984; 310:123–132. [PubMed: 6434154]

Liu Q, Wong-Riley MTT. Postnatal changes in tryptophan hydroxylase and serotonin transporter immunoreactivity in multiple brainstem nuclei of the rat: implications for a sensitive period. J Comp Neurol. 2010; 518:1082–1097. [PubMed: 20127812]

Liu JZ, Tozzi F, Waterworth DM, Pillai SG, Muglia P, Middleton L, Berrettini W, Knouff CW, Yuan X, Waeber G, Vollenweider P, Preisig M, Wareham NJ, Zhao JH, Loos RJF, Barroso I, Khaw K-T, Grundy S, Barter P, Mahley R, Kesaniemi A, McPherson R, Vincent JB, Strauss J, Kennedy JL, Farmer A, McGuffin P, Day R, Matthews K, Bakke P, Gulsvik A, Lucae S, Ising M, Brueckl T, Horstmann S, Wichmann H-E, Rawal R, Dahmen N, Lamina C, Polasek O, Zgaga L, Huffman J, Campbell S, Kooner J, Chambers JC, Burnett MS, Devaney JM, Pichard AD, Kent KM, Satler L, Lindsay JM, Waksman R, Epstein S, Wilson JF, Wild SH, Campbell H, Vitart V, Reilly MP, Li M, Qu L, Wilensky R, Matthai W, Hakonarson HH, Rader DJ, Franke A, Wittig M, Schäfer A, Uda M, Terracciano A, Xiao X, Busonero F, Scheet P, Schlessinger D, St Clair D, Rujescu D, Abecasis GR, Grabe HJ, Teumer A, Völzke H, Petersmann A, John U, Rudan I, Hayward C, Wright AF, Kolcic I, Wright BJ, Thompson JR, Balmforth AJ, Hall AS, Samani NJ, Anderson CA, Ahmad T, Mathew CG, Parkes M, Satsangi J, Caulfield M, Munroe PB, Farrall M, et al. Meta-analysis and imputation refines the association of 15q25 with smoking quantity. Nat Genet. 2010; 42:436–440. [PubMed: 20418889]

Manders EMM, Verbeek FJ, Aten JA. Measurement of co-localization of objects in dual3 colour confocal images. J Microsc. 1993; 169:375–382.

Marszalek JR, Williamson TL, Lee MK, Xu Z, Hoffman PN, Becher MW, Crawford TO, Cleveland DW. Neurofilament subunit NF-H modulates axonal diameter by selectively slowing neurofilament transport. J Cell Biol. 1996; 135:711–724. [PubMed: 8909545]

Matsumoto M, Hikosaka O. Lateral habenula as a source of negative reward signals in dopamine neurons. Nature. 2007; 447:1111–1115. [PubMed: 17522629]

Matsumoto M, Hikosaka O. Representation of negative motivational value in the primate lateral habenula. Nat Neurosci. 2009; 12:77–84. [PubMed: 19043410]

Morris JS, Smith KA, Cowen PJ, Friston KJ, Dolan RJ. Covariation of activity in habenula and dorsal raphé nuclei following tryptophan depletion. Neuroimage. 1999; 10:163–172. [PubMed: 10417248]

Neckers LM, Schwartz JP, Wyatt RJ, Speciale SG. Substance P afferents from the habenula innervate the dorsal raphe nucleus. Exp Brain Res. 1979; 37:619–623. [PubMed: 520447]

Olucha-Bordonau FE, Teruel V, Barcia-González J, Ruiz-Torner A, Valverde-Navarro AA, Martínez-Soriano F. Cytoarchitecture and efferent projections of the nucleus incertus of the rat. J Comp Neurol. 2003; 464:62–97. [PubMed: 12866129]

Park MR. Monosynaptic inhibitory postsynaptic potentials from lateral habenula recorded in dorsal raphe neurons. Brain Res Bull. 1987; 19:581–586. [PubMed: 3690368]

Paxinos, G.; Watson, C. The Rat Brain in Stereotaxic Coordinates. 6. New York: Elsevier/Academic Press; 2006.

Paxinos, G. The Rat Nervous System. 3. New York: Elsevier/Academic Press; 2004.

Quina LA, Wang S, Ng L, Turner EE. Brn3a and Nurr1 mediate a gene regulatory pathway for habenula development. J Neurosci. 2009; 29:14309–14322. [PubMed: 19906978]

Ranft K, Dobrowolny H, Krell D, Bielau H, Bogerts B, Bernstein H-G. Evidence for structural abnormalities of the human habenular complex in affective disorders but not in schizophrenia. Psychol Med. 2010; 40:557–567. [PubMed: 19671211]

Ren J, Qin C, Hu F, Tan J, Qiu L, Zhao S, Feng G, Luo M. Habenula "cholinergic" neurons co-release glutamate and acetylcholine and activate postsynaptic neurons via distinct transmission modes. Neuron. 2011; 69:445–452. [PubMed: 21315256]

Reisine TD, Soubrie P, Artaud F, Glowinski J. Involvement of lateral habenula-dorsal raphe neurons in the differential regulation of striatal and nigral serotonergic transmission cats. J Neurosci. 1982; 2:1062–1071. [PubMed: 6180148]

Roiser JP, Levy J, Fromm SJ, Nugent AC, Talagala SL, Hasler G, Henn FA, Sahakian BJ, Drevets WC. The effects of tryptophan depletion on neural responses to emotional words in remitted depression. Biol Psychiatry. 2009; 66:441–450. [PubMed: 19539268]

Salas R, Sturm R, Boulter J, de Biasi M. Nicotinic receptors in the habenulo-interpeduncular system are necessary for nicotine withdrawal in mice. J Neurosci. 2009; 29:3014–3018. [PubMed: 19279237]

Salas R, Baldwin P, de Biasi M, Montague PR. BOLD Responses to Negative Reward Prediction Errors in Human Habenula. Front Hum Neurosci. 2010; 4:36. [PubMed: 20485575]

Sartorius A, Henn FA. Deep brain stimulation of the lateral habenula in treatment resistant major depression. Med Hypotheses. 2007; 69:1305–1308. [PubMed: 17498883]

Sartorius A, Kiening KL, Kirsch P, von Gall CC, Haberkorn U, Unterberg AW, Henn FA, Meyer-Lindenberg A. Remission of major depression under deep brain stimulation of the lateral habenula in a therapy-refractory patient. Biol Psychiatry. 2010; 67:e9–e11. [PubMed: 19846068]

Sego C, Gonçalves L, Lima L, Furigo IC, Donato J, Metzger M. The lateral habenula and the rostromedial tegmental nucleus innervate neurochemically distinct subdivisions of the dorsal raphe nucleus in the rat. J Comp Neurol. 2014; 522:1454–1484. [PubMed: 24374795]

Sevigny CP, Bassi J, Williams DA, Anderson CR, Thomas WG, Allen AM. Efferent projections of C3 adrenergic neurons in the rat central nervous system. J Comp Neurol. 2012; 520:2352–2368. [PubMed: 22237784]

Shabel SJ, Proulx CD, Trias A, Murphy RT, Malinow R. Input to the lateral habenula from the basal ganglia is excitatory, aversive, and suppressed by serotonin. Neuron. 2012; 74:475–481. [PubMed: 22578499]

Sharp PE, Turner-Williams S, Tuttle S. Movement-related correlates of single cell activity in the interpeduncular nucleus and habenula of the rat during a pellet-chasing task. Behav Brain Res. 2006; 166:55–70. [PubMed: 16143407]

Sheffield EB, Quick MW, Lester RA. Nicotinic acetylcholine receptor subunit mRNA expression and channel function in medial habenula neurons. Neuropharmacology. 2000; 39:2591–2603. [PubMed: 11044729]

Shumake J, Gonzalez-Lima F. Functional opposition between habenula metabolism and the brain reward system. Front Hum Neurosci. 2013; 7:662. [PubMed: 24133441]

Sim LJ, Joseph SA. Dorsal raphe nucleus efferents: termination in peptidergic fields. Peptides. 1993; 14:75–83. [PubMed: 8441710]

Stamatakis AM, Stuber GD. Activation of lateral habenula inputs to the ventral midbrain promotes behavioral avoidance. Nature neuroscience. 2012; 15:1105–1107.

Sternberger LA, Harwell LW, Sternberger NH. Neurotypy: regional individuality in rat brain detected by immunocytochemistry with monoclonal antibodies. Proc Natl Acad Sci USA. 1982; 79:1326–1330. [PubMed: 7041117]

Stopper CM, Floresco SB. What's better for me? Fundamental role for lateral habenula in promoting subjective decision biases. Nature neuroscience. 2013; 17:33–35.

Takamori S, Rhee JS, Rosenmund C, Jahn R. Identification of a vesicular glutamate transporter that defines a glutamatergic phenotype in neurons. Nature. 2000; 407:189–194. [PubMed: 11001057]

Takamori S, Rhee JS, Rosenmund C, Jahn R. Identification of differentiation-associated brain-specific phosphate transporter as a second vesicular glutamate transporter (VGLUT2). J Neurosci. 2001; 21:RC182. [PubMed: 11698620]

Tapper AR, McKinney SL, Nashmi R, Schwarz J, Deshpande P, Labarca C, Whiteaker P, Marks MJ, Collins AC, Lester HA. Nicotine activation of alpha4* receptors: sufficient for reward, tolerance, and sensitization. Science. 2004; 306:1029–1032. [PubMed: 15528443]

Ullsperger M, von Cramon DY. Error monitoring using external feedback: specific roles of the habenular complex, the reward system, and the cingulate motor area revealed by functional magnetic resonance imaging. J Neurosci. 2003; 23:4308–4314. [PubMed: 12764119]

Valentino RJ, Bey V, Pernar L, Commons KG. Substance P Acts through Local Circuits within the Rat Dorsal Raphe Nucleus to Alter Serotonergic Neuronal Activity. J Neurosci. 2003; 23:7155–7159. [PubMed: 12904475]

Vincent SR, Staines WA, McGeer EG, Fibiger HC. Transmitters contained in the efferents of the habenula. Brain Res. 1980; 195:479–484. [PubMed: 6156737]

Viswanath H, Carter AQ, Baldwin PR, Molfese DL, Salas R. The medial habenula: still neglected. Front Hum Neurosci. 2013; 7:931. [PubMed: 24478666]

Wagner F, Stroh T, Veh RW. Correlating habenular subnuclei in rat and mouse using topographical, morphological and cytochemical criteria. J Comp Neurol. 2014

Wang RY, Aghajanian GK. Physiological evidence for habenula as major link between forebrain and midbrain raphe. Science. 1977; 197:89–91. [PubMed: 194312]

Ware JJ, van den Bree MBM, Munafò MR. Association of the CHRNA5-A3-B4 gene cluster with heaviness of smoking: a meta-analysis. Nicotine Tob Res. 2011; 13:1167–1175. [PubMed: 22071378]

Weissner W, Winterson BJ, Stuart-Tilley A, Devor M, Bove GM. Time course of substance P expression in dorsal root ganglia following complete spinal nerve transection. J Comp Neurol. 2006; 497:78–87. [PubMed: 16680762]

Wojcik SM, Rhee JS, Herzog E, Sigler A, Jahn R, Takamori S, Brose N, Rosenmund C. An essential role for vesicular glutamate transporter 1 (VGLUT1) in postnatal development and control of quantal size. Proc Natl Acad Sci USA. 2004; 101:7158–7163. [PubMed: 15103023]

Wouterlood FG, Härtig W, Groenewegen HJ, Voorn P. Density gradients of vesicular glutamate- and GABA transporter-immunoreactive boutons in calbindinand μ-opioid receptor-defined compartments in the rat striatum. Journal of Comparative Neurology. 2012; 520:2123–2142. [PubMed: 22173881]

Yang L-M, Hu B, Xia Y-H, Zhang B-L, Zhao H. Lateral habenula lesions improve the behavioral response in depressed rats via increasing the serotonin level in dorsal raphe nucleus. Behav Brain Res. 2008; 188:84–90. [PubMed: 18054396]

Zhao-Shea R, Liu L, Pang X, Gardner PD, Tapper AR. Activation of GABAergic neurons in the interpeduncular nucleus triggers physical nicotine withdrawal symptoms. Curr Biol. 2013; 23:2327–2335. [PubMed: 24239118]

Zhou J, Nannapaneni N, Shore S. Vessicular glutamate transporters 1 and 2 are differentially associated with auditory nerve and spinal trigeminal inputs to the cochlear nucleus. J Comp Neurol. 2007; 500:777–787. [PubMed: 17154258]

Zinchuk V, Grossenbacher-Zinchuk O. Quantitative colocalization analysis of fluorescence microscopy images. Curr Protoc Cell Biol. 2014; 62:4.19.1–4.19.14.

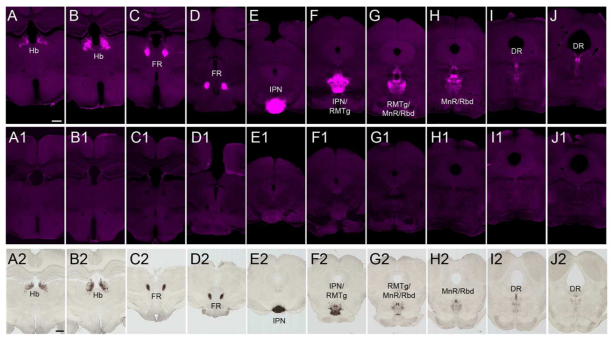

Figure 1. GPR151 is localized in habenular axonal projections in rat and mouse brain

Coronal brain sections of wildtype mouse (A–J) and rat (A2–J2) showing restricted expression of GPR151 in habenula (A–B, A2–B2), fasciculus retroflexus (C–D, C2–D2), interpeduncular nucleus (E–F, E2–F2), rostromedial tegmental nucleus (F–G, F2–G2), median and paramedian raphe (F–H, F2–H2), rhabdoid nucleus (F–H, F2–H2) and dorsal raphe (I–J, I2–J2). GPR151 immunoreactivity is completely absent in *Gpr151*$^{-/-}$ mice (A1–J1). Scale bar: 500 μm in A–J, 1000μm in A2–J2.

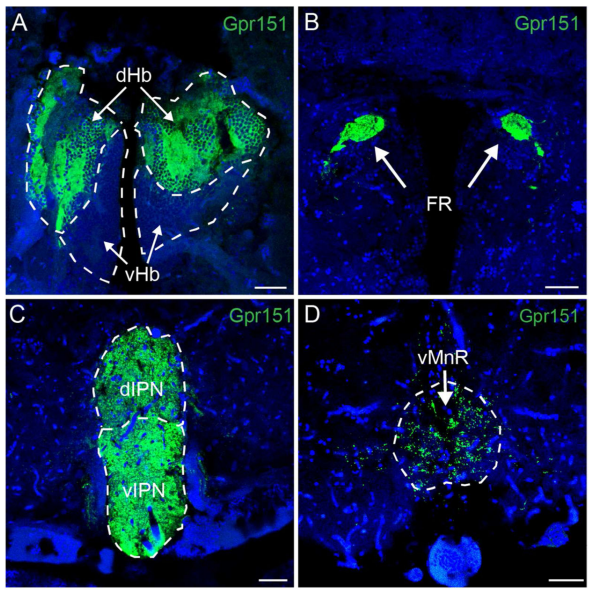

Figure 2. GPR151 is expressed in the habenular circuitry of zebrafish

Immunohistochemistry of coronal brain sections of adult zebrafish using a rabbit polyclonal antibody against human GPR151 yielded selective labeling of habenular axons projecting from the habenula (A), through the FR (B) to the dIPN and vIPN (C) as well as to the ventral median raphe (D). DAPI nuclear stain is shown in blue. Scale bar: 50μm.

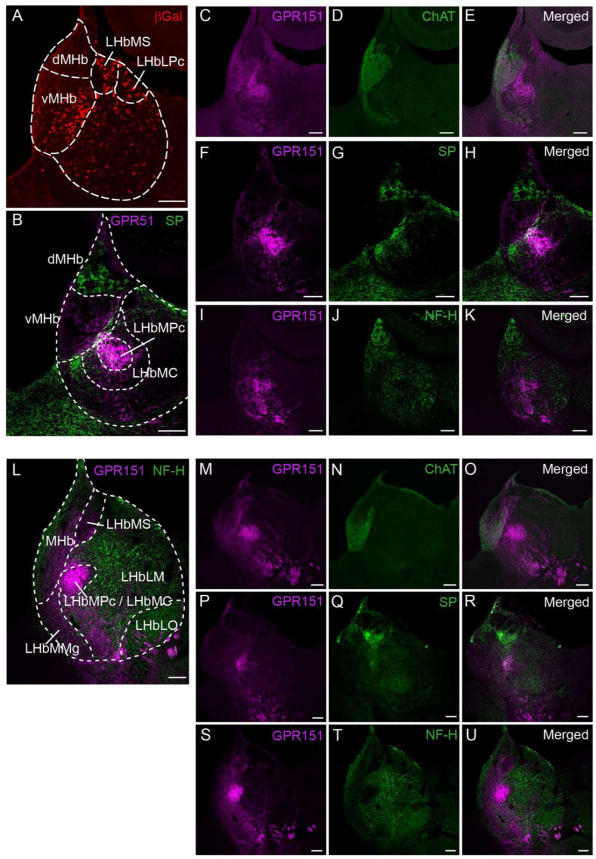

Figure 3. GPR151 labels specific subpopulations of medial and lateral habenula neurons

A: Coronal section of the habenula of *Gpr151*$^{-/-}$ mice showing immunostaining for the β-galactosidase reporter contained in the *Gpr151* gene deletion vector employed to generate *Gpr151*$^{-/-}$ mice. β-galactosidase positive cells are located mainly in the vMHb and the dorsal part of the LHb. B–K: Coronal sections of the wildtype mouse habenula showing immunostaining for GPR151 (magenta in B,C,E,F,H,I,K) relative to the immunostaining for acetylcholine transferase (ChAT, green in D,E), substance P (SP, green in B,G,H) and neurofilament-H (NF-H, green in J,K). L–U: Coronal sections of rat mouse habenula showing immunostaining for GPR151 (magenta in L,M,O,P,R,S,U) relative to the immunostaining for ChAT (green in N,O), SP (green in Q,R) and NF-H (green in L,T,U). In the LHb, GPR151 is mainly expressed in the LHbMPc and LHbMC subnuclei. In the MHb, GPR151 is expressed in the cholinergic vMHb, but not in the SP expressing dMHb. Scale bar: 100 μm.

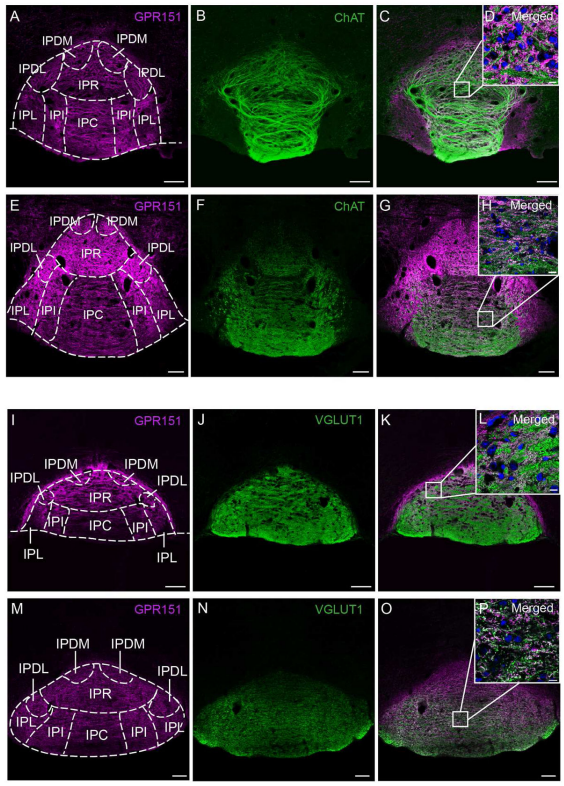

Figure 4. GPR151 immunoreactive habenular neurons project to the interpeduncular nucleus

Coronal sections of the interpeduncular nucleus of mouse (A–D, I–L) and rat (E–H, M–P) showing immunostaining for GPR151 (magenta in A,C,D,E,G,H,I,K,L,M,O,P) relative to the immunostaining for acetylcholine transferase (ChAT, green in B–D, F–H) and vesicular glutamate transporter 1 (VGLUT1, green in J–L,N–P). Colocalization of GPR151 and ChAT and GPR151 and VGLUT1 is observed in the rostral and central part of the IPN. Scale bar: 100 μm. D,H,L,P are higher magnifications of the boxed areas in the inset of each panel. DAPI nuclear stain is shown in blue. Scale bar: 10 μm.

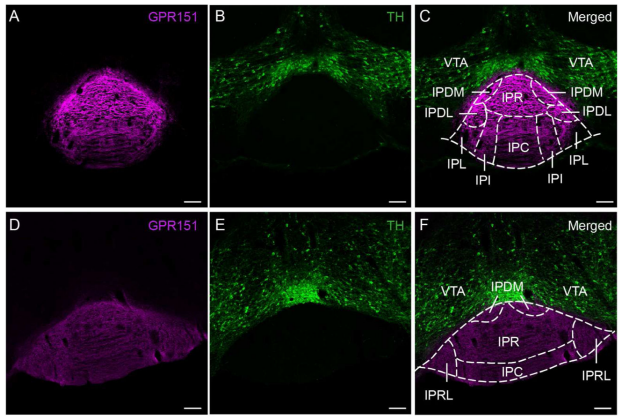

Figure 5. GPR151 habenular neurons do not project to the ventral tegmental area

Coronal sections of mouse (A–C) and rat (D–F) in the IPN and ventral tegmental area showing immunostaining for GPR151 (magenta in A,C,D,F) relative to the immunostaining for tyrosine hydroxylase (TH, green in B–C,E–F). GPR151 immunostaining is observed in the IPN but not in the ventral tegmental area. Scale bar: 100 μm.

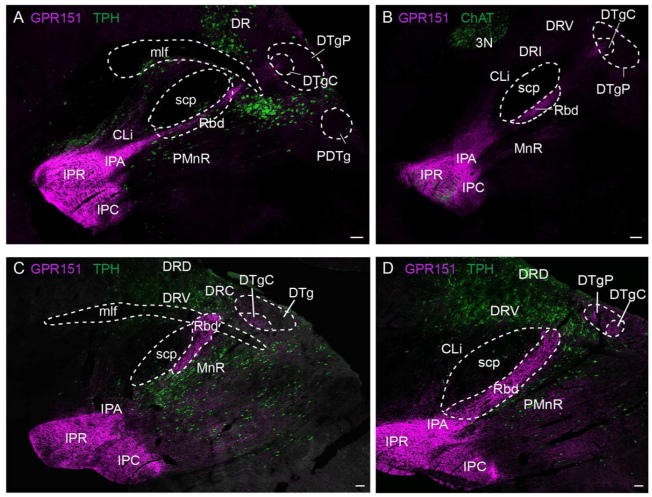

Figure 6. GPR151 habenular neurons project to the IPN, dorsal tegmental nucleus and mesencephalic raphe nuclei

Sagittal sections of mouse (A–B) and rat (C–D) in the midbrain and pons showing GPR151 immunostaining (magenta in A–D) relative to the immunostaining for tryptophan hydroxylase (TPH, green in A,C,D) or ChAT (green in B). GPR151 habenular neurons project to the IPN, the rhabdoid nucleus, the dorsal tegmental nucleus and the mesencephalic raphe nuclei. ChAT immunostaining is observed in the IPN and the oculomotor nucleus. TPH immunostaining labels the serotonergic neurons in the mesencephalic raphe nuclei. Scale bar: 100μm.

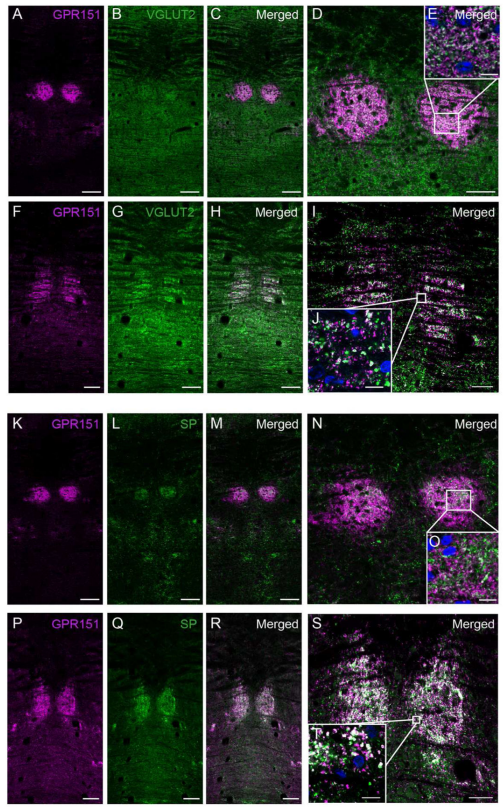

Figure 7. GPR151, substance P and VGLUT2 expression in the rhabdoid nucleus

Coronal sections of mouse (A–E, K–O) and rat (F–J, P–T) through the rhabdoid nucleus. GPR151 immunoreactivity is shown in magenta. Vesicular glutamate transporter 2 immunoreactivity is shown in green in B–E and G–J. Substance P immunoreactivity is shown in green in L–O and Q–T. E, J, O and T are higher magnifications of the boxed areas. DAPI nuclear stain is shown in blue. Colocalization of GPR151 and VGLUT2 as well as GPR151 and substance P is observed in the rhabdoid nucleus. Scale bar: 100μm in A–C, F–H, K–M, P–R; 50μm in D, I, N, S; 10μm in E, J, O, T.

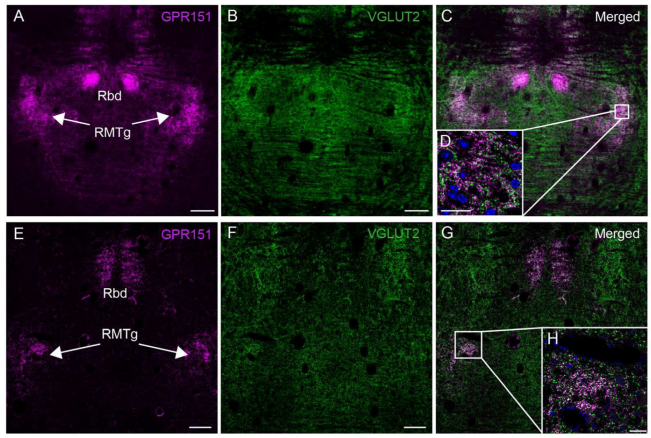

Figure 8. GPR151 immunoreactive habenular neurons project to the rostromedial tegmental nucleus

Coronal sections of mouse (A–D) and rat (E–H) in the midbrain showing GPR151 immunostaining (magenta in A,C,D,E,G,H) relative to the immunostaining for vesicular glutamate transporter 2 (VGLUT2, green in B–D,F–H). GPR151 immunostaining is observed in the rostromedial tegmental nucleus and rhabdoid nucleus. D,H are higher magnifications of the boxed areas in the inset of each panel. Colocalization of GPR151 and VGLUT2 is observed in the RMTg. DAPI nuclear stain is shown in blue. Scale bar: 100 μm in A–C, E–G; 10μm in D,H.

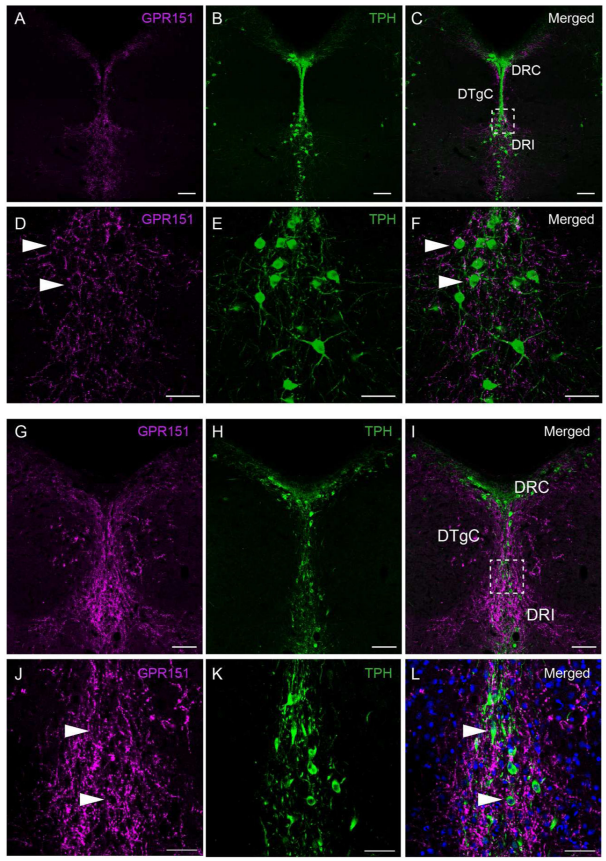

Figure 9. GPR151 expression in the caudal dorsal raphe nucleus

Coronal sections of mouse (A–F) and rat (G–L) through the caudal dorsal raphe nucleus. GPR151 immunoreactivity is shown in magenta and tryptophan hydroxylase (TPH) immunoreactivity is shown in green. DAPI nuclear stain is shown in blue. Panels D–F are magnifications of the boxed area in C. Panels J–L are magnifications of the boxed area in I. GPR151 positive fibers make close contact to serotonergic neurons (arrows). Scale bar: 100μm in A–C, G–I; 50μm in D–F, J–L.

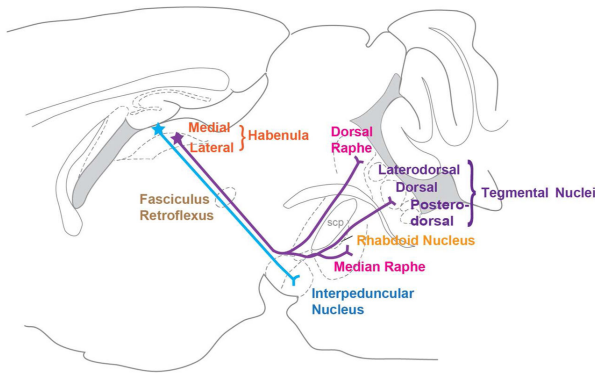

Figure 10. Schematic representation of GPR151 expressing habenular projections

Schematic sagittal view of a rodent brain depicting GPR151 expressing habenular projections. A prominent GPR151 positive projection arises in the ventral medial habenula and terminates in the interpeduncular nucleus (blue). From the lateral habenula, GPR151 immunoreactive axonal fibers project toward the interpeduncular nucleus, then travel through or adjacent to it, and then continue in a dorsal-caudal direction. The lateral habenular fibers travel both dorsally and ventrally to the superior cerebellar peduncle and terminate in the rostromedial tegmental nucleus, rhabdoid nucleus, dorsal tegmental nucleus as well as the median, paramedian and dorsal raphe nuclei.

Table 1

Primary antibodies

Antibody target	Immunogen	Manufacturer, cat. no, species	RRID	Working concentration or dilution
GPR151	Synthetic peptide derived from C-terminal of human GPR151 (aa 370–419, *EKEKPSSPSSGKGKTEKAEIPILPDVEQFWHERDTVPSVQDNDPIPWEHEDQETGEGVK*)	Sigma, SAB4500418, rabbit polyclonal	AB_10743815	0.2μg/ml (rat and mouse), 0.1μg/ml (zebrafish)
GPR151	Full length human GPR151 protein	Sigma, SAB1402000, mouse polyclonal	AB_10608138	0.5μg/ml (rat and mouse), 1μg/ml (zebrafish)
β-galactosidase	Full length native *ESCHERICHIA COLI* protein	Abcam, AB9361, chicken polyclonal	AB_307210	2μg/ml
Vesicular glutamate transporter 1 (VGLUT1)	Strep-Tag® fusion protein of rat VGLUT 1 (amino acids 456 – 560, *TLSGMVCPIIVGAMT*).	Synaptic Systems, 135303, rabbit polyclonal	AB_887876	1μg/ml
Vesicular glutamate transporter 1 (VGLUT1)	Purified recombinant protein of rat VGLUT 1 (amino acids 456 – 560, *TLSGMVCPIIVGAMT*).	Synaptic Systems, 135304, guinea pig polyclonal	AB_887878	1:1000
Vesicular glutamate transporter 2 (VGLUT2)	Strep-Tag® fusion protein of rat VGLUT 2 (amino acids 510 – 582, *EKQPWADPEETSEEKCGFIHEDELDEETGDITQNYINYGTTKSYGATSQENGGWPNGEKKEEFVQESAQDAYSYKDRDDYS*).	Synaptic Systems, 135403, rabbit polyclonal	AB_887883	1μg/ml
Vesicular glutamate transporter 2 (VGLUT2)	Purified recombinant protein of rat VGLUT 2 (amino acids 510 – 582, *EKQPWADPEETSEEKCGFIHEDELDEETGDITQNYINYGTTKSYGATSQENGGWPNGEKKEEFVQESAQDAYSYKDRDDYS*).	Synaptic Systems, 135404, guinea pig polyclonal	AB_887884	1:1000
Choline acetyltransferase (ChAT)	Human placental choline acetyltransferase enzyme	Millipore, AB144P, goat polyclonal	AB_2079751	2μg/ml
Neurofilament H - non phosphorylated	Homogenized hypothalami from Fischer 344 rat brain	Covance, SMI-32R, mouse monoclonal (clone SMI-32)	AB_10123643	1:4000 (rat), 1:1000 (mouse)
Tyrosine hydroxylase (TH)	Rat tyrosine hydroxylase	Sigma, T1299 mouse monoclonal (clone TH-2)	AB_477560	1:500
Tryptophan hydroxylase (TPH)	Recombinant rabbit tryptophan hydroxylase	Sigma, T0678, mouse monoclonal (clone WH-3)	AB_261587	2μg/ml
Tryptophan hydroxylase (TPH)	Recombinant rabbit tryptophan hydroxylase	Chemicon, AB1541, sheep polyclonal	AB_90754	0.4μg/ml
Substance P	Synthetic substance P coupled to keyhole limpet hemocyanin with carbodiimide	Immunostar, 20064, rabbit polyclonal	AB_572266	1:1000
Substance P	Eight amino acids of the COOH-terminal fragment of substance P (NC1/34HL)	Santa Cruz, sc-21715, rat monoclonal	AB_628299	0.8μg/ml

Table 2

Secondary antibodies

Target species	Produced in	Conjugation	Manufacturer, cat. no	Working concentration
Rabbit	Goat	Cy3	Jackson ImmunoResearch, 111-166-003	3μg/ml
Mouse	Goat	Alexa 488	Jackson ImmunoResearch, 115-545-003	3μg/ml
Mouse	Goat	DyLight 650	Nordic BioSite, IR-GTMU-003F650	5μg/ml
Mouse	Donkey	Cy5	Jackson ImmunoResearch, 711-175-152	3μg/ml
Mouse	Horse	Biotin	Vector Laboratories, BA-2000	3μg/ml
Rabbit	Donkey	Alexa 488	Jackson ImmunoResearch, 711-545-152	3μg/ml
Mouse	Donkey	Cy3	Jackson ImmunoResearch, 715-165-150	3μg/ml
Sheep	Donkey	Cy3	Jackson ImmunoResearch, 713-165-147	3μg/ml
Goat	Donkey	DyLight 549	Jackson ImmunoResearch, 705-505-147	3μg/ml
Rat	Donkey	Alexa 647	Jackson ImmunoResearch, 712-605-153	3μg/ml
Guinea pig	Donkey	Cy3	Jackson ImmunoResearch, 706-165-148	3μg/ml

Paper II

Received: 7 November 2016 | Revised: 16 June 2017 | Accepted: 19 June 2017
DOI: 10.1002/cne.24273

RESEARCH ARTICLE

WILEY The Journal of Comparative Neurology

Monosynaptic retrograde tracing of neurons expressing the G-protein coupled receptor Gpr151 in the mouse brain

Jonas Broms[1] | Matilda Grahm[1] | Lea Haugegaard[1] | Thomas Blom[2] | Konstantinos Meletis[3] | Anders Tingström[1]

[1]Psychiatric Neuromodulation Unit, Department of Clinical Sciences, Faculty of Medicine, Lund University, Lund, Sweden
[2]Biomedical Services Division, Faculty of Medicine, Lund University, Lund, Sweden
[3]Department of Neuroscience, Karolinska Institute, Stockholm, Sweden

Correspondence
Anders Tingström, Psychiatric Neuromodulation Unit, Biomedical Center, D11, Klinikgatan 30, Lund 221 84, Sweden.
Email: anders.tingstrom@med.lu.se

Funding information
Swedish Research Council; Royal Physiographic Society of Lund; Vetenskapsrådet; Stiftelsen Professor Bror Gadelius minnesfond; Kungliga Fysiografiska Sällskapet i Lund; Gyllenstiernska Krapperupsstiftelsen; Stiftelsen Ellen och Henrik Sjöbrings minnesfond

Abstract

GPR151 is a G-protein coupled receptor for which the endogenous ligand remains unknown. In the nervous system of vertebrates, its expression is enriched in specific diencephalic structures, where the highest levels are observed in the habenular area. The habenula has been implicated in a range of different functions including behavioral flexibility, decision making, inhibitory control, and pain processing, which makes it a promising target for treating psychiatric and neurological disease. This study aimed to further characterize neurons expressing the Gpr151 gene, by tracing the afferent connectivity of this diencephalic cell population. Using pseudotyped rabies virus in a transgenic Gpr151-Cre mouse line, monosynaptic afferents of habenular and thalamic Gpr151-expressing neuronal populations could be visualized. The habenular and thalamic Gpr151 systems displayed both shared and distinct connectivity patterns. The habenular neurons primarily received input from basal forebrain structures, the bed nucleus of stria terminalis, the lateral preoptic area, the entopeduncular nucleus, and the lateral hypothalamic area. The Gpr151-expressing neurons in the paraventricular nucleus of the thalamus was primarily contacted by medial hypothalamic areas as well as the zona incerta and projected to specific forebrain areas such as the prelimbic cortex and the accumbens nucleus. Gpr151 mRNA was also detected at low levels in the lateral posterior thalamic nucleus which received input from areas associated with visual processing, including the superior colliculus, zona incerta, and the visual and retrosplenial cortices. Knowledge about the connectivity of Gpr151-expressing neurons will facilitate the interpretation of future functional studies of this receptor.

KEYWORDS
habenula, rabies, thalamus, RRID: IMSR_JAX:000664, RRID: IMSR_JAX:024109, RRID: AB_10743815, RRID: AB_2571870, RRID: SCR_003070

1 | INTRODUCTION

The habenula is a paired epithalamic brain region whose structure and connectivity are largely conserved throughout the vertebrate subphylum (Bianco & Wilson, 2009; Díaz, Bravo, Rojas, & Concha, 2011; Stephenson-Jones, Floros, Robertson, & Grillner, 2011). In mammals, it can be further divided into two major subnuclei designated the medial and lateral habenula, homologous to the dorsal and ventral habenula in fish (Amo et al., 2010). In the mouse brain, the medial habenula receives input from the medial septal nucleus, the triangular nucleus of septum, the nucleus of the diagonal band, the bed nucleus of the anterior commissure, and the septofimbrial nucleus (Qin & Luo, 2009). The efferent axons from the medial habenula form the core of the fasciculus retroflexus fiber bundle and terminate in the interpeduncular nucleus. The afferent projections to the lateral habenula have not been investigated in detail in the mouse brain. In rats however, the most prominent

afferent connections arise in the lateral preoptic area, the entopeduncular nucleus and the lateral hypothalamic area, and to a minor extent in the lateral septal nucleus, the nucleus of the diagonal band, the prefrontal cortex, the median raphe, and the ventral tegmental area (Greatrex & Phillipson, 1982; Herkenham & Nauta, 1977; Vertes, Fortin, & Crane, 1999; Warden et al., 2012). Fibers from the lateral habenular neurons travel in the outer layer of fasciculus retroflexus and terminate primarily in the hypothalamus, the ventral tegmental area, the rostromedial tegmental nucleus, the rhabdoid nucleus, the median and dorsal raphe nuclei, and the pontine central gray (Broms, Antolin-Fontes, Tingström, & Ibañez-Tallon, 2015; Quina et al., 2014).

The habenula has been implicated in several apparently distinct brain functions, such as maternal behavior (Corodimas, Rosenblatt, & Morrell, 1992), aggressive behavior (Chou et al., 2016; Golden et al., 2016), social play (van Kerkhof, Damsteegt, Trezza, Voorn, & Vanderschuren, 2013), drug seeking (Jhou et al., 2013), noxious substance aversion (Donovick, Burright, & Zuromski, 1970; Fowler & Kenny, 2013), decision making (Stopper & Floresco, 2013), behavioral flexibility (Baker, Raynor, Francis, & Mizumori, 2016), and pain modulation (Shelton, Becerra, & Borsook, 2012). Subdivision of the habenular complex into smaller regions, defined by the expression of certain molecules or neuronal connectivity patterns, is a necessary strategy for deepening our understanding of its role in physiology and disease. This approach has been useful to target neuronal subpopulations and investigate their anatomical and functional features, especially in the medial habenula (Chou et al., 2016; Gardon et al., 2014; Hsu, Morton, Guy, Wang, & Turner, 2016; Hsu et al., 2014; Kobayashi et al., 2013).

G-protein coupled receptor 151 (GPR151; also known as PGR7, GALR4, GPCR-2037, and galanin-receptor like) is an orphan receptor phylogenetically related to the galanin receptor family (Berthold, Collin, Sejlitz, Meister, & Lind, 2003; Ignatov, Hermans-Borgmeyer, & Schaller, 2004; Vassilatis et al., 2003). In this work, we use capital letters to refer to GPR151 protein while the term Gpr151 is used for mRNA, promoter or gene. In a previous study using immunohistochemistry, we found that the protein expression of GPR151 was limited to habenular neurons targeting the interpeduncular nucleus, the rostromedial tegmental nucleus, the rhabdoid nucleus, the median raphe, the caudal dorsal raphe, and the dorsal tegmentum in rats and mice (Broms et al., 2015). The protein expression pattern was similar in zebrafish, with strong expression in habenular projections to the interpeduncular nucleus and ventral median raphe, and this distinct and phylogenetically conserved expression pattern suggests an important role of GPR151 in modulating habenular function.

Weak Gpr151 mRNA expression can also be detected in various thalamic areas such as the paraventricular, the reunions, the rhomboid, the central lateral, and the parafascicular nuclei (Ignatov et al., 2004; Lein et al., 2006; Wagner, French, & Veh, 2014). Surprisingly, these structures display no or very weak immunohistochemical staining of GPR151 protein (Broms et al., 2015). In a recent study, specific ablation of adult neurons exhibiting Gpr151 promoter activity resulted in several behavioral alterations, such as increased anxiety, inability to habituate to repeated exposure to a novel environment, increased impulsivity, impaired pre-pulse inhibition, and spatial memory deficits (Kobayashi et al., 2013). Decision making was also affected, where lesioned mice preferred effortless and immediate small rewards over larger rewards that required the animals to either wait longer for the reward or to climb an obstacle. The observed behavioral changes were accompanied by structural and neurochemical remodeling of the habenulo-interpeduncular system. The authors concluded that the Gpr151-expressing neurons may play an important role in inhibitory control and cognition-dependent executive functioning (Kobayashi et al., 2013).

In addition to the expression in the above mentioned juxtaposed diencephalic brain regions of the brain, Gpr151 mRNA is also detected in certain sensory ganglia and cranial nerve nuclei (Ignatov et al., 2004). In the spinal nerve ligation model of chronic neuropathic pain and in a model of heat induced pain, the expression of Gpr151 mRNA was strongly upregulated in dorsal root ganglia (Reinhold et al., 2015; Yin, Deuis, Lewis, & Vetter, 2016). Gpr151 mRNA expression is also increased in the facial nucleus of the brainstem in response to damage of the facial nerve (Gey et al., 2016). These findings suggest that GPR151, besides having a possible role in modulation of habenulothalamic functions, might also be important for pain modulation in cranial and peripheral nerves. However, a recent study utilizing mice carrying a Gpr151 loss-of-function mutation could not confirm this hypothesis (Holmes et al., 2017).

In a previous investigation (Broms et al., 2015), we characterized the *efferent* connectivity of habenular neurons expressing the GPR151 protein using immunohistochemistry. The aim of the current study was to identify the *afferent* regions projecting to Gpr151-expressing neurons using monosynaptic pseudotyped rabies virus tracing, to gain further knowledge about this diencephalic neuronal subpopulation. Using pseudotyped rabies virus, Gpr151-expressing neurons can be targeted specifically, avoiding some of the problems associated with conventional tracers, such as uptake in fibers of passage and diffusion of tracer to neighboring structures (Watabe-Uchida, Zhu, Ogawa, Vamanrao, & Uchida, 2012; Wickersham et al., 2007). A detailed anatomical characterization of the input and output of Gpr151-expressing neurons could facilitate future functional studies of this orphan receptor.

2 | MATERIALS AND METHODS

2.1 | Nomenclature

In this article, we will primarily use the nomenclature and area delineations (Table 1) of Franklin and Paxinos (2008). We use the nomenclature of Wagner, Stroh, and Veh, (2014) for the subnuclear organization of the habenula. The categorization of brain areas was done according to the hierarchy of the Allen Mouse Brain Atlas (Lein et al., 2006).

2.2 | Animals

All procedures described in the current investigation been approved by the Malmö-Lund Ethical Committee for the use and care of laboratory animals (permit no. M37-16). The Tg(Gpr151-Cre)#Ito transgenic mouse line containing random insertion of bacterial artificial chromosome (BAC) clone MSMg01-81G4 (Kobayashi et al., 2013) was kindly provided by Dr. Itohara (Laboratory for Behavioral Genetics, RIKEN

Brain Science Institute, Saitama, Japan) and maintained on a C57BL/6J background (RRID:IMSR_JAX:000664). To identify individual mice carrying the Cre recombinase allele, polymerase chain reaction genotyping was performed (Transnetyx, Cordova, TN) using the proprietary "CRE" probe set.

A total number of 46 adult (11–14 weeks old) mice was used in the experiment. Wild type litter mates (Cre-negative) were used as negative controls. The mice were housed in groups of two to six animals with free access to standard lab chow and water, in an air conditioned room at 22–23°C with a standard 12-hr light/dark cycle (lights on 07:00 a.m., off 07:00 p.m.). The cages (1284L Eurostandard Type II L, Techniplast, Italy) were enriched with aspen wooden bedding and nesting material.

2.3 | Retrograde Cre-dependent tracing using pseudotyped rabies virus

Monosynaptic tracing of the afferents of Cre-expressing neurons (Callaway & Luo, 2015; Watabe-Uchida et al., 2012) was carried out in two steps. First, Cre-dependent expression of an avian sarcoma-leukosis virus receptor (TVA) fused to the fluorescent protein mCherry (TVA-mCherry) and rabies glycoprotein (RG) was achieved by an intracerebral injection of adeno-associated virus (AAV) vectors. Second, SADΔG-eGFP(EnvA), a glycoprotein-deleted (ΔG) rabies vector pseudotyped with avian sarcoma-leukosis virus envelope protein (EnvA) was injected. In Cre-expressing neurons, TVA-mCherry then becomes expressed and acts as an entry receptor for the EnvA coated rabies vector, while infection should not be possible in TVA-negative neurons. RG allows budding of the viral particle and transsynaptic transport to afferent neurons. The rabies vector also carried the gene for enhanced green fluorescent protein (eGFP), allowing detection of infected neurons. We will hereafter refer to Cre-positive and TVA-mCherry/RG-expressing neurons that were infected by SADΔG-eGFP(EnvA) as *starter neurons*. The eGFP-positive/TVA-mCherry-negative afferent neuronal populations lack expression of RG which prohibits further propagation of the rabies virus (Figure 1).

The three AAV vectors, AAV8-Ef1a-FLEX-TVA-mCherry, AAV8-CA-FLEX-RG, and AAV8-hSyn1-FLEX-mCherry, were obtained from the UNC Vector Core (University of North Carolina at Chapel Hill, NC). The FLEX-switch makes these three vectors Cre-dependent by allowing one stable Cre-mediated inversion of the reversed transgene sequence (Atasoy, Aponte, Su, & Sternson, 2008). SADΔG-eGFP(EnvA) was obtained from the Gene Transfer, Targeting and Therapeutics Core (GT3) at Salk Institute (La Jolla, CA) and from Dr. Meletis at Karolinska Institute (Stockholm, Sweden).

Gpr151-Cre mice ($n = 38$) and wild type controls ($n = 5$) were anesthetized with isoflurane (induction at 5% and maintenance at 1–2%) and placed in a stereotaxic frame. The scalp was locally anesthetized with bupivacaine (0.25%) and the skull exposed. After adjusting the skull to a horizontal position, a hole was drilled through the skull, exposing the brain surface. Using a thin glass pipette, 0.6 μl of a 1:1 mixture of AAV8-Ef1a-FLEX-TVA-mCherry (5.4×10^{12} viral genomes/ml) and AAV8-CA-FLEX-RG (2.4×10^{12} viral genomes/ml) was injected unilaterally into the habenula at two different anterior-posterior levels (coordinates anteroposterior: −1.75, mediolateral: +0.35 or −0.35, dorsoventral: −2.7 and anteroposterior: −1.4, mediolateral: +0.35 or −0.35, dorsoventral: −2.7 relative to Bregma), the paraventricular thalamic nucleus (anteroposterior: −0.46, mediolateral: +0.1 or −0.1, dorsoventral: −3.25 relative to Bregma), or the lateral posterior thalamic nucleus (anteroposterior: −1.7, mediolateral: +1.3 or −1.3, dorsoventral: −2.7 relative to Bregma). In three of the animals injected in the habenula, AAV8-CA-FLEX-RG was omitted to verify that eGFP expression in neurons outside the injected area is a result of transsynaptic transport of rabies virus particles rather than direct infection of afferent terminals. After the injection, the pipette was left in the brain for 4 min to minimize back flow of the vector into the needle tract. The skin was sutured with absorbable suture, and the mouse was kept on a heat pad until recovered from the anesthesia, before returned to its home cage.

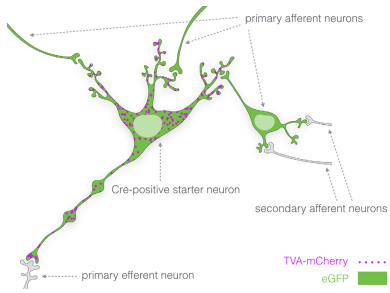

FIGURE 1 Distribution of fluorescent reporters in the Cre-dependent rabies virus retrograde tracing system. Cre-expressing neurons infected by AAV8-Ef1a-FLEX-TVA-mCherry express the sarcoma-leukosis virus receptor (TVA) fused to the fluorescent protein mCherry (TVA-mCherry; magenta). TVA enables entry of EnvA-coated pseudotyped glycoprotein-deleted rabies virus particles (SADΔG-eGFP(EnvA)) into Cre-positive neurons. Coinfection of these neurons with AAV8-CA-FLEX-RG leads to expression of rabies glycoprotein (RG) which enables transsynaptic retrograde transport of the rabies virus particles. Both the Cre-positive starter neurons and the primary afferent neurons will thus express the enhanced green fluorescent protein (eGFP; green) while TVA-mCherry expression will be limited to Cre-positive neurons

After 21 days, the stereotaxic procedure was repeated in order to inject the animals with 0.5 μl of the SADΔG-eGFP(EnvA) vector ($1.65–3.0 \times 10^7$ transforming units/ml). Seven days after the last vector injection, the mice were deeply anesthetized with an overdose of sodium pentobarbital and transcardially perfused with isotonic sodium chloride solution (0.9%) followed by cold phosphate buffered saline (PBS; 0.1M sodium phosphate buffer with 0.15M sodium chloride) containing 4% paraformaldehyde for 8 min (~100 ml per animal).

2.4 | Immunohistochemistry

The brains were dissected and postfixed in 4% paraformaldehyde for 18 hr at 4°C. After post-fixation, the brains were immersed in sucrose

solution (25% in PBS) at 4°C for 1–3 days until equilibration had occurred (i.e., the brains sank to the bottom of the vial). The brains were frozen on dry ice, sectioned in 30 μm sections using a sliding microtome (Thermo Scientific HM450) and cryoprotected in antifreeze solution (30% glycerol, 30% ethylene glycol, 40% 0.5M PBS) before storage at −20°C. During sectioning, the left hemisphere was marked with a needle to keep track of the orientation of the sections.

Immunohistochemistry was performed on free floating brain sections as described previously (Broms et al., 2015). The sections were washed in PBS, blocked with normal donkey serum (5%) in PBST (PBS containing 0.05% Tween-20) for 1 hr at room temperature and subsequently incubated in blocking solution with primary antibody over night at 4°C. The primary antibodies used in the experiment are described below. After repeated washing in PBS, the sections were incubated with biotinylated or Cy5-conjugated secondary antibodies at 3 μg/ml (Jackson ImmunoResearch Europe Ltd., Suffolk, United Kingdom) in PBST, 2 hr at room temperature. For immunofluorescent detection, sections were washed and mounted on Superfrost Plus glass slides (Menzel Gläser, Brunswick, Germany) with a polyvinyl alcohol and glycerol based mounting solution containing the anti-fading agent 1,4-diazabicyclo[2.2.2]octane (PVA-DABCO).

Fluorescent images were acquired using a Nikon Eclipse Ti confocal microscope with NIS-Elements (version 4.40) software (Nikon Instruments Europe BV, Amsterdam, The Netherlands). For automatic detection and marking of eGFP-expressing neurons in scanned images, ImageJ (version 2.0.0-rc-59/1.51n, RRID:SCR_003070) was used. The eGFP channel was thresholded to create a binary mask. The positions of eGFP-expressing cells were then obtained using the "Analyze Particles…" subroutine of ImageJ. Each location was marked with a green circle. A grayscale look-up table was applied to the mCherry channel and the background fluorescence of this channel provided a background for each micrograph.

For light microscopy detection, biotinylated secondary antibodies were used. After washing in PBS, the sections were incubated with avidin-biotin-peroxidase complex (diluted 1:125 in PBS) (VECTASTAIN Elite ABC Kit, Vector Laboratories, Burlingame, CA) and developed using 3,3'-diaminobenzidine (DAB, 0.5 mg/ml) with nickel chloride (0.5 mg/ml). Following the DAB reaction, sections were mounted, dehydrated in increasing concentrations of ethanol followed by xylene and finally coverslipped with *p*-xylene-bis-pyridinium bromide (DPX) (Fisher Scientific, Pittsburgh, PA). Low resolution micrographs were acquired using a slide scanner (PathScan Enabler 5, Meyer Instruments Inc., Houston, TX).

2.5 | Antibody characterization

Rabbit GPR151 polyclonal antibody (SAB4500418; Sigma-Aldrich, St. Louis, MO; RRID: AB_10743815) was raised against a synthetic peptide containing amino acids 370-419 (EKEKPSSPSSGKGKTEKAEIPILPDVEQFWHERDTVPSVQDNDPIPWEHEDQETGEGVK) of the C-terminal of human GPR151. It recognizes a single band of 46 kDa on western blots of lysate of GPR151-expressing K562 cells. The specificity was confirmed by pre-adsorption with the immunogen peptide (according to the manufacturer's technical information). In homozygous Gpr151-knockout mice, the immunoreactivity was completely abolished, further proving the specificity of the antibody (Broms et al., 2015). In the present experiment, a working concentration of 0.125 μg/ml was used.

Rabbit mCherry polyclonal antibody (ab167453; Abcam, Cambridge, MA; RRID:AB_2571870) was raised against recombinant full length mCherry protein (MVSKGEEDNMAIIKEFMRFKVHMEGSVNGHEFEIEGEGEGRPYEGTQTAKLKVTKGGPLPFAWDILSPQFMYGSKAYVKHPADIPDYLKLSFPEGFKWERVMNFEDGGVVTVTQDSSLQDGEFIYKVKLRGTNFPSDGPVMQKKTMGWEASSERMYPEDGALKGEIKQRLKLKDGGHYDAEVKTTYKAKKPVQLPGAYNVNIKLDITSHNEDYTIVEQYERAEGRHSTGGMDELYK), a fluorescent protein derived from the DsRed protein. According to the manufacturer's specifications, the antibody recognizes a ~27 kDa band in lysate of HEK293 cells transfected with a pFin-Ef1a-mCherry vector. In our experiment, the antibody (used at a working concentration of 0.2 μg/ml) produced a specific immunohistochemical signal in brains of Gpr151-Cre animals injected with the AAV8-Ef1a-FLEX-TVA-mCherry vector.

A different set of Gpr151-Cre mice ($n = 3$) were injected bilaterally in the habenula with AAV8-hSyn-FLEX-mCherry (0.6 μl, 6.1×10^{12} viral genomes/ml) to label cell bodies of Cre-expressing neurons. Four weeks following the injections the brains were prepared for in situ hybridization. Perfusion and postfixation in paraformaldehyde was carried out as described above. After equilibration in 25% phosphate buffered sucrose solution, 14 μm thick brain sections mounted onto Superfrost Plus glass slides using a cryostat. Detection of Gpr151-mRNA was performed using the RNAscope® Fluorescent Multiplex Assay with a probe set targeting base pairs 27–988 of mouse Gpr151-mRNA (Cat No. 317321, Advanced Cell Diagnostics, Inc., Newark, CA) (Wang et al., 2012). Briefly, the sections were air dried for 20 min, washed in PBS and subsequently immersed in boiling 1x Target Retrieval solution for 5 min. After washing in distilled water and 100% ethanol for 2 min each, the sections were incubated with Protease IV solution for 30 min at 40°C in a humidified tray. After washing in distilled water for 2 min, the sections were then hybridized with Gpr151 target probe for 2 hr at 40°C followed by amplification solutions 1 (30 min), 2 (15 min), 3 (30 min), and 4 (15 min) at 40°C. Between each amplification step, the sections were rinsed in 1x Wash Buffer for 2 min at room temperature. Finally, the sections were counterstained with 4',6-Diamidine-2'-phenylindole dihydrochloride (DAPI) for 30 s and coverslipped in PVA-DABCO. The fluorochrome used for detection in this system was Alexa488. Images were acquired using a Nikon Eclipse Ti confocal microscope with NIS-Elements software.

3 | RESULTS

3.1 | GPR151 protein and mRNA detected in Cre-expressing neurons

As previously reported, immunofluorescent GPR151 staining was pronounced in habenular axonal projections, while often barely above background level in the neuronal somata (Broms et al., 2015). To better visualize cell bodies with expression of Cre, we injected Gpr151-Cre

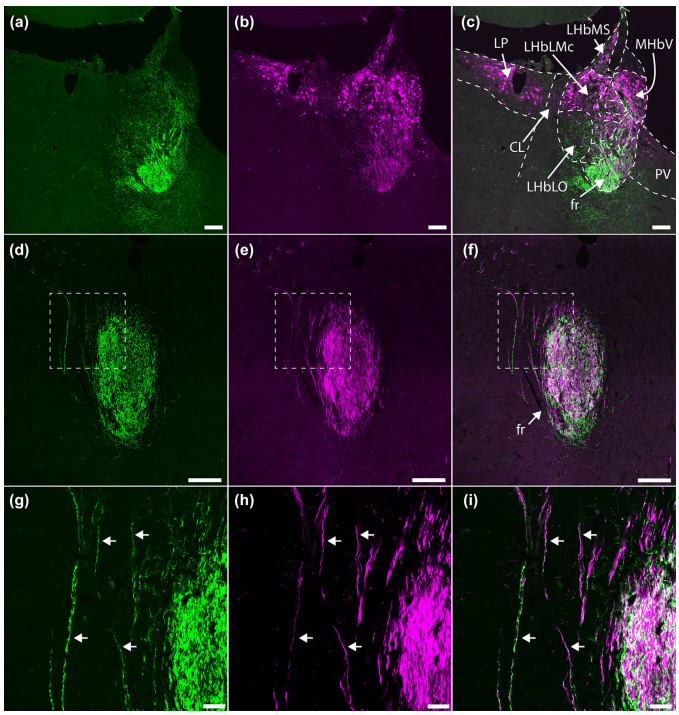

FIGURE 2 GPR151 protein expression in axons of Gpr151-Cre neurons. Coronal sections of a Gpr151-Cre mouse injected with AAV8-hSyn1-FLEX-mCherry in the habenular region. Panels (g–i) represent magnifications of the insets in (d–f). Cell bodies positive for mCherry (magenta) were observed in the ventral medial habenula, the lateral habenula (excluding the oval subnucleus of the lateral division of lateral habenula), the lateroposterior, and paraventricular thalamic nuclei (b, c; −1.94 mm posterior to Bregma). Fibers expressing mCherry and GPR151 protein (green) exited the habenula through the fasciculus retroflexus (a–i; −2.30 mm posterior to Bregma), where colocalization between mCherry and GPR151 was observed (arrows; g–i). Scale bar (a–f) = 100 μm, (g–i) = 20 μm

mice with AAV8-hSyn1-FLEX-mCherry in the habenular region (Figure 2).

Colocalization between GPR151 protein and mCherry could be observed in fibers in the fasciculus retroflexus (Figure 2d–i), which contains the efferent axons from the habenula. In the habenula, mCherry-expressing cell bodies were localized in the ventral division of the medial habenula and in most lateral habenular subnuclei, excluding the oval subnucleus of the lateral division of lateral habenula (Figure 2c). Furthermore, mCherry-positive neurons were also observed in the paraventricular thalamic nucleus, and in the lateral dorsal and lateral posterior thalamic nuclei. No GPR151 protein could be detected in these thalamic areas using immunohistochemistry (Figure 2c; Broms et al., 2015).

Next, we performed fluorescent in situ hybridization using a RNAscope® probe targeting mouse Gpr151 mRNA on brain sections of mice that had been injected with AAV8-hSyn1-FLEX-mCherry into the habenula. In Figure 3, expression of Gpr151 mRNA in mCherry-expressing neurons is seen in neurons located in the habenula, paraventricular thalamic nucleus and the lateral posterior thalamic nucleus. The strongest Gpr151 mRNA expression was observed in medial and lateral habenula, compared to much weaker expression in the paraventricular thalamic nucleus while only a very faint expression was observed in neurons of the lateral posterior thalamic nucleus. In the habenula (Figure 3e) and the paraventricular thalamic nucleus, mCherry colocalized with the Gpr151 mRNA signal. In the lateral posterior

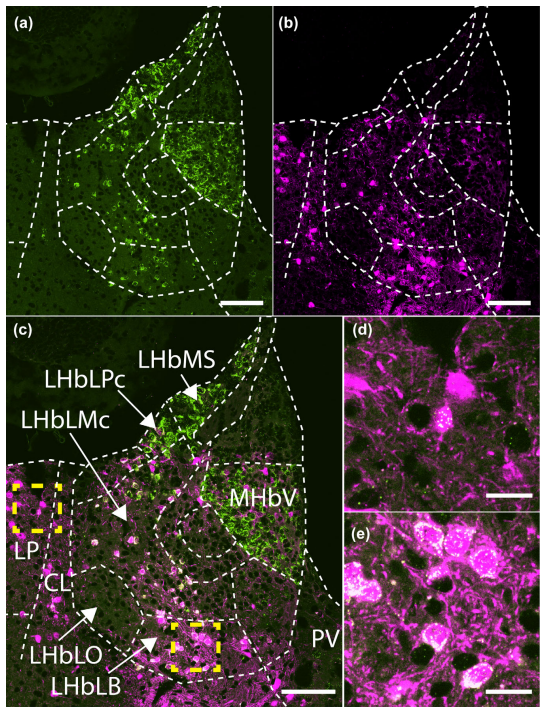

FIGURE 3 Gpr151 mRNA expression in Gpr151-Cre neurons. Coronal section of a Gpr151-Cre mouse injected with AAV8-hSyn1-FLEX-mCherry in the habenular region (−1.82 mm posterior to Bregma). Gpr151 mRNA expression (green) can be seen in the ventral medial habenula, lateral habenula (excluding the oval subnucleus of the lateral division), as well as in the lateral posterior, central lateral, and paraventricular thalamic nuclei (panels a, c, d, e). Expression of mCherry (magenta, panels b–e) show partial overlap with Gpr151 mRNA. Transduction efficiency and injection localization could explain the lack of mCherry expression in certain Gpr151-positive subregions like the LHbMS. Examples of coexpression of mCherry and Gpr151 mRNA in the lateral posterior thalamic nucleus and lateral habenula are shown in panel (d) and (e) (magnifications of insets in panel c). Scale bar (a–c) = 100 μm, (d, e) = 20 μm

thalamic nucleus, Gpr151 was undetectable in some mCherry-positive neurons (Figure 3d). This finding is further considered in the discussion.

Using a crossing between Gpr151-Cre mice and two different ß-galactosidase reporter strains, Kobayashi et al. (2013) identified Cre-expressing cells in the medial and lateral habenula, paraventricular thalamic nucleus and the reuniens thalamic nucleus. This expression pattern largely agrees with our findings, except that more Cre-expressing cells were detected in the laterodorsal and lateral posterior thalamic nucleus in the current investigation. Given that Gpr151 mRNA expression is accentuated in the habenula and paraventricular thalamic nucleus (Ignatov et al., 2004; Lein et al., 2006), no viral injections targeting the reuniens thalamic nucleus were performed in the current investigation.

3.2 | Monosynaptic tracing of afferents to Cre-expressing neurons

Using the Cre-dependent rabies virus tracing system, Gpr151-Cre starter neurons were labeled with TVA-mCherry and eGFP, while monosynaptic afferents to these starter neurons were labeled with eGFP only. Not all TVA-mCherry-expressing neurons coexpressed eGFP. This may be explained by different transduction efficiency of the

TABLE 1 Abbreviations

Abbreviation	Area	Abbreviation	Area
3V	3rd ventricle	Me	medial amygdaloid nucleus
aca	anterior commissure, anterior part	MG	medial geniculate nucleus
Acb	accumbens nucleus	MHb	medial habenular nucleus
AD	anterodorsal thalamic nucleus	MHbD	dorsal subnucleus of the MHb
AH	anterior hypothalamic area	MHbS	superior subnucleus of the MHb
AI	agranular insular cortex	MHbV	ventral part of the MHb
Arc	arcuate hypothalamic nucleus	MHbVc	central subnucleus of the MHbV
Au	auditory cortex	MHbVl	lateral subnucleus of the MHbV
AV	anteroventral thalamic nucleus	MHbVm	medial subnucleus of the MHbV
BAC	bed nucleus of the anterior commissure	MnPO	median preoptic nucleus
BL	basolateral amygdaloid nucleus	MnR	median raphe nucleus
BM	basomedial amygdaloid nucleus	MPA	medial preoptic area
CG	cingulate cortex	MPT	medial pretectal nucleus
Cg1	cingulate cortex, area 1	MPtA	medial parietal association cortex
Cg2	cingulate cortex, area 2	mRt	mesencephalic reticular formation
CL	centrolateral thalamic nucleus	MS	medial septal nucleus
CI	claustrum	MTu	medial tuberal nucleus
CPu	caudate putamen (striatum)	Pa	paraventricular hypothalamic nucleus
DB	nucleus of the diagonal band	PAG	periaqueductal gray
DG	dentate gyrus	Pe	periventricular hypothalamic nucleus
DLG	dorsal lateral geniculate nucleus	PF	parafascicular thalamic nucleus
DM	dorsomedial hypothalamic nucleus	PG	pregeniculate nucleus
DR	dorsal raphe nucleus	PH	posterior hypothalamic nucleus
EP	entopeduncular nucleus	PLH	peduncular part of lateral hypothalamus
f	fornix	PnO	pontine reticular nucleus, oral part
fmi	forceps minor of the corpus callosum	Po	posterior thalamic nuclear group
fr	fasciculus retroflexus	PrC	precommissural nucleus
IC	inferior colliculus	PrL	prelimbic cortex
IF	interfascicular nucleus	PT	paratenial thalamic nucleus
IL	infralimbic cortex	PV	paraventricular thalamic nucleus
		PVA	paraventricular thalamic nucleus, anterior part
IP	interpeduncular nucleus	PVP	paraventricular thalamic nucleus, posterior part
LD	laterodorsal thalamic nucleus	RCh	retrochiasmatic area
LDTg	laterodorsal tegmental nucleus	RLi	rostral linear nucleus (midbrain)
LHb	lateral habenular nucleus	RMg	raphe magnus nucleus
LHbA	anterior division of the LHb	RSD	retrosplenial dysgranular cortex
LHbL	lateral division of the LHb	Rt	reticular nucleus (prethalamus)
LHbLB	basal subnucleus of the LHbL	S1	primary somatosensory cortex
LHbLMc	magnocellular subnucleus of the LHbL	S2	secondary somatosensory cortex

(Continues)

TABLE 1 (Continued)

Abbreviation	Area	Abbreviation	Area
LHbLMg	marginal subnucleus of the LHbL	SC	superior colliculus
LHbLO	oval subnucleus of the LHbL	SCh	suprachiasmatic nucleus
LHbLPc	parvocellular subnucleus of the LHbL	SFi	septofimbrial nucleus
LHbM	medial division of the LHb	SHy	septohypothalamic nucleus
LHbMC	central subnucleus of the LHbM	sm	stria medullaris
LHbMMg	marginal subnucleus of the LHbM	ST	bed nucleus of the stria terminalis
LHbMPc	parvocellular subnucleus of the LHbM	TS	triangular septal nucleus
LHbMS	superior subnucleus of the LHbM	V1	primary visual cortex
LHbP	posterior division of the LHb	V2	secondary visual cortex
LP	lateral posterior thalamic nucleus	VMH	ventromedial hypothalamic nucleus
LPO	lateral preoptic area	VP	ventral pallidum
LS	lateral septal nucleus	VTA	ventral tegmental area
M	medial mammillary nucleus	ZI	zona incerta
ME	median eminence	ZIR	zona incerta, rostral part

Abbreviations of mouse brain regions according to Franklin and Paxinos (2008) and Wagner, Stroh, et al. (2014).

AAV and rabies vectors or that the vectors were injected at slightly different locations due to the margin of error of the stereotaxic technique. The injections targeted one of three areas, the habenula, the paraventricular thalamic nucleus, or the lateral posterior thalamic nucleus. The starter neurons at the injection sites and the resulting eGFP expression in afferent structures are summarized in Tables 2 and 3.

In wild type animals, occasional neurons expressing mCherry and eGFP could be observed close to the injection tract in the habenula, which implies minor local Cre-independent expression (Figure 4j–l; Table 2). However, no eGFP+ neurons were detected outside of the injected area, so the analysis of eGFP+ neurons far from the injected site is not impacted.

SADΔG-(EnvA) is capable of infecting neurons with minute expression of TVA (Callaway & Luo, 2015). Since it has been shown that trace amounts of TVA-expression can result from retrograde transport of AAV-TVA (Menegas et al., 2015), it is important to confirm that the starter neurons are indeed restricted to the injected area. By omitting AAV8-CA-FLEX-RG, transsynaptic transport is inhibited and eGFP expression should be restricted to local TVA-expressing neurons. In Gpr151-Cre animals where AAV8-CA-FLEX-RG was omitted, a strong expression of TVA-mCherry and eGFP was only observed in the vicinity of the injection, but not anywhere else in the brain (Figures 4g–i and 5; Table 2). This confirms that any eGFP+ neurons found outside of the injected area result from RG-dependent transsynaptic transport of rabies virus.

3.3 | Afferents to Gpr151-Cre neurons in the habenula

Seven cases with good quality injections targeting the habenula were considered for further analysis (Figure 4a–f; Table 2). In all cases, a majority of starter neurons were detected in the habenula, although a varying degree of spread to neighboring thalamic structures, such as the paraventricular thalamic nucleus and the lateral posterior thalamic nucleus was also observed.

Very few eGFP+ neurons were detected in the cerebral cortex (Figure 6; Table 3). Occasional eGFP+ neurons were observed in medial prefrontal areas, most notably bilaterally in the prelimbic and infralimbic cortices.

Several structures in the pallidum contained large numbers of eGFP+ neurons (Table 3). Moderate numbers of eGFP+ neurons were detected in the medial (Figure 7a) and triangular septum (Figure 7d). The nucleus of the diagonal band contained many eGFP+ neurons, both in the vertical and horizontal limb (Figure 7a). Moderate numbers of eGFP+ neurons were also observed in the bed nucleus of the anterior commissure (Figure 7d). The bed nucleus of the stria terminalis contained great numbers of eGFP+ neurons, especially in case M17 (Figure 7c). In two cases (M18 and M104), a dense network of eGFP+ neurons was seen in the entopeduncular nucleus (Figure 7e,f). Interestingly, these specific cases were distinguished by a large number of starter neurons in lateral division of the lateral habenula as well as spread into the lateral posterior thalamic nucleus.

The hypothalamus was another major source of input to the Gpr151-Cre neurons of the habenula (Table 3). A continuous group of eGFP-expressing neurons stretching from the lateral preoptic area to the peduncular part of the lateral hypothalamus was observed in all cases (Figures 6 and 7b,e,f). Scattered neurons were also observed in several medial hypothalamic nuclei (Table 3). In two cases (M18 and M104), the same animals which displayed eGFP+ neurons in the entopeduncular nucleus, eGFP+ neurons could also be observed in the zona incerta.

Because undetectable expression of TVA-mCherry may be sufficient to allow entry of the rabies vector (Callaway & Luo, 2015), it

TABLE 2 Starter neuron populations

		Habenula							Paraventricular thalamic nucleus				
		M17	M18	M80	M102	M103	M104	M105	M74	M112	M113	M120	M121
Medial habenula	MHbD												
	MHbS												
	MHbVl	+++++		+++++	+++	++	++	++++					
	MHbVc	+++++		+++++	+++	++	++	+++					
	MHbVm	+			+								
Lateral habenula	LHbA	+	+++	+	++			++			+		
	LHbMS	+++++	++	+++++	++++		++	++++					
	LHbMPc				+	+++		++					
	LHbMC		++	++	+++	++		+++					
	LHbMMg				+++			+					
	LHbLMg	++	++	++		+							
	LHbLPc	++	++	+++	+++	++++							
	LHbLMc	+	+++++	+++	+++++	+++++	++	++					
	LHbLB		++++		++++	++++	++						
	LHbLO												
	LHbP		+	++++	++++	+++	++	+					
Paraventricular thalamic nucleus	PVA								+++	+++++	+++++	+++	+++++
	PV			+	+	+++	+	+		+	++	++	+++++
	PVP				+								
Lateral thalamic nuclei	LP		++				++						
	LD	+	++										
	CL		+			+	+						
Posterior thalamic nuclei	PF												
	PrC			+									
	Po												
	MPT							+					

		Lateral posterior thalamic nucleus				Habenula no RG			Habenula wild type					
		M114	M115	M116	M119	M106	M117	M118	M113	M16 M77		M78	M81	
Medial habenula	MHbD													
	MHbS													
	MHbV													
	MHbVc													
	MHbVm													
Lateral habenula	LHbA		++	++	++	+								
	LHbMS	+++	+++	+++	++++	++		+						
	LHbMPc	+	++	+		+	+	++						
	LHbMC	+++		++	++	+++		++						

(Continues)

TABLE 2 (Continued)

		Lateral posterior thalamic nucleus				Habenula no RG			Habenula wild type					
		M114	M115	M116	M119	M106	M117	M118	M113	M16	M77	M77	M78	M81
	LHbMMg							++						
	LHbLMg			++				+++						
	LHbLPc	++		++	+++	++++		+++						
	LHbLMc	+++		++		+++++						+		
	LHbLB							++++						
	LHbLO													
	LHbP	+++		++	+++	+++++	+++++	+++++						
Paraventricular thalamic nucleus	PVA													
	PV					+		++						
	PVP						++	+++						
Lateral thalamic nuclei	LP	+++++	+++++	+++++	+++++	+++		++						
	LD	+++++	+++++	+++++	+++++	++++								
	CL	+	++	+++	+			+++						
Posterior thalamic nuclei	PF				+		++	++++						
	PrC			+	+	++	+++	+++						
	Po	++++	++		++++									
	MPT	+	++		++		+	++						

Semiquantitative estimate of neurons coexpressing TVA-mCherry and eGFP (starter neurons) in target areas and neighboring structures. Each area was graded from + to +++++ depending on the number of mCherry/eGFP coexpressing cells observed.

cannot be ruled out that eGFP+ neurons close to the injected area that appear to lack mCherry are indeed afferent neurons and not starter neurons. Because of the proximity of the injection target area to some Gpr151-expressing thalamic nuclei, it makes interpretation of eGFP+ neurons in these areas uncertain. Scattered eGFP+ neurons were detected in the pregeniculate, dorsolateral geniculate, and medial geniculate nuclei which are far from the injected area. The parafascicular thalamic nucleus and the precommissural nucleus also contained a small number of eGFP+ neurons, along with occasional starter neurons. Occasionally, eGFP+ neurons were visible in the medial or lateral habenula contralateral to the injected side which suggests minor contribution from an intrahabenular projection.

In the midbrain, scattered eGFP+ neurons were observed in the pretectal area, superior colliculus, and the periaqueductal gray. A few eGFP+ cells could also be detected in the interpeduncular nucleus, which is the projection target of neurons in the medial habenula. This implies a reciprocal connection between the habenular complex and the interpeduncular nucleus. EGFP+ neurons were also observed in many monoaminergic midbrain areas such as the ventral tegmental area (primarily the interfascicular nucleus), rostral linear nucleus, median, and dorsal raphe nuclei.

Very few eGFP+ neurons were detected in hindbrain areas, including the laterodorsal tegmental nucleus, pontine reticular nucleus, and raphe magnus nucleus.

3.4 | Afferents to Gpr151-Cre neurons in the paraventricular thalamic nucleus

Five animals where starter neurons could be observed in the paraventricular thalamic nucleus (Table 2) were further analyzed regarding afferents (Figures 8 and 9; Table 3). The starter neuron population was entirely restricted to the target area except for one case (M113) where a few cells were also observed in the anterior division of the lateral habenula.

Cortical afferents were restricted to frontal cortical areas such as the prelimbic, infralimbic, and agranular insular cortices. In two cases (M113 and M121), a few eGFP+ neurons could also be observed in the claustrum.

The distribution of eGFP+ neurons in the pallidum was remarkably similar to that of the afferents to the habenular Gpr151-Cre population (Table 3). The nucleus of the diagonal band, bed nucleus of stria terminalis, and the ventral pallidum contained many eGFP+ neurons. No eGFP+ neurons were observed in the medial septal nucleus or the

TABLE 3 Locations of primary afferents to Gpr151-Cre neurons.

		Habenula							Paraventricular thalamic nucleus					Lateral posterior thalamic nucleus			
		M17	M18	M80	M102	M103	M104	M105	M74	M112	M113	M120	M121	M114	M115	M116	M119
Cerebral cortex	AI										+/+						
	Au													+/-			+/-
	BL					+/+											
	BM										+/-						
	Cg1		+/-				+/-						+/-	++/-	+++/-	+++/-	++/-
	Cg2		+/-	+/-			+/-			-/+				++/+	+++/-	+/-	++/+
	CI				+/-		+/-				+/+		+/+				+/-
	DG	+/-						+/-							+/-		
	IL			+/-			+/+	+/-	+/-				-/+	+/-		+/+	++/-
	MPtA															+/-	
	PrL		+/+				++/+		+/-	+/+	+++/++	-/+	++/+	+/-	+/-	++/+	+++/+
	RSD														+/-	+/-	+++/-
	S1													+/-	++/-		
	S2														+/-		
	V1															++/-	+/-
	V2													++/-		+/-	+/-
Pallidum	BAC	+++/++	+/-	+/-			+/-	++/-						+/-	+/-	++/-	++/++
	DB	+++/++	++++/+	++++/+	++/+	+/+	+++/++	+++/+		++/++	++/-	+/+	++/++	++/-	++/-	+/-	+++/+
	EP	++/-	+++ ++/+				+++++/+	+/-						++/-	+/-		+++/+
	MS	++	+	++			++	+							+	+	+
	ST	++++/+++	+++/-	++/-	+/-	+++/-	++/++				++/++	+/-	+/+	++++/++	+++/+	++++/++	+++/++
	TS	+/-		+/-		+/+	+++/+	+/-									
	VP	++/++	++/-	++/+	+/-	++/-	+++/++	+++/+		+/+	+/-	-/+	+/+	+++/+	++/-	+/-	++++/++
Striatum	Acb						+/-			++/++	++/++	+/-	+/+				+/-

(Continues)

TABLE 3 (Continued)

		Habenula						Paraventricular thalamic nucleus					Lateral posterior thalamic nucleus				
		M17	M18	M80	M102	M103	M104	M105	M74	M112	M113	M120	M121	M114	M115	M116	M119
	CPu						++/-		+ /+		+/-		++/++	+ /+	++/-	+/-	+ +/-
	LS	+/-	+/-	+ /+			+/-	+/-		+/-	+ /+	+/-	+/-	+ +/+	+/-	+/-	+ /+
	Me										+/-						+/-
Hypothalamus	AH		+/-		+/-	+/-	+/+	+/-	+/-	+/+	++/++	+/-		+ /+			+ /+
	Arc	+/-	-/+			+/-	+/-	++/++	+/+	+/-	++/++		+/-	+/-		++/-	-/+
	DM	++/-	+/-	+/-				+/+		+/+	+++/ +++		-/+	+/+	+/-	+/-	+/-
	LPO	+++/ ++	++++/ ++	+/-	++/+	++/+	+++++/ ++	++/-	+/+	+/+	++/++		+/+	++++/+	+++/+	+++++/+	++++/ ++
	M			+/-				+/+			+/-			+ /+		+/-	+ +/+
	MnPO			+		+				+	++	+	+				
	MPA				-/+	+/+	++/-		+/-	+ +/++	+++ +/ +++	+/+	++/ +++		+/-	+ +/+	+ +/+
	MTu										+/+		-/+				
	Pa		+/-		+/-						++/+					+/-	
	Pe					+/-				+/+	++/++		+/+				
	PH			-/+	+/-									+/-		+/-	
	PLH	+++/ ++	+++++/ +++	++/+	+++/+	++++/ ++	+++++/ ++	++++/ ++	+/-	+/++	+++/++	+/-	++/ ++	+++++/ ++	+++/ ++	+++++/ +++	+++++/ +++
	RCh					+/+	+/+			++/-	+++/++			-/+			
	SCh					+/-				+/+	++/+	+/-	+/+				
	SFi						++/-	++/-									
	SHy	+/-		+/+				++/-			++/++						
	VMH	+/-		+/-	++/-		+/-			+/+	+++/+++		++/+				+/-
	ZI		++/-			+/-	++ +/-	+/-	+/-	+ ++/+++	++++/ +++++	++/+	+++/ +++	+++/-	++/-	+ ++++/+	+ ++++/+
Thalamus	AD																+/-
	LD/LP (contralateral side)												+				

(Continues)

TABLE 3 (Continued)

		Habenula						Paraventricular thalamic nucleus					Lateral posterior thalamic nucleus			
		M17	M18	M80	M102	M103	M104	M105	M74 M112	M113	M120	M121	M114	M115	M116	M119
	LHb (contralateral side)		+					+					+		+	
	MD		+/-							++/-		+/+			+/-	
	MG/PG/DLG	+/+		+/-	+/-		+++/+	+/-					++/-	+/-	+++/+	+++/+
	MHb (contralateral side)	+						+							+	
	PF	+/-	+/+	+/-		+/-	+++/+	+/-	+/-	+/+		++/+	++/-		+/-	
	Po												++ +/-			
	PrC	+/-	+/-	+/-	++/-		+/-		+/-							
	PVA			+/-	++/-	+/-	+/+	+/-					++ +/++	+/-	+/-	
	Rt						+++/-		-/+				++++/+	+++/-	+++++/-	+++++/+
Midbrain	DR		+/-		+/-	+/-	+++/+	+	+/-	+/+			++	+/+	+++/+	++/-
	IC															+/-
	IP	+ /+			+/-	-/+	+/+	++/-		+/-			+			+/+
	MnR	+++/+	+/-	+/-	+/+	+/+	+++/+	+	+/+	+/-		+/+	++		+	+/+
	MPT		++/-		++/-			++/+					+++/ ++			+++/++
	mRT		+++/+	+/-			+++/+			+/+	-/+	+/+	+/-	+/-		++/-
	PAG	+/-		+/-			+++/+	+/-	+/+	++/++	+/-	+/+	+/-	++/-		+/+
	RLi	+				+	+								+	
	SC	+/-	+/-	+/-	-/+	+/-		+/+		+/+			+++++/+	++++/ ++	+++++/++	+++++/ ++
	VTA	+/-	+/-	+/-	+/-	+/-	+++/+	+/-				+/+	+/-		+/-	+/+
Hindbrain	LDTg		+/-	+/-	+/-		+/-									++/-
	PnO		+/+		+/-		+/+	+/-					+/-			
	RMg		+/-	+/-												

Semiquantitative estimate of primary afferents to Gpr151-Cre neurons. The entire brain was investigated and areas were graded from + to ++++ depending on the number of eGFP expressing cells found. In paired structures, the ipsilateral estimate is shown to the left and the contralateral estimate to the right (ipsilateral/contralateral).

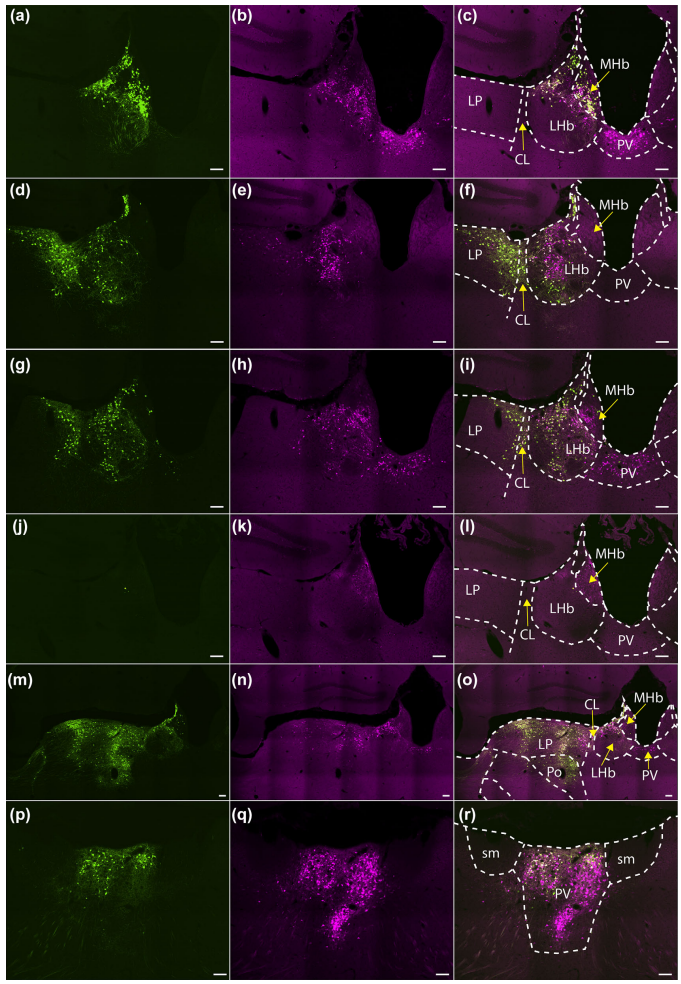

FIGURE 4 Expression of TVA-mCherry and eGFP after injections of viral vectors at target sites. Coronal sections through the target areas of cases M80 (habenula; a–c), M18 (habenula; d–f), M118 (habenula, no RG; g–i), M77 (habenula, wild type; j–l), M119 (lateral posterior thalamic nucleus; m–o), and M113 (paraventricular thalamic nucleus; p–r) showing sarcoma-leukosis virus receptor (TVA) fused to the fluorescent protein mCherry (TVA-mCherry; magenta; b, e, h, k, n, q), eGFP expression (green; a, d, g, j, m, p), and an overlay between the two (c, f, i, l, o, r). Scale bar = 100 μm

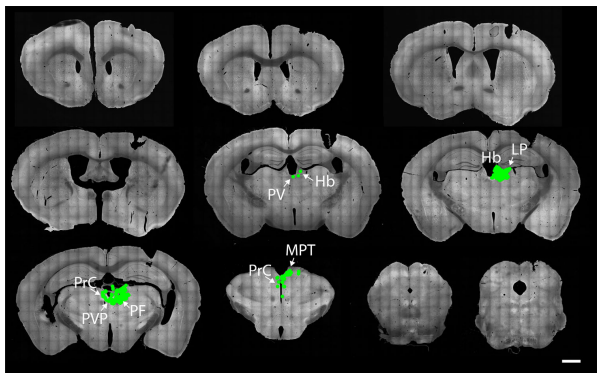

FIGURE 5 Omission of RG limits eGFP expression to the injected area. Coronal brain sections from 1.34 to −4.84 mm relative to Bregma of a Gpr151-Cre mouse (case M118) in which AAV8-Ef1a-FLEX-TVA-mCherry and SADΔG-eGFP(EnvA) was injected unilaterally in the habenula. Since AAV8-CA-FLEX-RG was omitted, transsynaptic transport of the rabies vector is inhibited. Although many eGFP positive (green) neurons could be seen in various nuclei in the targeted area (medial and lateral habenula, lateral posterior thalamic nucleus, parafascicular thalamic nucleus, paraventricular thalamic nucleus, and precommissural nucleus), no eGFP expressing neurons were detected elsewhere in the brain. Scale bar = 1000 μm

entopeduncular nucleus however, in contrast to the afferents of the Gpr151-Cre neurons in the habenula.

In the striatum, moderate numbers of eGFP+ neurons were detected in the accumbens nucleus, caudate putamen, and the lateral septum.

The main source of input to the paraventricular thalamic Gpr151-Cre population was the hypothalamus (Table 3). Similarly to the habenular Gpr151-Cre population, eGFP+ neurons could be detected in the lateral preoptic area and the peduncular part of the lateral hypothalamus (Figure 9e). Great numbers of eGFP+ neurons were also seen in the medial preoptic area, and to a lesser extent the median preoptic area (Figure 9b). Medial hypothalamic areas such as the anterior, ventromedial, dorsomedial, arcuate, paraventricular, and periventricular hypothalamic nuclei also contained many eGFP+ neurons (Figure 9b,d, e,f). Some afferent neurons were also seen in the retrochiasmatic (Figure 9d) and suprachiasmatic nuclei. The strongest projection arose from a cluster of cells in the rostral part of the zona incerta (Figure 9c).

Some eGFP+ neurons were also detected in thalamic areas such as the parafascicular and mediodorsal thalamic nuclei. In the midbrain, there were also a small number of eGFP+ neurons in the periaqueductal gray and the mesencephalic reticular formation.

3.5 | Efferent projections of the Cre-expressing population in the paraventricular thalamic nucleus

Since the paraventricular thalamic Gpr151-Cre population could be targeted specifically without spread into other Gpr151-expressing populations, we decided to also analyze the efferent connectivity of this population. Immunohistochemistry using mCherry antiserum was performed to visualize the efferent projections of the TVA-mCherry-expressing neurons (Figure 10). The cell bodies of these neurons were confined to the paraventricular nucleus, while dense fields of mCherry-immunoreactivity could be observed in the prelimbic area, the shell and core regions of accumbens nucleus, the basolateral amygdala, and the zona incerta. It should be noted that while no GPR151 protein could be detected by immunohistochemistry in any of these areas (Broms et al., 2015), Gpr151 mRNA was observed in the paraventricular thalamic nucleus in the current study (Figure 3c) and has also been reported previously (Ignatov et al., 2004; Wagner, French, et al., 2014).

3.6 | Afferents to Gpr151-Cre neurons in the lateral posterior thalamic nucleus

Four animals with injections targeting the lateral posterior thalamic nucleus were analyzed (Figure 11; Table 3). Large quantities of starter neurons were observed in a group of neurons in the lateral dorsal and lateral posterior thalamic nuclei. In two cases, the labeled population also extended into the posterior thalamic group (M114 and M119). Unfortunately, all cases also contained a varying number of starter neurons in the habenula which impose a limit on the analysis of the afferents to the lateral thalamic group. Some striking differences between the cases targeting the lateral posterior thalamic Gpr151-Cre population and the habenular Gpr151-Cre population could nonetheless be observed. The cingulate cortical area 1 and area 2, as well as the prelimbic cortex, contained many eGFP+ neurons in animals with starter neurons in the lateral posterior thalamic nucleus, but were completely devoid of eGFP+ cells when the injections were restricted to the habenula. Similarly, other cortical areas such as the retrosplenial dysgranular cortex as well as the primary and secondary visual cortex and primary and secondary somatosensory cortex, only contained eGFP+ neurons in cases with lateral posterior thalamic starter neurons.

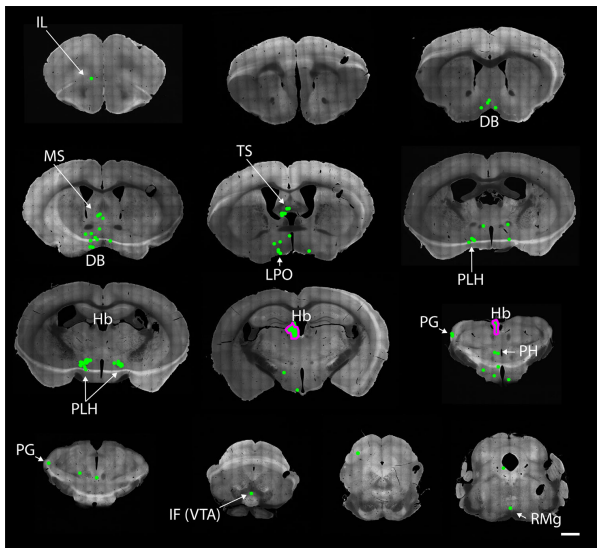

FIGURE 6 Afferents of habenular Gpr151-Cre neurons. Coronal brain sections from 1.98 to −4.96 mm relative to Bregma of a Gpr151-Cre mouse (case M80) where AAV8-Ef1a-FLEX-TVA-mCherry, AAV8-CA-FLEX-RG and SADΔG-eGFP(EnvA) was injected unilaterally in the habenula. Neurons coexpressing eGFP and mCherry (starter neurons; magenta outline) were almost exlusively located in the medial and lateral habenula. EGFP positive neurons (green) were found throughout the brain, most notably in the medial septal nucleus, nucleus of the diagonal band, lateral preoptic area, and the lateral hypothalamus (peduncular part). Scale bar = 1000 μm

Similar to what was observed when the habenula was targeted, many eGFP+ neurons could be observed in the bed nucleus of the anterior commissure, nucleus of the diagonal band, ventral pallidum, bed nucleus of stria terminalis, lateral preoptic area, lateral hypothalamic area, and the entopeduncular nucleus. The caudate putamen also contained eGFP+ positive neurons in contrast to habenula-targeting injections. Large number of eGFP+ neurons was observed in the zona incerta, mainly in the caudal part.

In the thalamus, dense populations of eGFP+ neurons were observed in pregeniculate, dorsolateral geniculate, and medial geniculate nuclei as well as the reticulate and paraventricular thalamic nuclei. In the midbrain, great numbers of eGFP+ neurons were detected in the superior colliculus as well as in the pretectal region. In the hindbrain, only a few eGFP+ neurons were detected in the laterodorsal tegmental nucleus.

4 | DISCUSSION

In this study, monosynaptic tracing using pseudotyped rabies virus was used to identify primary afferents to populations of Gpr151-Cre neurons in the mouse diencephalon.

In the medial habenula, TVA-mCherry+/eGFP+ starter neurons were observed in the ventral part of the medial habenula (Table 2). This distribution is consistent with the pattern of Gpr151 mRNA and protein expression (Figures 2 and 3). Several nuclei in the pallidum, including the triangular septal nucleus, septofimbrial nucleus, bed nucleus of the anterior commissure, medial septal nucleus, and the nucleus of the diagonal band have previously been identified as afferents to the medial habenula (Herkenham & Nauta, 1977; Qin & Luo, 2009; Yamaguchi, Danjo, Pastan, Hikida, & Nakanishi, 2013). All of these areas contained eGFP+ neurons in cases where starter neurons were found in the medial habenula, although the most prominent and consistent projection appeared to arise in the nucleus of the diagonal band and the medial septal nucleus. This projection is reported to be GABAergic (Contestabile & Fonnum, 1983; Qin & Luo, 2009), although we did not test whether the neurons that project onto Gpr151-expressing cells have this phenotype.

In the lateral habenula, Cre expression could be detected in all subnuclei except for the oval subnucleus of the lateral division (Figures 2 and 3; Table 2). Afferent neurons were observed in many areas (Figure 7; Table 3) that have previously been reported to contain afferents to the lateral habenula, including the nucleus of the diagonal band, bed

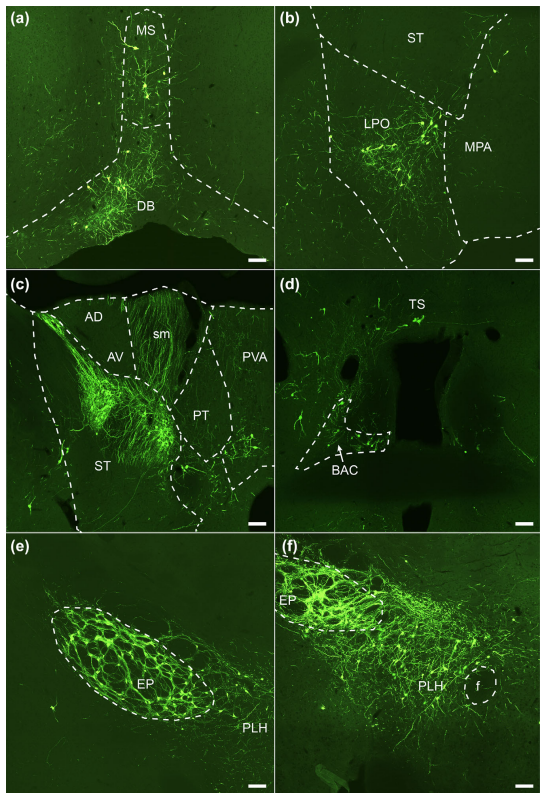

FIGURE 7 Main afferent neuronal populations of the habenular Gpr151-Cre starter neurons. Coronal sections showing eGFP-expressing afferent neurons (green cell bodies and fibers) in the medial septal nucleus and the nucleus of the diagonal band (a; case M17), the lateral and medial preoptic area (b; case M18), the bed nucleus of stria terminalis and the paraventricular thalamic nucleus (c; case M17), the triangular nucleus of the septum and the bed nucleus of the anterior commissure (d; case M17), the entopeduncular nucleus and the lateral hypothalamus (e, f; case M18). Scale bar = 100 μm

nucleus of stria terminalis, ventral pallidum, lateral preoptic area, lateral hypothalamic area and entopeduncular nucleus and the median raphe nucleus (Dong & Swanson, 2004; Herkenham & Nauta, 1977; Wallace et al., 2017).

In a recent study, the nucleus of the diagonal band was shown to provide a possible source of input to the lateral habenula, which allowed the habenular neurons to phase lock with hippocampal theta oscillations during anesthesia and rapid-eye-movement (REM) sleep (Aizawa et al., 2013). Lesions of the lateral habenula and the fasciculus retroflexus reduce theta power in the hippocampus and substantially decrease REM sleep duration, while non-REM sleep remains unaffected (Aizawa et al., 2013; Valjakka et al., 1998). Since Gpr151-Cre neurons receive input from the nucleus of the diagonal band and in turn project to the interpeduncular nucleus and median raphe, structures that has been implicated in theta oscillations and REM sleep (Funato et al., 2010; Vertes, Kinney, Kocsis, & Fortin, 1994), it is possible that this neuronal population (or a subset of it) plays a role in controlling these functions.

A fruitful approach for determining the valence of experiencing activation or inhibition of specific neurons is by optogenetic stimulation,

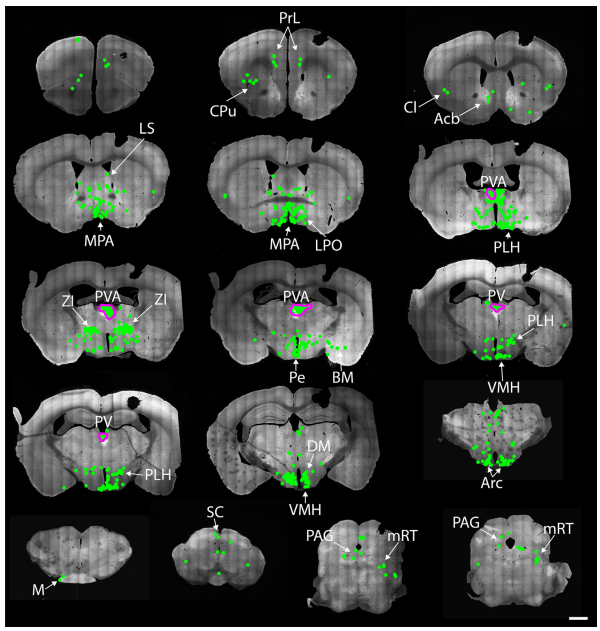

FIGURE 8 Afferents of Gpr151-Cre neurons in the paraventricular thalamic nucleus. Coronal brain sections from 1.98 to −4.84 mm relative to Bregma of a Gpr151-Cre mouse (case M113) where AAV8-Ef1a-FLEX-TVA-mCherry, AAV8-CA-FLEX-RG, and SADΔG-eGFP(EnvA) was injected into the anterior part of the paraventricular thalamic nucleus. Afferent eGFP expressing neurons (green) were found in great numbers in the zona incerta, medial preoptic area, medial and lateral hypothalamus and to a minor extent in the prelimbic cortex, accumbens nucleus, lateral preoptic area, bed nucleus of stria terminalis, and periaqueductal gray. Neurons coexpressing eGFP and mCherry (starter neurons; magenta outline) were located in the paraventricular thalamic nucleus. Scale bar = 1000 μm

combined with the real-time place preference test. In this test, the animals may freely choose to enter or avoid an area where the laser light is activated. It has been shown that activation of projections from the lateral hypothalamic area and entopeduncular nucleus to the lateral habenula is aversive, that is, the animals avoid stimulation (Shabel, Proulx, Trias, Murphy, & Malinow, 2012; Stamatakis et al., 2016). In line with this finding, inhibition of the projection from the lateral hypothalamic area to the lateral habenula using an inhibitory light-sensitive chloride channel, or activation of inhibitory afferents from the ventral tegmental area, was appetitive (Stamatakis et al., 2013). Stimulation of lateral habenular efferents to the rostromedial tegmental nucleus also produced an aversive response (Stamatakis & Stuber, 2012). It was recently demonstrated that activation of a projection from the paraventricular thalamic nucleus to accumbens nucleus evoked the similar avoidance behavior (Zhu, Wienecke, Nachtrab, & Chen, 2016). Given that the aforementioned projections were observed in our study, it is tempting to speculate that modulation of GPR151-expressing neurons could alter the affective component of an experience. Indeed, selective ablation of Gpr151-Cre neurons resulted in increased anxiety in the elevated plus maze and open field tests (Kobayashi et al., 2013).

Two distinct populations of entopeduncular neurons project to the lateral habenula (Wallace et al., 2017). Glutamatergic parvalbumin-expressing neurons preferentially targets the oval subnucleus of the lateral division of the lateral habenula, while a GABA/glutamate co-releasing somatostatin-expressing population display a more distributed terminal pattern within the lateral habenula. Given that no Gpr151-Cre was observed in the oval subnucleus, the entopeduncular afferents may belong to this population of somatostatin-expressing neurons.

4.1 | Similarities and differences between habenular and thalamic Gpr151-Cre populations

It is clear from the efferent connectivity pattern that Gpr151-Cre neurons of the habenula and the paraventricular thalamic nucleus are distinct populations. The Gpr151-Cre neurons in paraventricular nucleus

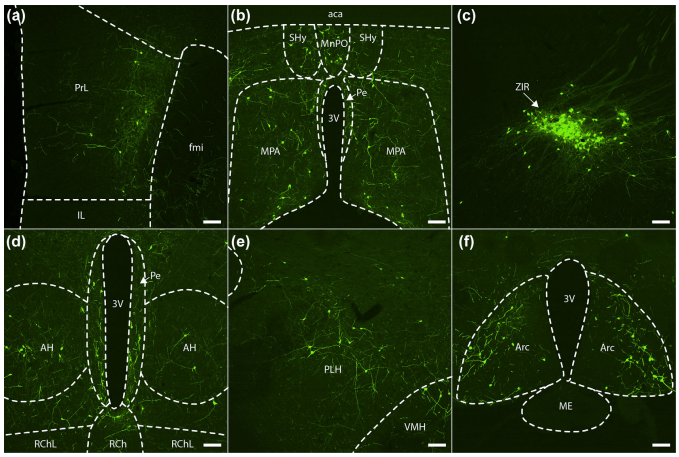

FIGURE 9 Main afferent neuronal populations of Gpr151-Cre starter neurons in the paraventricular thalamic nucleus. Coronal sections (case M113) showing eGFP-expressing afferent neurons (green cell bodies and fibers) in the prelimbic cortex (a, left hemisphere), the septohypothalamic nucleus (b), the median preoptic nucleus (b), the periventricular hypothalamic nucleus (b, d), the medial preoptic area (b), the zona incerta (c, right hemisphere), the anterior hypothalamic area (d), the retrochiasmatic area (d), the peduncular part of lateral hypothalamus (e, right hemisphere), the ventromedial hypothalamic nucleus (e, right hemisphere), and the arcuate hypothalamic nucleus (f). Scale bar = 100 μm

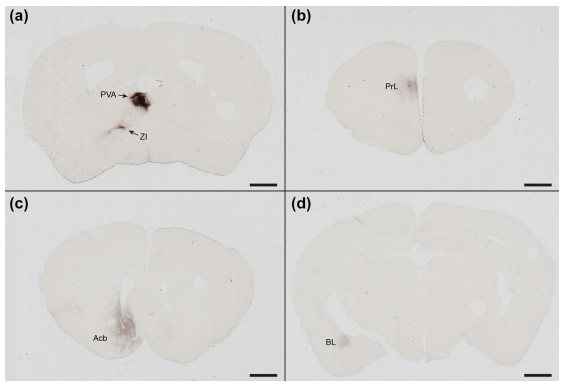

FIGURE 10 Efferent projections of Gpr151-Cre neurons in the paraventricular thalamic nucleus. Coronal sections of a Gpr151-Cre mouse injected with AAV8-hSyn1-FLEX-mCherry in the paraventricular nucleus of the thalamus (case M74) showing 3,3'-diaminobenzidine enhanced mCherry immunostaining in cell bodies in the injected area and in efferent projections to the zona incerta (a), the prelimbic area (b), the shell and core of accumbens nucleus (c), and the basolateral amygdala (d). Scale bar = 1000 μm

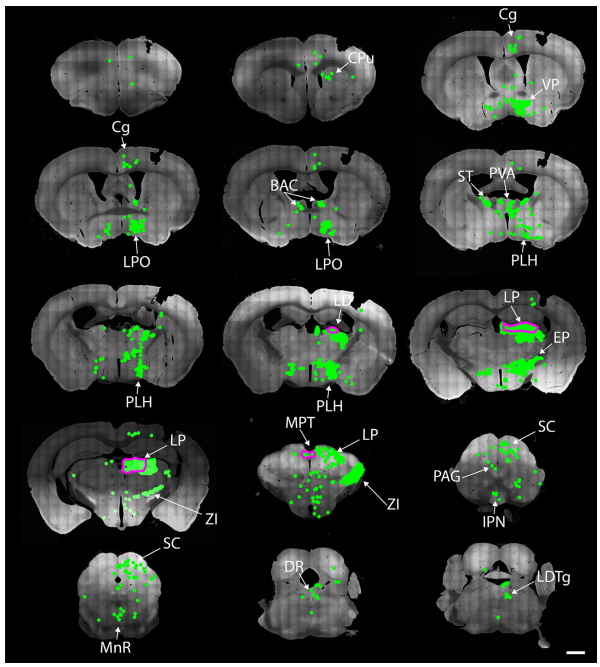

FIGURE 11 Afferents of Gpr151-Cre neurons in lateral thalamic nuclei. Coronal brain sections from 1.98 to −5.02 mm relative to Bregma of a Gpr151-Cre mouse (case M119) where AAV8-Ef1a-FLEX-TVA-mCherry, AAV8-CA-FLEX-RG, and SADΔG-eGFP(EnvA) was injected into the lateral posterior thalamic nucleus. Starter neurons expressing both mCherry and eGFP (outlined in magenta) were not restricted to the target area, but were also found in the laterodorsal thalamic nucleus, central lateral thalamic nucleus, parafascicular thalamic nucleus, posterior thalamic group, lateral habenula, precommissural nucleus, and medial pretectal nucleus. Afferent eGFP expressing neurons (green) were detected in many areas throughout the brain including the cingulate and prelimbic cortices, bed nucleus of stria terminalis, ventral pallidum, reticular thalamic nucleus, lateral preoptic area, lateral hypothalamic area, zona incerta, and superior colliculus. Scale bar = 1000 μm

project to the accumbens nucleus, zona incerta, basolateral amygdala, and prelimbic area, a pattern that is distinct from the mesencephalic projection of the habenular GPR151-expressing neurons (Figure 10; Broms et al., 2015). On the other hand, many similarities in afferent connectivity could be noted between the habenular and paraventricular thalamic Gpr151-Cre populations. Both populations were targeted by neurons in the bed nucleus of stria terminalis, ventral pallidum, nucleus of the diagonal band, lateral preoptic area, and lateral hypothalamic area. However, some striking differences in afferent connectivity were observed. The zona incerta produced a heavy projection onto paraventricular thalamic Gpr151-Cre neurons, while habenular afferents from this area were sparse. The same held true for the medial preoptic area. In contrast to the habenular population, afferents to the paraventricular thalamic population could not be detected in the bed nucleus of the anterior commissure, entopeduncular nucleus, or in the triangular septum.

The paraventricular nucleus has been implicated in food and drug reward seeking (reviewed in Matzeu, Zamora-Martinez, & Martin-Fardon, 2014). In a recent study, it was demonstrated that inhibition of a projection from the paraventricular nucleus to the accumbens nucleus ameliorates symptoms of opiate withdrawal (Zhu et al., 2016). The lateral habenula has been implicated in cocaine-induced avoidance behavior (Jhou et al., 2013) and the medial habenula contributes to nicotine aversion (Fowler, Lu, Johnson, Marks, & Kenny, 2011). It is therefore an interesting possibility that, despite differences in connectivity patterns, the diencephalic GPR151-expressing neurons could be functionally related by involvement in the modulation of drug seeking behavior.

4.2 | Afferent connectivity of the lateral thalamic Gpr151-Cre population, involvement in visual processing?

Many neurons in the lateral posterior nucleus, lateral dorsal nucleus, and posterior group of the thalamus displayed Cre recombinase activity (Table 2; Figure 4m–o). In animals where the viral vector injections were targeted on the lateral posterior nucleus, there was always some degree of spread in to the habenula. This precludes clear conclusions to be drawn from these experiments. However, some characteristics of the eGFP+ neuronal distribution nonetheless provide clues regarding the connectivity and function of this thalamic population. Compared to the afferents of the habenular Gpr151-Cre neurons, a large number of afferents to lateral thalamic Gpr151-Cre neurons were detected in prefrontal cortical areas (primarily the cingulate cortex), the visual cortex, the caudate putamen, the reticular nucleus, and most notably in the zona incerta and the superior colliculus (Figure 11; Table 3).

Several studies have previously implicated the lateral posterior thalamic nucleus, the superior colliculus, and the zona incerta in visual information processing (Benevento & Fallon, 1975; Gale & Murphy, 2014; Krauzlis, Lovejoy, & Zénon, 2013; Legg, 1979; Power, Leamey, & Mitrofanis, 2001). Interestingly, it has been demonstrated that the lateral posterior thalamic nucleus contains multimodal neurons that are sensitive to both pain and light (Noseda et al., 2010). To clarify if GPR151 is involved in the processing of visual or somatosensory information will require further investigation.

4.3 | Cre-independent expression of viral constructs

In wild type mice injected with Cre-dependent viral vectors, we occasionally saw TVA-mCherry and eGFP expression in the vicinity of the injection tract. This finding suggests that there is a certain degree of leakiness in the FLEX switch, but that this ectopic expression of TVA-mCherry (and presumably also RG) is not strong enough to enable transsynaptic transport of rabies virus particles. This problem has also been noted by other researchers using the same pseudotyped rabies tracing system (Callaway & Luo, 2015; Pollak Dorocic et al., 2014). In Cre-expressing animals, neurons that are TVA-mCherry-positive/eGFP-positive as a result of leakiness are impossible to distinguish from true starter neurons. We can therefore not conclude that all TVA-mCherry-positive/eGFP-positive neurons in the vicinity of the injection tract are actual starter neurons. Nevertheless, since no neurons were observed outside of the injected area in wild type mice, the Cre-independent expression does not affect the validity of the analysis of long-range projections.

4.4 | Different sensitivity of the methods used for Gpr151 detection

There are notable differences in expression pattern of GPR151 protein, Gpr151 mRNA, and Gpr151 promoter activity. Immunohistochemistry reveals strong GPR151 protein expression in habenular projections (Broms et al., 2015). In situ hybridization detects Gpr151 mRNA in the habenula, but also in certain thalamic areas (Figure 3; Berthold et al., 2003; Ignatov et al., 2004; Lein et al., 2006; Vassilatis et al., 2003). The expression of Cre-dependent reporters found in the current study largely corresponds to the mRNA distribution. One exception is the lateral posterior thalamic nuclei, in which only very few neurons expressing Gpr151 mRNA has been detected using in situ hybridization (Figure 3c,d; Lein et al., 2006), but ample Cre-dependent mCherry expression was seen in the current study (Figures 2, 3, and 4m–o). A possible explanation for this discrepancy is that there is a difference in the sensitivity of the different detection methods. The constructs for the viral reporter employ strong promoters and enhancer sequences (woodchuck hepatitis virus posttranscriptional regulatory element) for improved expression, elements that the endogenous Gpr151 gene is lacking. Furthermore, the reporter constructs are permanently activated by Cre recombination, meaning that even a transient surge in Cre expression will result in persistent tagging of that neuron. As long as a no specific GPR151 agonists or antagonists are available, there is no gold standard for assessing functional GPR151 expression. In the future when such substances have possibly been discovered, the Cre-expressing populations described in this study should be examined electrophysiologically, in order to verify that GPR151 is expressed at physiologically relevant levels.

4.5 | Caveats of using BAC transgenic Cre mice

Gpr151 mRNA and protein could be detected in many, but not all, neurons that exhibited Cre recombinase activity. One possibility is that Cre mediated activation of the reporter construct can occur even at low or transient Gpr151 promoter activation. This would result in persistent reporter expression, while GPR151 protein and Gpr151 mRNA would remain undetectable. Although the Gpr151-Cre BAC construct is large (108 kbp) and should contain most of the regulatory elements of the endogenous Gpr151 gene, we cannot rule out that the BAC transgenic approach used in this study suffers from ectopic Cre expression independent of the Gpr151 promoter. This could be the result of inserting the BAC transgene into the vicinity of a strong promoter or enhancer (Liu, 2013). Ectopic expression could also arise if the endogenous Gpr151 promoter is epigenetically silenced, while the Gpr151 promoter of the BAC construct remains active. In future studies, knock-in animals targeting the endogenous Gpr151 gene could be used to minimize the risk of ectopic Cre expression.

5 | CONCLUSION

Here, we present a map of the afferent connectivity of a diencephalic neuronal population defined by Gpr151 expression. The connectivity of thalamic versus habenular Gpr151-expressing neurons differed substantially, indicating a neuroanatomical heterogeneity within the Gpr151-system. In depth knowledge of the connectivity of this, neuronal population will facilitate the design of investigations regarding the function of GPR151 as well as the interpretation of the effects of pharmacological modulators of this system.

ACKNOWLEDGMENTS

We sincerely thank Maria Ekemohn, Alice Lagebrant, Joakim Ekstrand, and Martin Lundblad for valuable input on the manuscript. This work was supported by the Swedish Research Council, the Royal Physiographic Society of Lund, Stiftelsen Professor Bror Gadelius minnesfond, Gyllenstiernska Krapperupsstiftelsen, and Stiftelsen Ellen och Henrik Sjöbrings minnesfond.

CONFLICT OF INTEREST

The authors declare no conflicts of interest.

AUTHOR CONTRIBUTION

All authors had full access to all the data in the study and take responsibility for the integrity and presentation of the data. Study concept and design: JB, MG, TB, and AT. Acquisition of data: JB, MG, and LH. Analysis and interpretation of data: JB, LH, and AT. Writing of the manuscript: JB and AT. Conceptualization and critical revision of the manuscript for intellectual content: AT and KM. Obtained funding: JB and AT. Study supervision: AT.

REFERENCES

Aizawa, H., Yanagihara, S., Kobayashi, M., Niisato, K., Takekawa, T., Harukuni, R., … Okamoto, H. (2013). The synchronous activity of lateral habenular neurons is essential for regulating hippocampal theta oscillation. *Journal of Neuroscience*, *33*(20), 8909–8921.

Amo, R., Aizawa, H., Takahoko, M., Kobayashi, M., Takahashi, R., Aoki, T., & Okamoto, H. (2010). Identification of the zebrafish ventral habenula as a homolog of the mammalian lateral habenula. *Journal of Neuroscience*, *30*(4), 1566–1574.

Atasoy, D., Aponte, Y., Su, H. H., & Sternson, S. M. (2008). A FLEX switch targets Channelrhodopsin-2 to multiple cell types for imaging and long-range circuit mapping. *Journal of Neuroscience*, *28*(28), 7025–7030.

Baker, P. M., Raynor, S. A., Francis, N. T., & Mizumori, S. J. Y. (2016). Lateral habenula integration of proactive and retroactive information mediates behavioral flexibility. *Neuroscience*, *345*, 89–98.

Benevento, L. A., & Fallon, J. H. (1975). The ascending projections of the superior colliculus in the rhesus monkey (Macaca mulatta). *Journal of Comparative Neurology*, *160*(3), 339–361.

Berthold, M., Collin, M., Sejlitz, T., Meister, B., & Lind, P. (2003). Cloning of a novel orphan G protein-coupled receptor (GPCR-2037): In situ hybridization reveals high mRNA expression in rat brain restricted to neurons of the habenular complex. *Molecular Brain Research*, *120*, 22–29.

Bianco, I. H., & Wilson, S. W. (2009). The habenular nuclei: A conserved asymmetric relay station in the vertebrate brain. *Philosophical Transactions of the Royal Society of London. Series B, Biological Sciences*, *364*, 1005–1020.

Broms, J., Antolin-Fontes, B., Tingström, A., & Ibañez-Tallon, I. (2015). Conserved expression of the GPR151 receptor in habenular axonal projections of vertebrates. *Journal of Comparative Neurology*, *523*(3), 359–380.

Callaway, E. M., & Luo, L. (2015). Monosynaptic circuit tracing with glycoprotein-deleted rabies viruses. *Journal of Neuroscience*, *35*, 8979–8985.

Chou, M.-Y., Amo, R., Kinoshita, M., Cherng, B.-W., Shimazaki, H., Agetsuma, M., … Okamoto, H. (2016). Social conflict resolution regulated by two dorsal habenular subregions in zebrafish. *Science*, *352*, 87–90.

Contestabile, A., & Fonnum, F. (1983). Cholinergic and GABAergic forebrain projections to the habenula and nucleus interpeduncularis: Surgical and kainic acid lesions. *Brain Research*, *275*, 287–297.

Corodimas, K. P., Rosenblatt, J. S., & Morrell, J. I. (1992). The habenular complex mediates hormonal stimulation of maternal behavior in rats. *Behavioral Neuroscience*, *106*, 853–865.

Díaz, E., Bravo, D., Rojas, X., & Concha, M. L. (2011). Morphologic and immunohistochemical organization of the human habenular complex. *Journal of Comparative Neurology*, *519*, 3727–3747.

Dong, H.-W., & Swanson, L. W. (2004). Projections from bed nuclei of the stria terminalis, posterior division: Implications for cerebral hemisphere regulation of defensive and reproductive behaviors. *Journal of Comparative Neurology*, *471*, 396–433.

Donovick, P. J., Burright, R. G., & Zuromski, E. (1970). Localization of quinine aversion within the septum, habenula, and interpeduncular nucleus of the rat. *Journal of Comparative and Physiological Psychology*, *71*(3), 376–383.

Fowler, C. D., & Kenny, P. J. (2013). Nicotine aversion: Neurobiological mechanisms and relevance to tobacco dependence vulnerability. *Neuropharmacology*, *76*(Pt. B), 533–544.

Fowler, C. D., Lu, Q., Johnson, P. M., Marks, M. J., & Kenny, P. J. (2011). Habenular α5 nicotinic receptor subunit signalling controls nicotine intake. *Nature*, *471*, 597–601.

Franklin, K., & Paxinos, G. (2008). *The mouse brain in stereotaxic coordinates, compact* (3rd ed.). Amsterdam, The Netherlands. Elsevier.

Funato, H., Sato, M., Sinton, C. M., Gautron, L., Williams, S. C., Skach, A., … Yanagisawa, M. (2010). Loss of Goosecoid-like and DiGeorge syndrome critical region 14 in interpeduncular nucleus results in altered regulation of rapid eye movement sleep. *Proceedings of the National Academy of Sciences of the United States of America*, *107*, 18155–18160.

Gale, S. D., & Murphy, G. J. (2014). Distinct representation and distribution of visual information by specific cell types in mouse superficial superior colliculus. *Journal of Neuroscience*, *34*(40), 13458–13471.

Gardon, O., Faget, L., Chu Sin Chung, P., Matifas, A., Massotte, D., & Kieffer, B. L. (2014). Expression of mu opioid receptor in dorsal diencephalic conduction system: New insights for the medial habenula. *Neuroscience*, *277*, 595–609.

Gey, M., Wanner, R., Schilling, C., Pedro, M. T., Sinske, D., & Knöll, B. (2016). Atf3 mutant mice show reduced axon regeneration and impaired regeneration-associated gene induction after peripheral nerve injury. *Open Biology*, *6*(8). pii: 160091.

Golden, S. A., Heshmati, M., Flanigan, M., Christoffel, D. J., Guise, K., Pfau, M. L., … Russo, S. J. (2016). Basal forebrain projections to the lateral habenula modulate aggression reward. *Nature*, *534*, 688–692.

Greatrex, R. M., & Phillipson, O. T. (1982). Demonstration of synaptic input from prefrontal cortex to the habenula in the rat. *Brain Research*, *238*, 192–197.

Herkenham, M., & Nauta, W. J. (1977). Afferent connections of the habenular nuclei in the rat. A horseradish peroxidase study, with a note on the fiber-of-passage problem. *Journal of Comparative Neurology*, *173*, 123–146.

Holmes, F. E., Kerr, N., Chen, Y.-J., Vanderplank, P., McArdle, C. A., & Wynick, D. (2017). Targeted disruption of the orphan receptor Gpr151 does not alter pain-related behaviour despite a strong induction in dorsal root ganglion expression in a model of neuropathic pain. *Molecular and Cellular Neuroscience*, *78*, 35–40.

Hsu, Y.-W. A., Morton, G., Guy, E. G., Wang, S. D., & Turner, E. E. (2016). Dorsal medial habenula regulation of mood-related behaviors and primary reinforcement by tachykinin-expressing habenula neurons. *eNeuro*, *3*. ENEURO.0109-16.2016.

Hsu, Y.-W. A., Wang, S. D., Wang, S., Morton, G., Zariwala, H. A., de la Iglesia, H. O., & Turner, E. E. (2014). Role of the dorsal medial habenula in the regulation of voluntary activity, motor function, hedonic state, and primary reinforcement. *Journal of Neuroscience*, *34*, 11366–11384.

Ignatov, A., Hermans-Borgmeyer, I., & Schaller, H. C. (2004). Cloning and characterization of a novel G-protein-coupled receptor with homology to galanin receptors. *Neuropharmacology*, *46*, 1114–1120.

Jhou, T. C., Good, C. H., Rowley, C. S., Xu, S.-P., Wang, H., Burnham, N. W., … Ikemoto, S. (2013). Cocaine drives aversive conditioning via delayed activation of dopamine-responsive habenular and midbrain pathways. *Journal of Neuroscience*, *33*, 7501–7512.

Kobayashi, Y., Sano, Y., Vannoni, E., Goto, H., Suzuki, H., Oba, A., … Itohara, S. (2013). Genetic dissection of medial habenula-interpeduncular nucleus pathway function in mice. *Frontiers in Behavioral Neuroscience*, *7*, 17.

Krauzlis, R. J., Lovejoy, L. P., & Zénon, A. (2013). Superior colliculus and visual spatial attention. *Annual Review of Neuroscience*, *36*, 165–182.

Legg, C. R. (1979). Visual discrimination impairments after lesions in zona incerta or lateral terminal nucleus of accessory optic tract. *Brain Research*, *177*, 461–478.

Lein, E. S., Hawrylycz, M. J., Ao, N., Ayres, M., Bensinger, A., Bernard, A., … Jones, A. R. (2006). Genome-wide atlas of gene expression in the adult mouse brain. *Nature*, *445*(7124), 168–176.

Liu, C. (2013). Strategies for designing transgenic DNA constructs. In Lita A. Freeman (Ed.), *Lipoproteins and cardiovascular disease. Methods in molecular biology* (Vol. 1027, pp. 183–201). Totowa, NJ: Humana Press.

Matzeu, A., Zamora-Martinez, E. R., & Martin-Fardon, R. (2014). The paraventricular nucleus of the thalamus is recruited by both natural rewards and drugs of abuse: Recent evidence of a pivotal role for orexin/hypocretin signaling in this thalamic nucleus in drug-seeking behavior. *Frontiers in Behavioral Neuroscience*, *8*, 117.

Menegas, W., Bergan, J. F., Ogawa, S. K., Isogai, Y., Umadevi Venkataraju, K., Osten, P., … Watabe-Uchida, M. (2015). Dopamine neurons projecting to the posterior striatum form an anatomically distinct subclass. *Elife*, *4*, e10032.

Noseda, R., Kainz, V., Jakubowski, M., Gooley, J. J., Saper, C. B., Digre, K., & Burstein, R. (2010). A neural mechanism for exacerbation of headache by light. *Nature Neuroscience*, *13*, 239–245.

Pollak Dorocic, I., Fürth, D., Xuan, Y., Johansson, Y., Pozzi L., Silberberg, G., … Meletis, K. (2014). A whole-brain atlas of inputs to serotonergic neurons of the dorsal and median raphe nuclei. *Neuron*, *83*, 663–678.

Power, B. D., Leamey, C. A., & Mitrofanis, J. (2001). Evidence for a visual subsector within the zona incerta. *Visual Neuroscience*, *18*, 179–186.

Qin, C., & Luo, M. (2009). Neurochemical phenotypes of the afferent and efferent projections of the mouse medial habenula. *Neuroscience*, *161*, 827–837.

Quina, L. A., Tempest, L., Ng, L., Harris, J., Ferguson, S., Jhou, T., & Turner, E. E. (2014). Efferent pathways of the mouse lateral habenula. *Journal of Comparative Neurology*, *523*(1), 32–60.

Reinhold, A. K., Batti, L., Bilbao, D., Buness, A., Rittner, H. L., & Heppenstall, P. A. (2015). Differential transcriptional profiling of damaged and intact adjacent dorsal root ganglia neurons in neuropathic pain. *PLoS One*, *10*, e0123342.

Shabel, S. J., Proulx, C. D., Trias, A., Murphy, R. T., & Malinow, R. (2012). Input to the lateral habenula from the basal ganglia is excitatory, aversive, and suppressed by serotonin. *Neuron*, *74*, 475–481.

Shelton, L., Becerra, L., & Borsook, D. (2012). Unmasking the mysteries of the habenula in pain and analgesia. *Progress in Neurobiology*, *96*, 208–219.

Stamatakis, A. M., Jennings, J. H., Ung, R. L., Blair, G. A., Weinberg, R. J., Neve, R. L., … Stuber, G. D. (2013). A unique population of ventral tegmental area neurons inhibits the lateral habenula to promote reward. *Neuron*, *80*, 1039–1053.

Stamatakis, A. M., & Stuber, G. D. (2012). Activation of lateral habenula inputs to the ventral midbrain promotes behavioral avoidance. *Nature Neuroscience*, *15*(8), 1105–1107.

Stamatakis, A. M., Van Swieten, M., Basiri, M. L., Blair, G. A., Kantak, P., & Stuber, G. D. (2016). Lateral hypothalamic area glutamatergic neurons and their projections to the lateral habenula regulate feeding and reward. *Journal of Neuroscience*, *36*, 302–311.

Stephenson-Jones, M., Floros, O., Robertson, B., & Grillner, S. (2011). Evolutionary conservation of the habenular nuclei and their circuitry controlling the dopamine and 5-hydroxytryptophan (5-HT) systems. *Proceedings of the National Academy of Sciences of the United States of America*, *109*(3), E164–E173.

Stopper, C. M., & Floresco, S. B. (2013). What's better for me? Fundamental role for lateral habenula in promoting subjective decision biases. *Nature Neuroscience*, *17*(1), 33–35.

Valjakka, A., Vartiainen, J., Tuomisto, L., Tuomisto, J. T., Olkkonen, H., & Airaksinen, M. M. (1998). The fasciculus retroflexus controls the integrity of REM sleep by supporting the generation of hippocampal theta rhythm and rapid eye movements in rats. *Brain Research Bulletin*, *47*, 171–184.

van Kerkhof, L. W. M., Damsteegt, R., Trezza, V., Voorn, P., & Vanderschuren, L. J. M. J. (2013). Functional integrity of the habenula is necessary for social play behaviour in rats. *European Journal of Neuroscience*, *38*, 3465–3475.

Vassilatis, D. K., Hohmann, J. G., Zeng, H., Li, F., Ranchalis, J. E., Mortrud, M. T., … Gaitanaris, G. A. (2003). The G protein-coupled receptor repertoires of human and mouse. *Proceedings of the National Academy of Sciences of the United States of America*, *100*, 4903–4908.

Vertes, R. P., Fortin, W. J., & Crane, A. M. (1999). Projections of the median raphe nucleus in the rat. *Journal of Comparative Neurology*, *407*(4), 555–582.

Vertes, R. P., Kinney, G. G., Kocsis, B., & Fortin, W. J. (1994). Pharmacological suppression of the median raphe nucleus with serotonin1a agonists, 8-OH-DPAT and buspirone, produces hippocampal theta rhythm in the rat. *Neuroscience*, *60*, 441–451.

Wagner, F., French, L., & Veh, R. W. (2014). Transcriptomic-anatomic analysis of the mouse habenula uncovers a high molecular heterogeneity among neurons in the lateral complex, while gene expression in the medial complex largely obeys subnuclear boundaries. *Brain Structure and Function*, *221*(1), 39–58.

Wagner, F., Stroh, T., & Veh, R. W. (2014). Correlating habenular subnuclei in rat and mouse using topographical, morphological and cytochemical criteria. *Journal of Comparative Neurology*, *522*(11), 2650–2662.

Wallace, M. L., Saunders, A., Huang, K. W., Philson, A. C., Goldman, M., Macosko, E. Z., … Sabatini, B. L. (2017). Genetically distinct parallel pathways in the entopeduncular nucleus for limbic and sensorimotor output of the basal ganglia. *Neuron*, *94*, 138–152.

Wang, F., Flanagan, J., Su, N., Wang, L.-C., Bui, S., Nielson, A., … Luo, Y. (2012). RNAscope: A novel in situ RNA analysis platform for formalin-fixed, paraffin-embedded tissues. *The Journal of Molecular Diagnostics*, *14*, 22–29.

Warden, M. R., Selimbeyoglu, A., Mirzabekov, J. J., Lo, M., Thompson, K. R., Kim, S.-Y., … Deisseroth, K. (2012). A prefrontal cortex-brainstem

neuronal projection that controls response to behavioural challenge. *Nature*, *92*(7429), 428–432.

Watabe-Uchida, M., Zhu, L., Ogawa, S. K., Vamanrao, A., & Uchida, N. (2012). Whole-brain mapping of direct inputs to midbrain dopamine neurons. *Neuron*, *74*, 858–873.

Wickersham, I. R., Lyon, D. C., Barnard, R. J. O., Mori, T., Finke, S., Conzelmann, K.-K., … Callaway, E. M. (2007). Monosynaptic restriction of transsynaptic tracing from single, genetically targeted neurons. *Neuron*, *53*, 639–647.

Yamaguchi, T., Danjo, T., Pastan, I., Hikida, T., & Nakanishi, S. (2013). Distinct roles of segregated transmission of the septo-habenular pathway in anxiety and fear. *Neuron*, *78*, 537–544.

Yin, K., Deuis, J. R., Lewis, R. J., & Vetter, I. (2016). Transcriptomic and behavioural characterisation of a mouse model of burn pain identify the cholecystokinin 2 receptor as an analgesic target. *Molecular Pain*, *28*, pii: 1744806916665366.

Zhu, Y., Wienecke, C. F. R., Nachtrab, G., & Chen, X. (2016). A thalamic input to the nucleus accumbens mediates opiate dependence. *Nature*, *530*, 219–222.

How to cite this article: Broms J, Grahm M, Haugegaard L, Blom T, Meletis K, Tingström A. Monosynaptic retrograde tracing of neurons expressing the G-protein coupled receptor Gpr151 in the mouse brain. *J Comp Neurol*. 2017;525:3227–3250. https://doi.org/10.1002/cne.24273

Manuscript III

Manuscript IV

Habenula and circuit psychiatry

Novel tools and technologies in neuroscience are currently reshaping our understanding of the brain. Anatomical and functional mapping of the brain circuits that constitute the mind is now possible at an unprecedented level of detail, using the current molecular biological toolbox. Careful dissection of the complex circuitry involved in psychiatric syndromes such as depression, is probably necessary for making significant progress in the understanding of the neurobiological mechanisms. In this thesis, I focus on a specific brain area, the habenula, which appears to be implicated in depression. The localization and pharmacology of GPR151, a receptor that can possibly be targeted for modulating habenular activity, is investigated. Furthermore inhibitory neurons within the habenula are identified and classified, something that previously has largely been overlooked. This thesis is only a small contribution to a field that is likely to expand tremendously within the coming decades, the field of circuit psychiatry.

Printed by Media-Tryck, Lund 2018 NORDIC SWAN ECOLABEL 3041 0903

LUND UNIVERSITY

FACULTY OF MEDICINE

Department of Clinical Sciences, Lund

Lund University, Faculty of Medicine
Doctoral Dissertation Series 2018:139
ISBN 978-91-7619-707-3
ISSN 1652-8220

9 789176 197073